PLT 27 GAS TURBINE ENGINE EXHAUST EMISSION AND NOISE MEASUREMENTS

Philip M. Rubins, et al

Avco Lycoming Division

Prepared for:

Army Air Mobility Research and Development Laboratory

September 1974

EUSTIS DIRECTORATE POSITION STATEMENT

An effort is under way within the Government and in private industry to categorize and catalog the exhaust gas emission and noise characteristics of turbine engines of all types. The objective of this work was to measure the exhaust gas and noise characteristics of the Lycoming PLT 27 engine. The data obtained in this program will be used as a guide in assessing the environmental impact of future Army helicopter operations.

The work was performed under the technical management of Messrs. R. G. Furgurson and R. G. Dodd, Technology Applications Division.

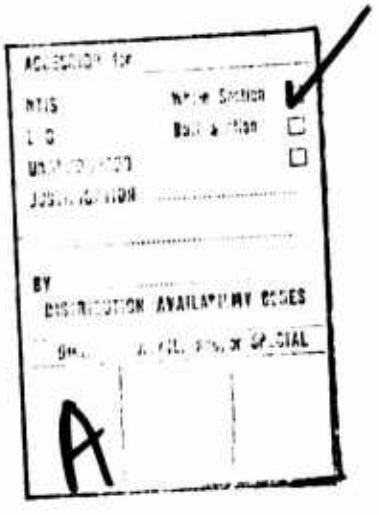

Unclassified

SECURITY CLASSIFICATION OF THIS PAGE (When Data Entered)

AD/A-001728

REPORT DOCUMENTATION PAGE

READ INSTRUCTIONS BEFORE COMPLETING FORM

1. REPORT NUMBER: USAAMRDL-TR-74-61	2. GOVT ACCESSION NO.
3. RECIPIENT'S CATALOG NUMBER	
4. TITLE (and Subtitle): PLT 27 GAS TURBINE ENGINE EXHAUST EMISSION AND NOISE MEASUREMENTS	5. TYPE OF REPORT & PERIOD COVERED: Final Report, 21 May 1973 through 31 Dec. 1973
	6. PERFORMING ORG. REPORT NUMBER: LYC 74-7
7. AUTHOR(s): Philip M. Rubins, Edward Auerbach, Jochen A. Deman	8. CONTRACT OR GRANT NUMBER(s): DAAJ02-73-C-0068
9. PERFORMING ORGANIZATION NAME AND ADDRESS: Avco Lycoming Division, Stratford, Connecticut 06497	10. PROGRAM ELEMENT, PROJECT, TASK AREA & WORK UNIT NUMBERS: Task 1G162204AA7110
11. CONTROLLING OFFICE NAME AND ADDRESS: Eustis Directorate, U.S. Army Air Mobility Research and Development Laboratory, Fort Eustis, Virginia 23604	12. REPORT DATE: September 1974
	13. NUMBER OF PAGES: 111
14. MONITORING AGENCY NAME & ADDRESS (if different from Controlling Office)	15. SECURITY CLASS. (of this report): Unclassified
	15a. DECLASSIFICATION/DOWNGRADING SCHEDULE: N/A

16. DISTRIBUTION STATEMENT (of this Report)

Approved for public release; distribution unlimited

17. DISTRIBUTION STATEMENT (of the abstract entered in Block 20, if different from Report)

18. SUPPLEMENTARY NOTES

19. KEY WORDS (Continue on reverse side if necessary and identify by block number)

Gas Turbines
Exhaust Gases
Combustion
Smoke
Noise
Free Field
Sound Pressure
Engines
Emission

20. ABSTRACT (Continue on reverse side if necessary and identify by block number)

PLT 27 gas turbine engine exhaust gas and noise were measured and analyzed.

The results of the exhaust gas emission analysis show that the exhaust gases have a low content of unburned combustion products, i. e., hydrocarbons and carbon monoxide, down to idle power due to the high combustion efficiency of this engine. The combustion efficiency is 99.5 percent at idle and 99.9 percent above 10 percent of maximum-rated power. The smoke numbers of the PLT 27 engine are extremely low. No visible smoke was produced at any power setting with any of the injector systems tested. The PLT 27 engine meets the exhaust gas emission standards set by the EPA for 1979 for fixed-wing aircraft.

DD FORM 1 JAN 73 1473 EDITION OF 1 NOV 65 IS OBSOLETE

Unclassified

SECURITY CLASSIFICATION OF THIS PAGE (When Data Entered)

20. ABSTRACT (Continued)

The near-field and far-field noise emissions were determined. The emitted sound pressure levels were compared with the noise emission criteria established by the U.S. Army for advanced turboshaft engines. This comparison shows that the PLT 27 as a bare engine without inlet particle separator satisfies these criteria with a few exceptions in particular frequency bands. The overall near-field sound pressure level is 104.5 dBA, and the far-field (200-feet) sound pressure level is 90 dBA at 2000 shaft horsepower.

TABLE OF CONTENTS

LIST OF ILLUSTRATIONS

LIST OF TABLES

INTRODUCTION

GENERAL

The general objective of the work completed under this contract was to provide smoke, invisible exhaust gas, and noise level information for an advanced gas turbine engine in the medium-power class in order to facilitate the categorization of these engines with respect to these emission characteristics. Advanced gas turbines are characterized by a high compressor pressure ratio and high turbine inlet temperature.

This report, comprising two major subsections, describes the measurement and analysis the exhaust gas emissions and the noise emission levels from a Lycoming PLT 27 gas turbine engine, which is an advanced technology turboshaft engine of 2000 shaft horsepower.

The first section discusses the measurement of the contents of carbon monoxide (CO), carbon dioxide (CO_2), hydrocarbon (C_nH_m), nitric oxide (NO), total oxides of nitrogen (NO_x), and smoke in the engine exhaust gas for three different fuel injector configurations used in the engine.

The measured exhaust gas data have been recorded, reduced, and analyzed according to the methods described in SAE ARP 1256 and ARP 1179. The emission indices are presented as functions of the fuel-air ratio and engine power output and are also related to the combustor operating conditions to show trends and relationships between the emission components and combustor performance and the fuel injection systems. The combustor efficiency and the fuel-air ratio have been determined by carbon-balance procedures.

The second section describes the measurement and analysis of the engine noise emission characteristics. Far-field noise data were taken at the Lycoming noise test facility at radial distances of 200 and 100 feet and at a near-field point (10 feet). To obtain a complete picture of the acoustical characteristics of the engine, both a 1/3-octave band spectrum level and a narrow-band 40-Hz bandwidth spectrum analysis were performed. Directivity plots of the sound pressure level are presented for various engine power outputs. The narrow-band analysis identifies individual noise sources of the engine.

ENGINE DESCRIPTION

The PLT 27 turboshaft engine (Figure 1) has a nominal power output of 2000 shaft horsepower.

Output power is produced by a two-stage free-power turbine driven by the exhaust gases of the gas generator. The power takeoff connection is located at the front of the engine.

The engine intake airflow at the design point is 12.5 pounds per second. The overall compression ratio is 16:1.

The gas generator consists of a tandem arrangement of a low- and a high-pressure compressor, an annular reverse-flow atomizing combustor, and a high- and low-pressure turbine driving the high- and low-pressure compressor, respectively, through a pair of concentric shafts.

The low-pressure spool consists of a five-stage axial compressor with variable inlet guide vanes, single-stage turbine, and the drive shaft. The high-pressure spool is made up of a four-stage axial/single-stage centrifugal compressor, a single-stage turbine, and drive shaft. The two spools are mechanically independent. Their speed relationship is established by the aerothermodynamic interrelationship between the compressors and turbines.

The reverse-flow, annular type combustor is wrapped around the turbine section. It receives air from the radial diffuser of the high-pressure compressor and ducts the air through two 180-degree turns before discharging it axially into the turbine section. The fuel is injected at the aft end through 16 nozzles. The standard injector used is a Parker-Hannifin air-blast atomizing injector.

To obtain comparative exhaust emission data, the engine was also run with production-type T53-L-13 engine dual-orifice injectors and Delavan air-blast injectors.

Fuel flow to the engine was automatically metered by a hydromechanical fuel control that is driven by the high-pressure spool through the accessory gearbox mounted on top of the engine. The fuel control also positions the variable inlet guide vanes and a compressor bleed valve that bleeds air from the second high-compressor stage to provide proper compressor matching during starting and at low power levels.

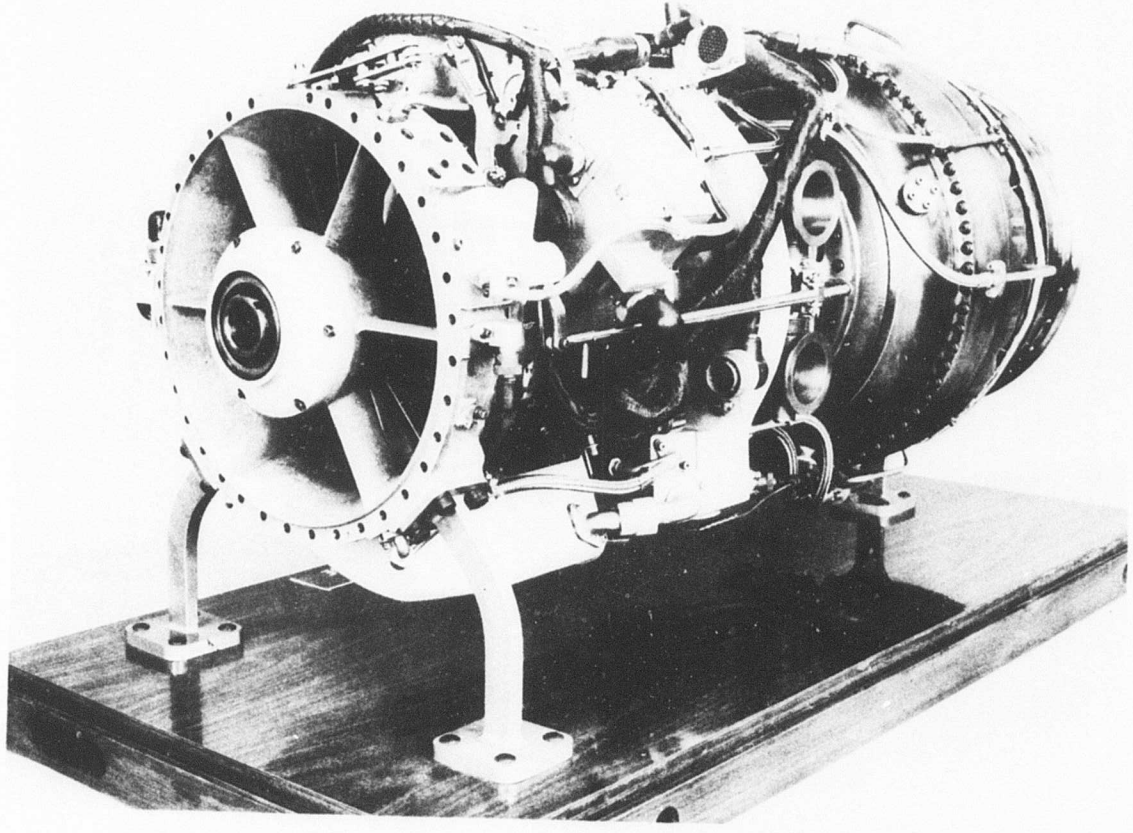

Figure 1. PLT 27 Turboshaft Engine.

ENGINE TEST

Emission Measurement

For the exhaust gas emission measurement, the engine was installed in a development test cell. Prior to the emission measurement test, the engine was subjected to a checkout run to determine its functional, operational, and performance characteristics. All engine testing was performed using MIL-T-5161, Grade 1 (JP-4) fuel and MIL-L-23699 lubricating oils.

The engine was instrumented to measure engine performance, engine condition parameters, and to extract exhaust gas samples from the tailpipe. These gas samples were extracted by two cruciform probes in tandem and ducted to gas sampling equipment.

Output power was absorbed by a waterbrake, which was supported from the engine on four calibrated strain-gaged beams sensing the output torque. The strain-gage signal was converted into engineering units and displayed in inch-pounds on a digital readout.

The engine inlet airflow was measured with a calibrated inlet bellmouth set, consisting of an inner and outer bellmouth. The static pressure was measured with four static probes located around the inner bellmouth surface. A single total-pressure probe was used to measure the total pressure in the inlet airstream. The pressures were indicated on Bourdon tube gages. The relationship between the static and the total pressure yields the engine airflow. The engine compressor bleed airflow was measured with a Meriam laminar airflow meter.

Total pressure and temperature rakes were installed in the engine to measure the low- and high-pressure compressor discharge conditions. The combustor pressure drop was measured by two differential static probes.

Power turbine inlet temperature was measured with the 12-point chromel-alumel engine thermocouple harness indicating the average and local temperature.

The low-spool and power turbine speeds were determined with magnetic pulse generators. The high-spool speed was obtained from the engine alternator. These speed signals were displayed digitally.

Engine fuel flow and oil flows were measured with Cox turbine elements and read digitally. Fuel and oil temperatures were monitored with I. C. thermocouples. The oil reservoir was instrumented to indicate engine oil consumption.

Vibration pickups were installed on the compressor case, air diffuser housing, and power turbine nozzle. Engine vibrations were indicated in terms of displacement and velocity.

Noise Measurement

After completion of the exhaust gas emission measurements, the engine was installed on an adjustable turntable at the Lycoming free-field acoustical test site for noise measurements. This test site is equipped with all the services required for basic engine testing and the acquisition of noise and atmospheric data.

The engine instrumentation was the same as that used for the emission testing; however, fewer performance parameters were recorded.

EXHAUST EMISSION MEASUREMENTS

SUMMARY

A single combustor assembly was tested on the PLT 27 engine over the full power spectrum, using MIL-T-5161 JP-4 fuel. Exhaust gas and smoke samples were analyzed while three different fuel injector configurations were tested:

1. Parker-Hannifin air-blast
2. Parker-Hannifin dual-orifice
3. Delavan air-blast

An analysis of the results showed that the PLT 27 engine produces a high combustion efficiency with all three configurations (approximately 99.9% above 10% of full power). The engine produces essentially zero smoke level with either of the air-blast fuel injectors, and a low smoke number (not in the visible range) with the dual-orifice injector. NO_x production is on the high side of the range of typical gas turbine data. NO_x consisted primarily of NO, with low, scattered values of NO_2. Combustor exit temperature peak values were considerably less with the air-blast injectors than with dual-orifice injection, a strong point in favor of air-blast.

The air-blast injectors produced slightly higher combustion efficiency, and considerably more uniform exhaust gas temperature. Maximum power could not be reached with the dual-orifice injector because the allowable maximum local temperature was exceeded. This problem did not exist for the Parker-Hannifin air-blast injector.

The lowest total emissions when operating in the Army helicopter duty cycle were obtained with the dual-orifice fuel injector. This was caused by its lower contribution of NO_x. However, because of the lower combustor exit peak temperature and lower smoke emissions, the air-blast injectors are attractive. Additional development work is recommended to further develop the low emission capabilities of the air-blast injector.

The results indicate that all of these configurations will meet the EPA 1979 P-2 standard for fixed-wing turboprop engines.

INTRODUCTION

The objective of the exhaust emission measurements portion of this program was to obtain exhaust gas and smoke emission data from a PLT 27 engine with the following combustor manifold configurations:

1. Manifold 1, Parker-Hannifin air-blast fuel injectors, standard PLT 27 injector, Part number PH-6700230.

2. Manifold 2, Parker-Hannifin dual-orifice injectors, Part number 1-300-347-01.

3. Manifold 3, Delavan air-blast injectors, Part number DLN 33033.

4. Repeat of Manifold 1.

The results of the tests were used to define emission levels for the present PLT 27 engine and also to determine which fuel injector configurations offer the best potential for reduced emission in conjunction with the combustor design.

Engine Configuration

The test program was performed using PLT 27 engines P2 and P3 (Figure 2), and testing was performed in one experimental engine test cell at Avco Lycoming. JP-4 referee grade fuel was used throughout the test.

The combustor, with a liner part number 3-131-020X04, serial number 0K001, illustrated in Figures 3 and 4, is a reverse-flow style typical of Avco Lycoming engines. A fuel manifold fastened to the rear side of the combustor housing is easily changed without disturbing the other engine components.

The three fuel injector designs are shown schematically in Figures 5, 6, and 7. The Parker-Hannifin and Delavan air-blast injectors incorporate different schemes for using air to break up and vaporize the fuel. The Parker-Hannifin dual-orifice injector design is more conventional in Avco Lycoming engines, and this particular design has a long record of dependable operation in the T53-L-13 engine model.

The spray quality of the three fuel injectors was checked before and after each group of engine tests to determine if fuel flow at each injector was the same and if the flow spray pattern had changed from start to finish of the tests.

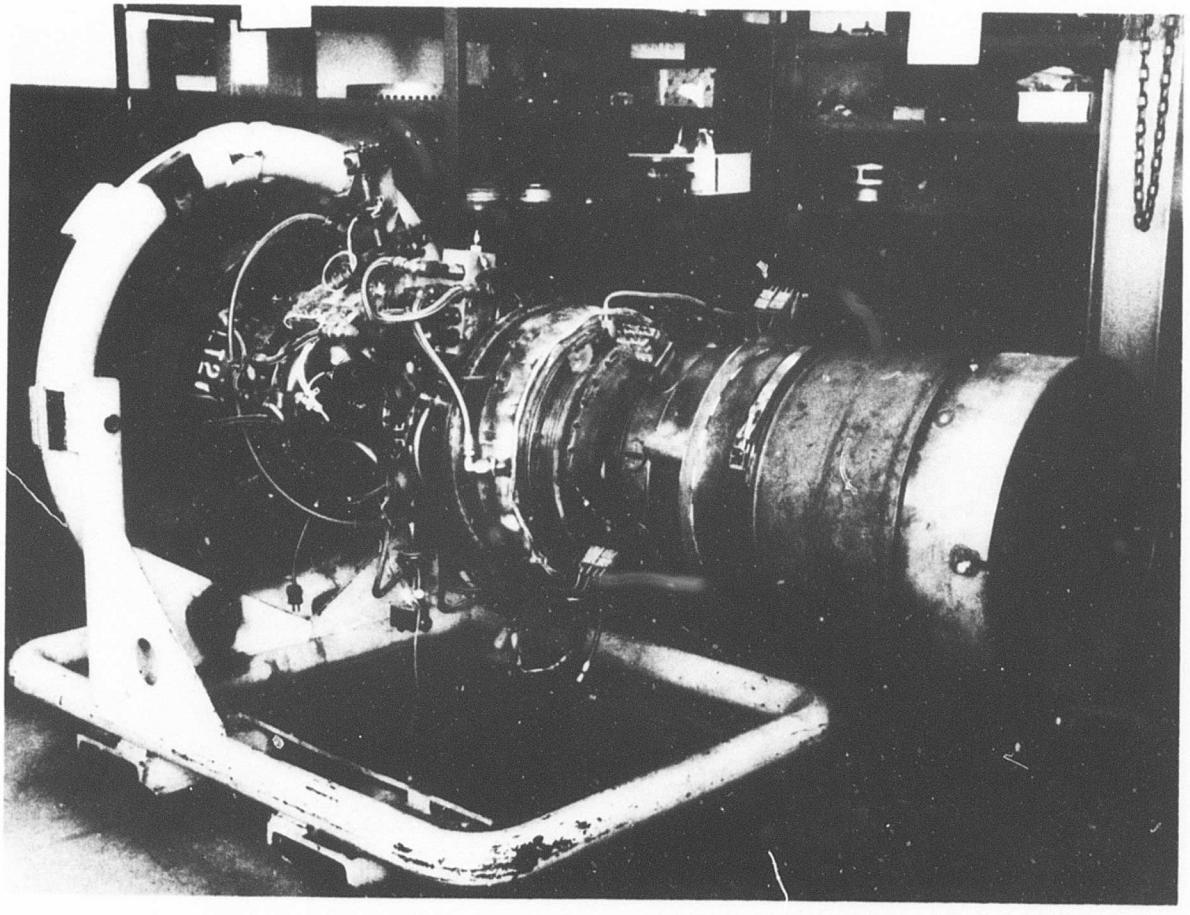

Figure 2. PLT 27 Engine Assembled With Exhaust Sampling Probe Attached.

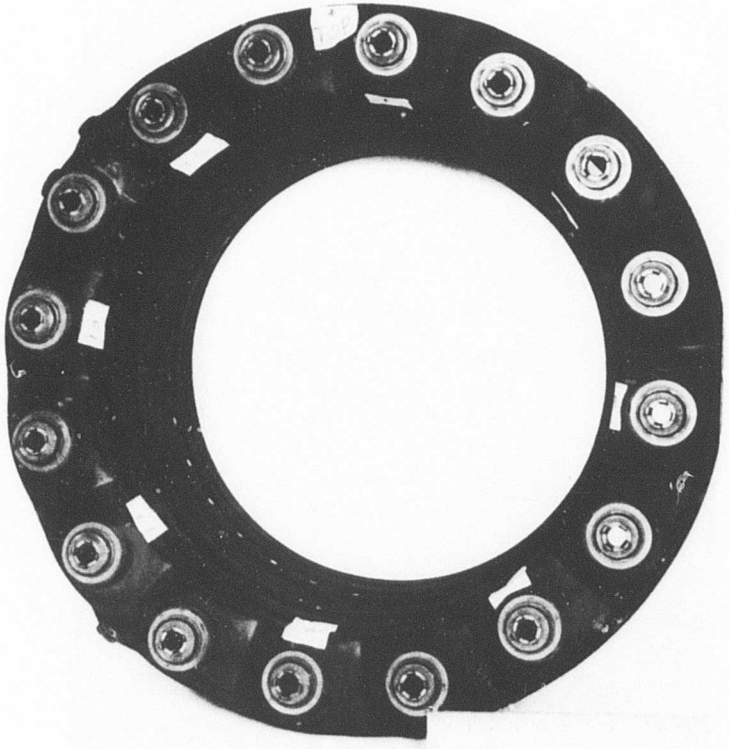

Figure 3. PLT 27 Combustor Liner, Serial 0K001, After Completion of Tests, View Looking Forward.

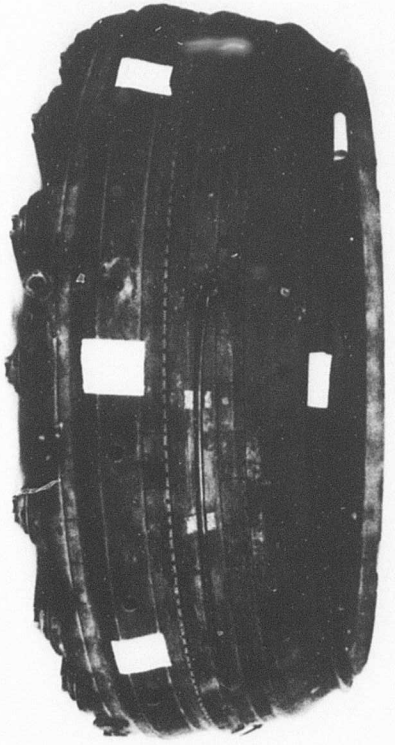

Figure 4. PLT 27 Combustor Liner, Serial 0K001, After Completion of Tests, Side View.

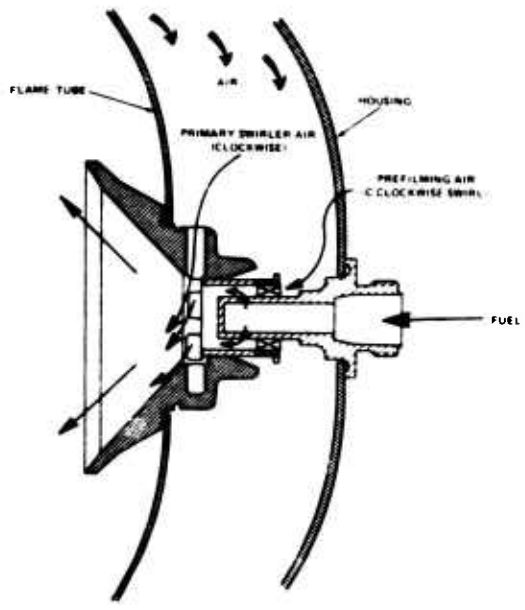

Figure 5. Parker-Hannifin Air-Blast Injector for Manifold 1.

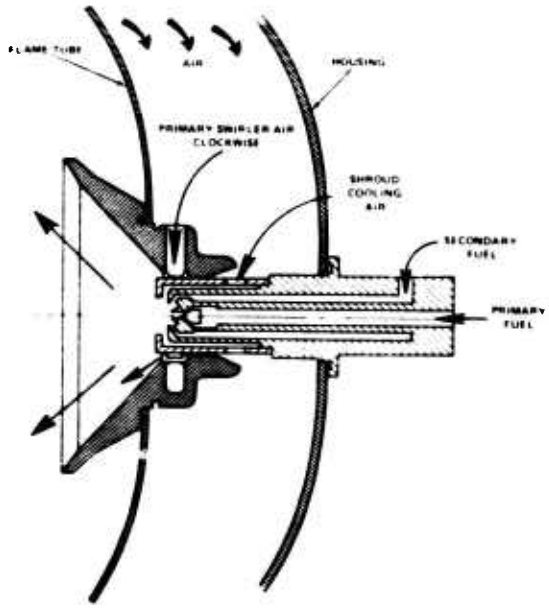

Figure 6. Dual-Orifice Injector for Manifold 2.

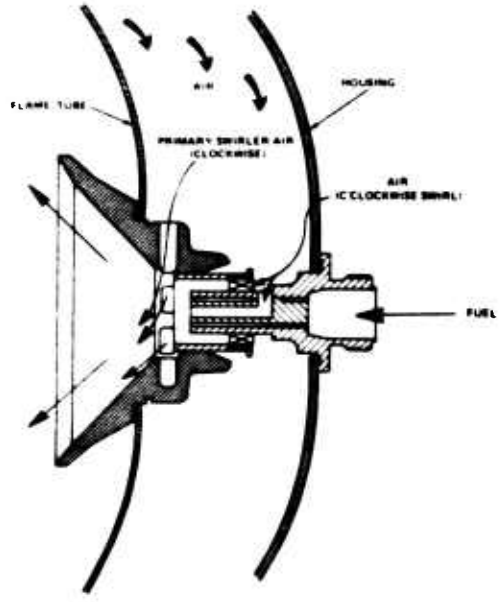

Figure 7. Delavan Air-Blast Fuel Injector for Manifold 3.

Engine Exhaust Gas Measurements

Exhaust gas and smoke samples were acquired with a cruciform configuration averaging-type gas sample probe positioned in the exhaust gas stream (Figure 8). The gas smoke samples were fed directly to the analysis equipment through heated lines. The dimensions of the tubes and sampling ports were based on a similar design used at the Naval Air Propulsion Test Center (References 1 and 2). The smoke probe was installed in tandem with the gas sampling probe approximately 3 inches downstream of the gas sampler and at an angle of 45 degrees to it (Figure 8). A photograph of the installed probe is shown in Figure 9.

The Avco Lycoming on-line exhaust gas analysis system is based on the specifications of SAE ARP 1256 (Reference 3) and SAE ARP 1179 (Reference 4). It consists of detectors for measuring CO, CO_2, unburned hydrocarbons (HC), NO and NO_x, and a filter paper smoke collector. The gas analysis system schematically shown in Figure 10 consists of the following:

1. A high-speed pumping system to transport the sample from the engine to the analyzer

2. A "hot" sampling leg for HC and NO_x analysis, in order to prevent water and HC condensation

3. A "cold" sampling leg for the CO_2, CO, and NO analyzers

4. Calibration valving for a wide range of gas compositions and ranges of measurement

Data were recorded both on strip chart recorders and on punched tape. The punched tape data were converted to cards, and these were used in a program to calculate all desired parameters.

Specific instruments in the system, their ranges, accuracy, and response times are listed in Table 1. A photograph of the console is shown in Figure 11. The equipment and procedures used were similar to those used in previous tests of Avco Lycoming T53-L-13A and T53-L-11A engines as reported in Reference 5.

A special TECO converter was used with the NDIR NO analyzer, so that, by means of conversion of any NO_2 component present to NO, both NO and NO_x could be measured in two passes. However, this converter did

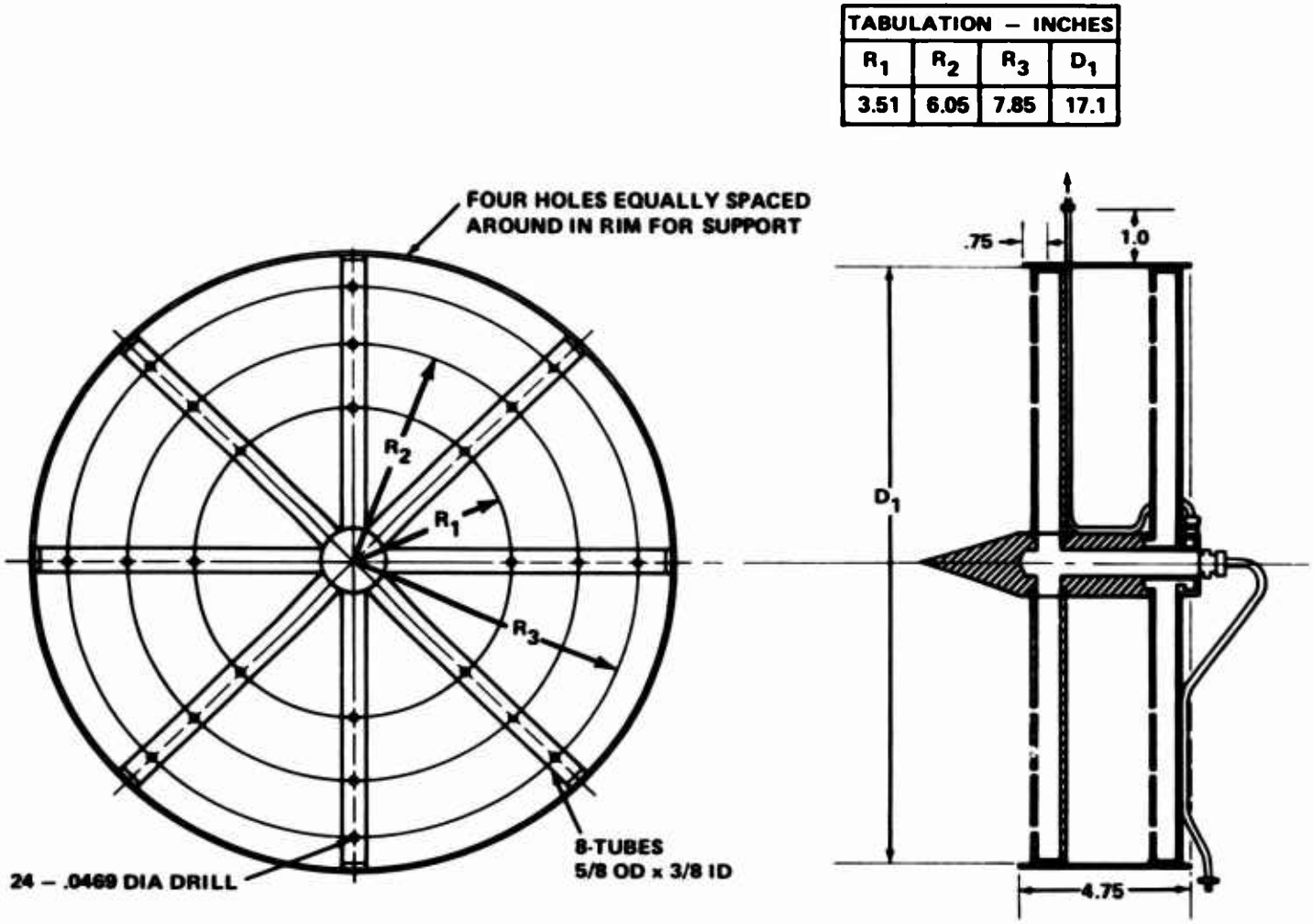

Figure 8. Dual Exhaust Averaging Gas Sampling Probe (Gas and Smoke) for PLT 27 Engine.

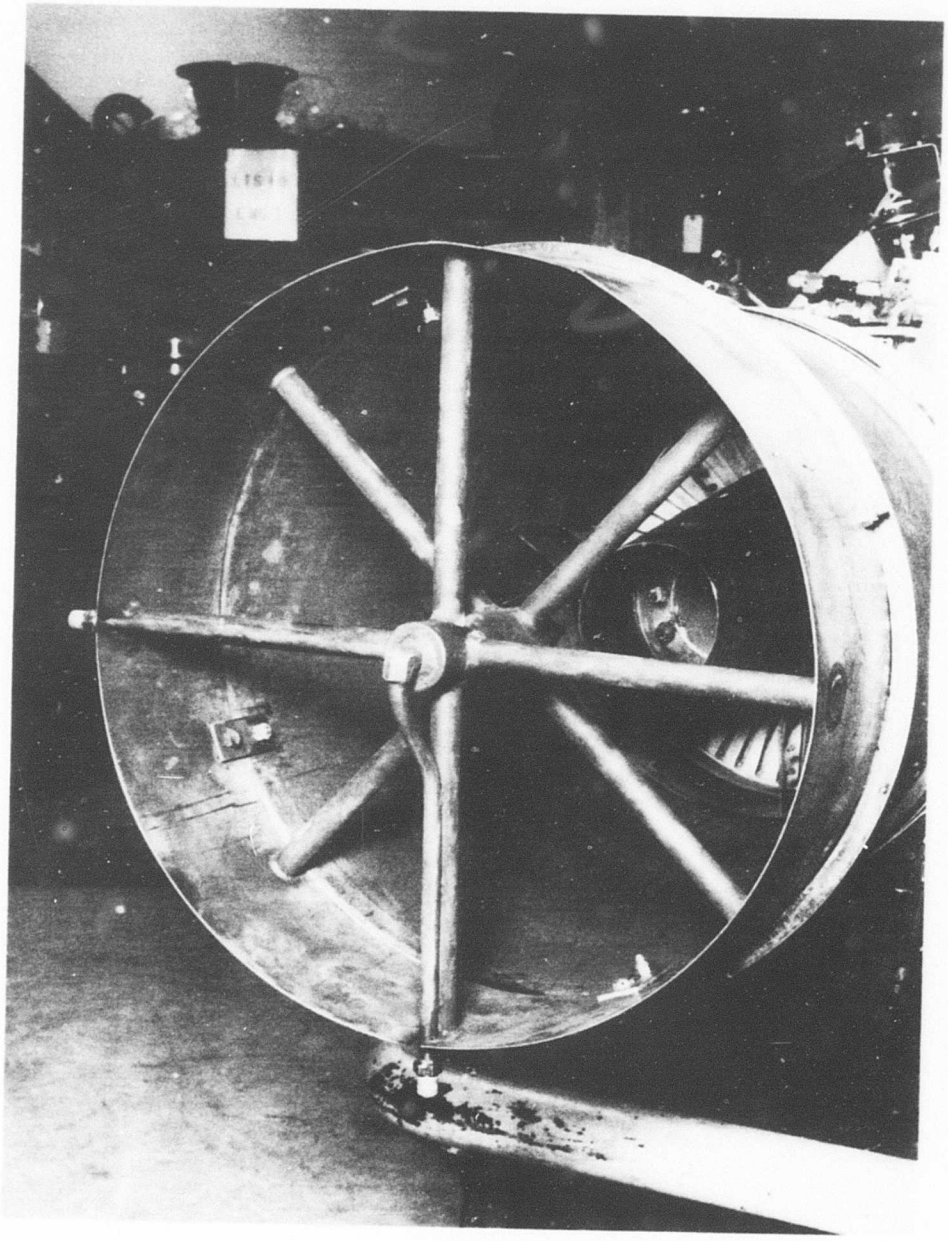

Figure 9. Exhaust Sampling Probe Attached to PLT 27 Engine Tail Pipe.

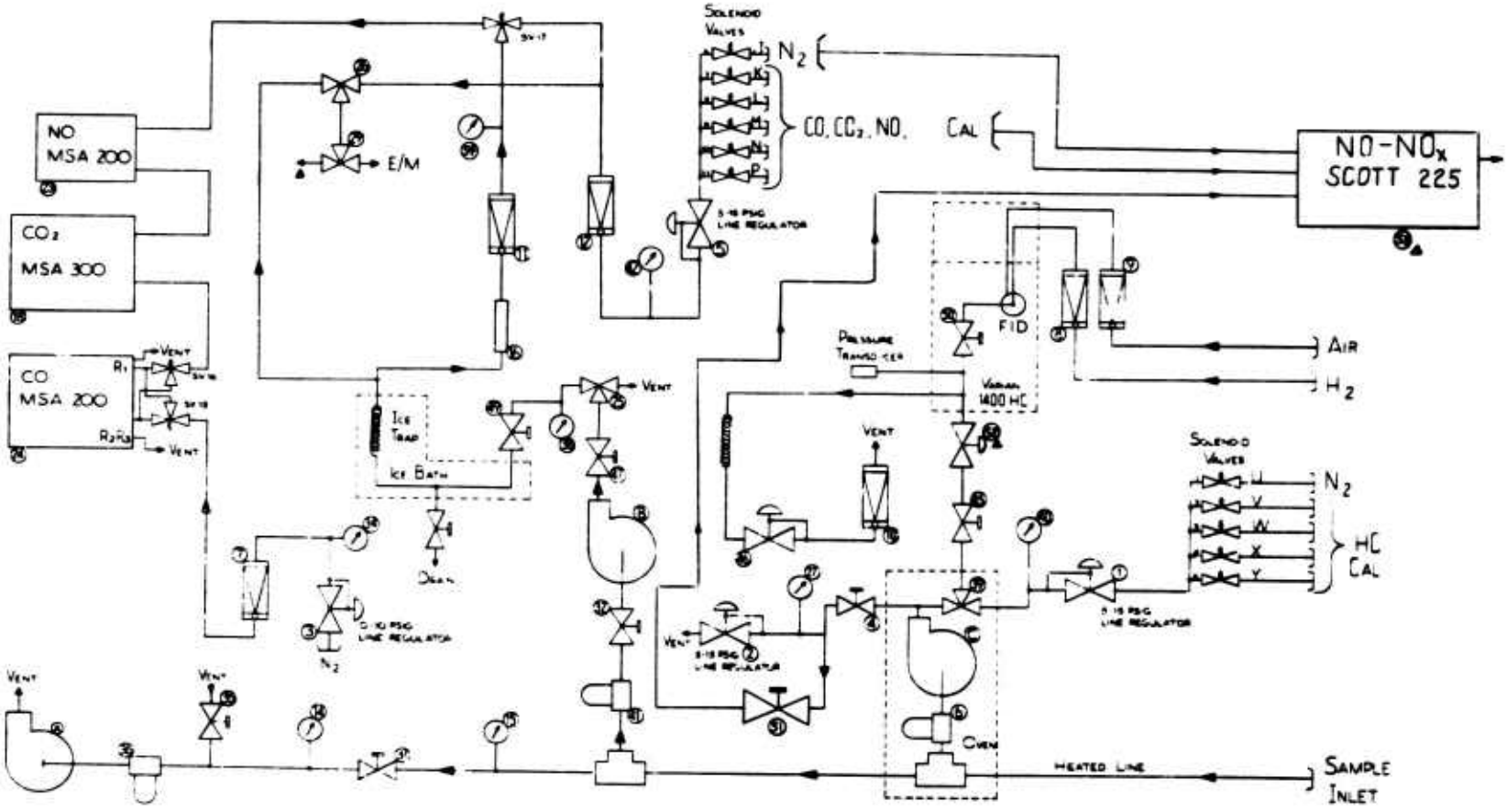

Figure 10. Schematic of Lycoming On-Line Exhaust Gas Analyzer System, DS-16A.

TABLE 1. GAS ANALYSIS DETECTOR COMPONENTS

Gas	Model	Ranges	Full-Scale Accuracy*	Response Time*
Nitric Oxide (NO)	MSA-200S Infrared detector	0-300 ppm 0-1500 ppm	±1%	90% in 5 sec
Carbon Monoxide	MSA-200 Dual tube infrared detector	Tube No. 1 0-200 ppm 0-800 0-3200	±1%	90% in 5 sec
		Tube No. 2 0-5%	±1%	
Carbon Dioxide	MSA-300 Infrared detector	0-8% 0-40%	±1% ±1%	90% in 5 sec
Hydrocarbons	Varian 1400 Flame ionization detector	0-100 ppm to approx. 0-20,000 ppm	±2% in low range ±1% in high range	Approximately 90% in 10 sec
Nitrogen Oxides (NO & NO_x)	Scott-132 Chemiluminescent detector	0-1 ppm to 0-10,000 ppm	±1%	90% in 2 to 4 sec

*Per manufacturer's specifications

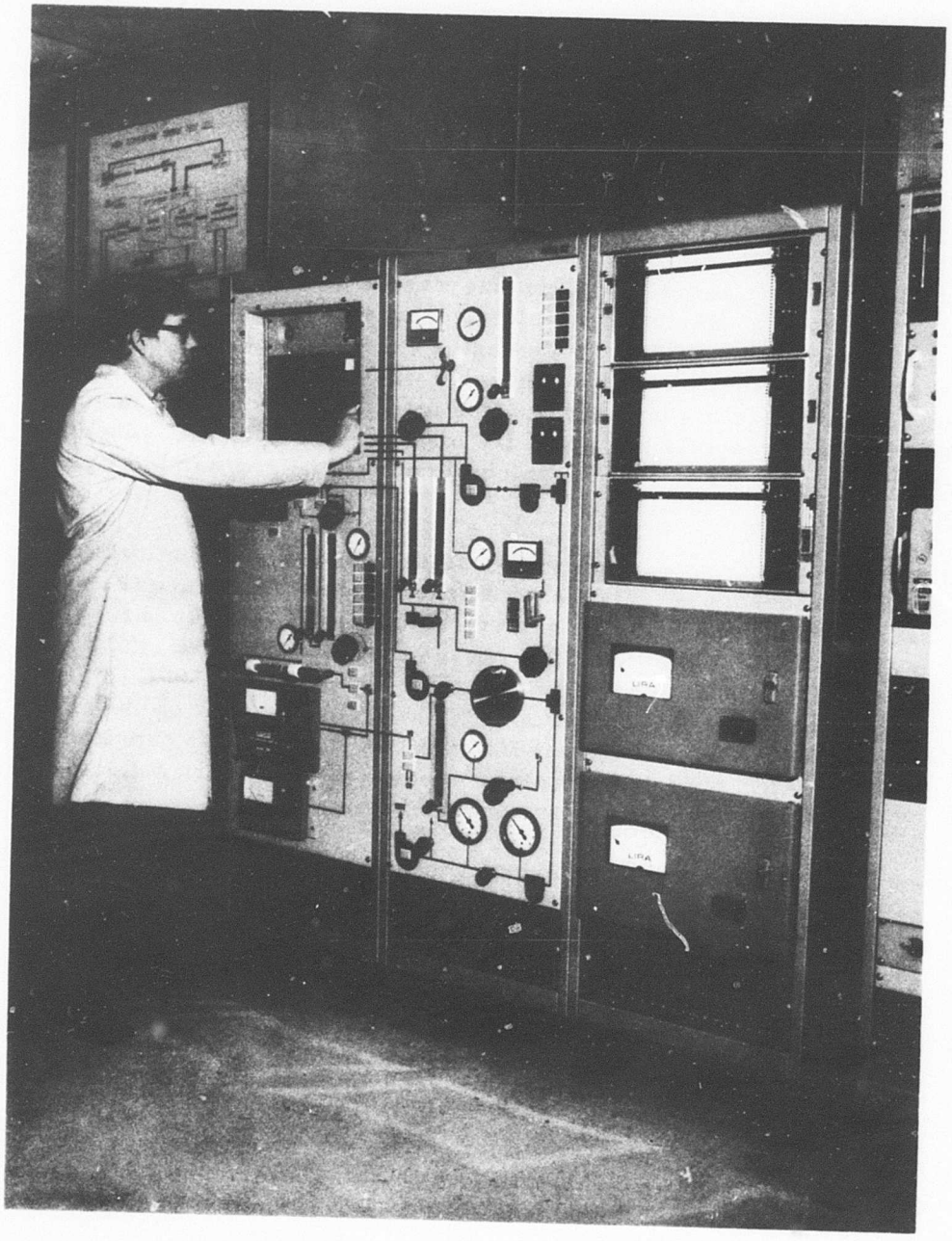

Figure 11. Gas Analysis Console DS-16A Used for PLT 27 Exhaust Gas Measurements.

not prove satisfactory under the existing operating conditions. Data were obtained, however, for NO from two measurements (NDIR and chemiluminescence), and for NO_x from the chemiluminescence detector.

The sample transport lines were 60 feet long and were made of 3/8-inch stainless steel tubing, electrically heated, and insulated with layers of fiberglass and asbestos wool. A temperature controller was installed and set at 300°F ±10.

The velocity of gas in the sampling line was calculated to be 50 to 75 ft/sec under conditions of atmospheric inlet pressure and properly adjusted flows, such as would be found with engine exhaust sampling. Sample pressure drop to the gas analysis console was calculated to be 5 psi, under normal operating conditions. The method of calculation included Fanno line compressible gas pressure loss in a 0.25-inch ID tube with gas temperature held at 300°F, which simulated the gas sample line used.

The Avco Lycoming smoke analyzer was designed to conform to SAE ARP 1179 (Reference 4). It is shown schematically in Figure 12. The analyzer consists of a pumping system which pulls a sample through heated lines, meters the flow, and passes the gas through a standardized filter paper. The sample lines are heated to about 150°F to prevent water condensation. The reflectance of the smoke deposit on the filter paper is measured with a Macbeth Model RD-400 reflecting densitometer (Figure 13). ARP 1179 procedures are followed to convert reflectance from the smoke deposit to AIA smoke number.

The entire system was pressure-checked before and after each test to ensure that the sample lines did not leak.

PROCEDURES

Exhaust Gas Analysis Chemistry

The chemical reaction for a typical hydrocarbon fuel that is not completely reacted is assumed to be as follows (Reference 6):

$$\begin{aligned}
&\emptyset\, C_nH_m + (O_2 + 3.73N_2 + .04A)(n + m/4) \longrightarrow \\
&n\emptyset\left[(1 - a - b)CO_2 + aCO + bCH_{m/n}\right] + \emptyset(m/2)(1 - b)H_2O \\
&+ \left[(n + m/4) - \emptyset\,(n\left[1 - a/2 - b\right] + \left[m/4\right]\left[1 - b\right])O_2\right. \\
&+ \left[.04A + 3.73N_2\right](n + m/4) \qquad (1)
\end{aligned}$$

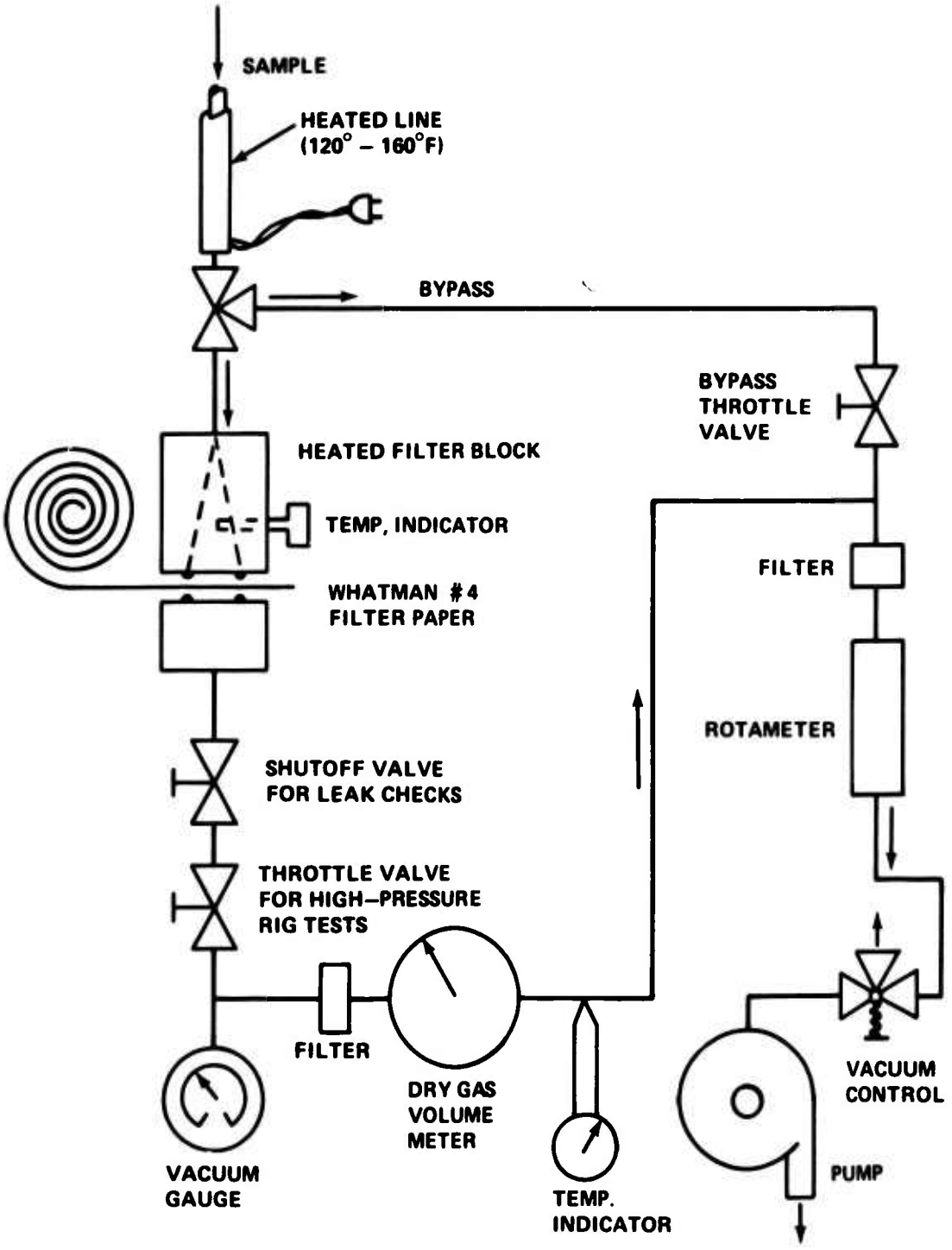

Figure 12. Schematic of the Lycoming Stained Filter Paper Smoke Analyzer.

a. Reflecting Densitometer - Zero Calibration.

b. Reflecting Densitometer Smoke Spot Measurement.

Figure 13. Method of Measuring Smoke Deposit Reflectance With Reflecting Densitometer, Macbeth RD-400.

where

$$a = \frac{CO}{CO_2 + CO + CH_{m/n}} \quad (2)$$

$$b = \frac{CH_{m/n}}{CO_2 + CO + CH_{m/n}} \quad (3)$$

and CO, CO_2, and $CH_{m/n}$ are measured volume fractions on a dry basis.

The hydrocarbon product, $CH_{m/n}$, is used because the flame ionization detector measures effective carbon atoms.

It is assumed that unburned hydrocarbons remain as a combination of C-H atoms, and that the only other unburned component is CO. Smoke or carbon particles are not considered. Hydrogen is present in such small quantities at high combustion efficiency levels that its effect on combustion efficiency is assumed to be negligible (Reference 7).

Point equivalence ratio can then be calculated from Equation (1) from a knowledge of the CO, CO_2, and unburned hydrocarbons ($CH_{m/n}$) on a dry basis

$$\phi = \frac{4.77(1 + m/4n)}{1/(CO + CO_2 + CH_{m/n}) - a/2 - b(1 + m/4n) + m/4n} \quad (4)$$

The stoichiometric F/A for any hydrocarbon fuel may be calculated from Equation (1):

$$(F/A)_{stoich.} \equiv \frac{(12)n + m}{(n + m/4)(32 + 3.73 \times 28 + .04 \times 40)} \quad (5)$$

where

approximate molecular weights of C, O_2, N_2, and A are 12, 32, 28, and 40, respectively. For a JP-4R fuel used at Lycoming, n = 7.82; m = 13.76; and $(F/A)_{stoich.}$ can be calculated to be 0.0692. The atomic proportions of hydrogen and carbon are average values from an analysis of the fuel*. The F/A can then

*The Federal Environmental Protection Agency specifies a factor "a" to represent the hydrogen-carbon ratio in the fuel.

be calculated from equivalence ratio:

$$F/A = (F/A)_{stoich.}\ \phi \tag{6}$$

Combustion efficiency for fuel can be determined from equivalence ratio and a measure of the total unburned components, CO and $CH_{m/n}$. This equation is valid for all lean mixtures, and for rich mixtures at low values of η_b where some oxygen is still unused:

$$\eta_{b\ fuel} = 1 - \left[\frac{\left(W_{CH_{m/n}} + \left[\frac{\Delta H(CO)}{\Delta H(fuel)}\right] W_{CO}\right) \Big/ \left(W_a + W_f\right)}{W_f/(W_a + W_f)}\right] \tag{7}$$

where

$$\frac{W_{CH_{m/n}}}{W_a + W_f} = \text{Mass concentration of unburned fuel in the exhaust gas}$$

$$\frac{\left[\frac{\Delta H(CO)}{\Delta H(fuel)}\right] W_{CO}}{W_a + W_f} = \text{Mass CO equivalent to heating value of fuel in the exhaust gas}$$

$$W_f/(W_a + W_f) = \text{Total fuel/gas ratio} = 1/(W_a/W_f + 1)$$

For the fuels used in these tests, a mean value of $\frac{\Delta H(CO)}{\Delta H(fuel)}$

$$= \frac{4,343}{18,702} = .232.$$

For the data reduction used in the work reported here, Equation 4 was used to calculate equivalence ratio, Equations 5 and 6 to calculate F/A, and Equation 7 to calculate combustion efficiency. Periodic bomb calorimeter tests for lower heating value of the JP-4(referee grade) fuel indicate a range of 18,300 to 18,700 Btu/lb. The value used in Equation (7) was 18,400 Btu/lb. The heat of combustion of CO was obtained from Reference 8.

Calculation Programs

Calculation programs were available for:

1. Engine data, where data recorded from engine instrumentation during the test are used to calculate fuel flow, airflow, and other engine parameters.

2. Gas analysis data, where instrument calibration and output signals are converted to ppm, lb/1000 lb fuel, F/A, and combustion efficiency (Reference 9).

Engine Test Instrument Calibrations

Instrumentation used to measure the engine performance is calibrated in accordance with "Measurements and Test Equipment Calibration Systems" standard (Reference 10). This standard operating procedure for instrument calibrations was also written to conform to MIL-45662-A (Reference 11).

Gas Analyzer Calibration

The Lycoming gas analyzer system comprises the detectors listed in Table 1. Calibration curves were supplied by the manufacturer for the infrared analyzers (CO, CO_2, and NO). For each test, a calibration gas was used to set the electrical output for each instrument at a range convenient to read on the chart recorder.

The flame ionization detector (FID), used to measure total hydrocarbons, was calibrated on two ranges, a factor of 10 apart. The calibration curve of this instrument appears linear. Data in reports from the manufacturer also show linearity (Reference 12).

The calibration procedures recommended in ARP 1256 (Reference 3) were followed as closely as practicable.

Smoke Meter Calibration

The smoke meter contains a flowmeter, pressure gages, and thermocouples. These undergo periodic calibration to ensure proper operation. No calibrations are required for each test. However, the smoke meter and the entire sample line were pressure-checked before and after each test. Leakage would dilute the sample and produce an erroneously low smoke number.

Engine Test Procedures

Initial functional engine tests were completed for calibration purposes and to check out the installation and equipment prior to testing each manifold.

After completion of the functional tests, an initial low-power engine test was performed in order to select two power level points between "idle" and 30% power which would be useful in plotting data and determining the loci of points in the sharp bend normally found in gas turbine emissions data. The fuel flows for the two in-between points were approximately the same for all three fuel injector configurations, as follows:

Power	Approximate Fuel Flow (pph)
Idle	110
Intermediate 1	130
Intermediate 2	200
30%	400
60%	630
75%	740
100%	950

For emission tests covering the full range of engine operation, the engine was operated from the specified idle condition, increasing the power in steps up to full power, then back down to idle. This was repeated. Approximately 5 minutes was required to stabilize the engine operation at each power level and record the data. Both gas samples and smoke samples were recorded simultaneously with the double cruciform probe.

Gas samples were recorded when composition was observed to stabilize on the chart recorders. Instrument calibration checks were recorded normally before the test, after one power cycle, and at the end of the second power cycle.

DISCUSSION OF DATA AND RESULTS

An explanation of the precision of our measurements is justified in order to judge the value of the results. Precision of results can be divided as follows:

1. Measurement precision of the instruments only.

2. Correlation of gas analysis measurement with fuel-air calculations by other means (fuel and airflow measurements).

3. Effect of measurement precision on emission determination.

Instrument Precision

Instrument precision specified by the manufacturers is shown in Table 2. The specifications here can be judged to be as close to reality as is possible if the instruments are carefully maintained, calibrated, and checked, and if calibration curves are indeed correct. However, as noted in Reference 5, accuracy propounded by the manufacturer cannot always be maintained. As a result of these experiences, it would seem more reasonable to expect dependable accuracies of the order of ±3 to 4 percent of full scale rather than 1 percent (Table 2). These values of accuracy (Table 2) represent a "best" and a "realistic" view of accuracy of gas analysis. The effect of these error quantities on the emission measurements is reviewed in the following.

Correlation of F/A (Gas Analysis) With F/A (Measurements)

In considering the precision of gas analysis discussed here, two completely independent methods of F/A measurement - (1) gas analysis and (2) engine fuel and air metering - may be compared. Engine fuel flows were measured directly, and engine airflow was determined from the inlet bellmouth calibration. The F/A correlation can be taken as a measure of just how representative are the emission concentrations if it is assumed that the gases are all mixed in the same proportion and that there is no selective momentum separation of exhaust gas components. These are thought to be reasonable assumptions.

This type of fuel-air ratio correlation data is plotted in Figures 14 through 18 for Manifolds 1, 2, and 3, and repeat of Manifold 1. We note at the outset that all of the data lie within the 10 percent margin, and well within the ARP 1256 specification of 15 percent. Except for low-power bleed-open points, nearly all of the F/A data agree within 3 to 4%. An indication of the quantity of air ejected at the compressor bleed at low power is shown in these figures. This quantity was separately measured to be 10 to 18% during idle. It is known that the bypass control closes gradually as power increases and does not suddenly shut off the bleed. This is substantiated by the exhaust gas analysis, within the data accuracy.

TABLE 2. OPTIMUM AND EXPERIMENTAL GAS SAMPLE MEASUREMENT PRECISION

	Manufacturer's Specification* (%)	Root Mean Square, Optimum Error (%)	Maximum Experimental Error (%)	Root Mean Square, Experimental Error (%)
Instrument Zero Drift	±1		±1 to 5	1 25
Instrument Span Shift	±1		±1 to 5	1 25
Calibration Bottle Accuracy	±1**		±2	4 4
Cumulative Error	±3	±1.7	±4 to 12	±2.5 to 7.3

*Percent of Full Scale

**Calibration Bottles are Obtainable for ±1% Accuracy

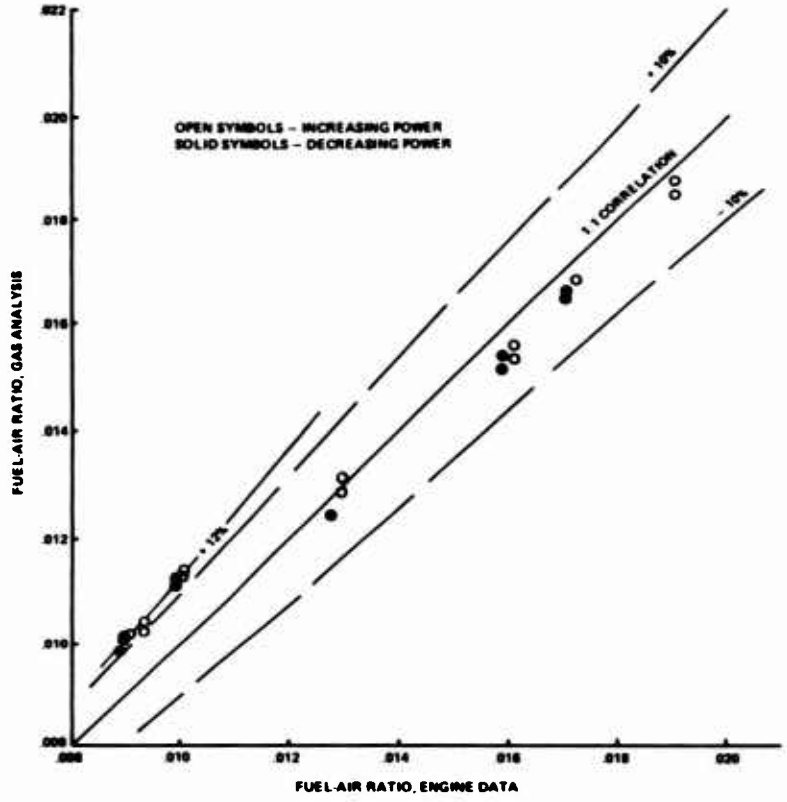

Figure 14. Comparison of Fuel-Air Ratio, Engine Data With Fuel-Air Ratio, Gas Analysis for Engine P2-J, Manifold 1.

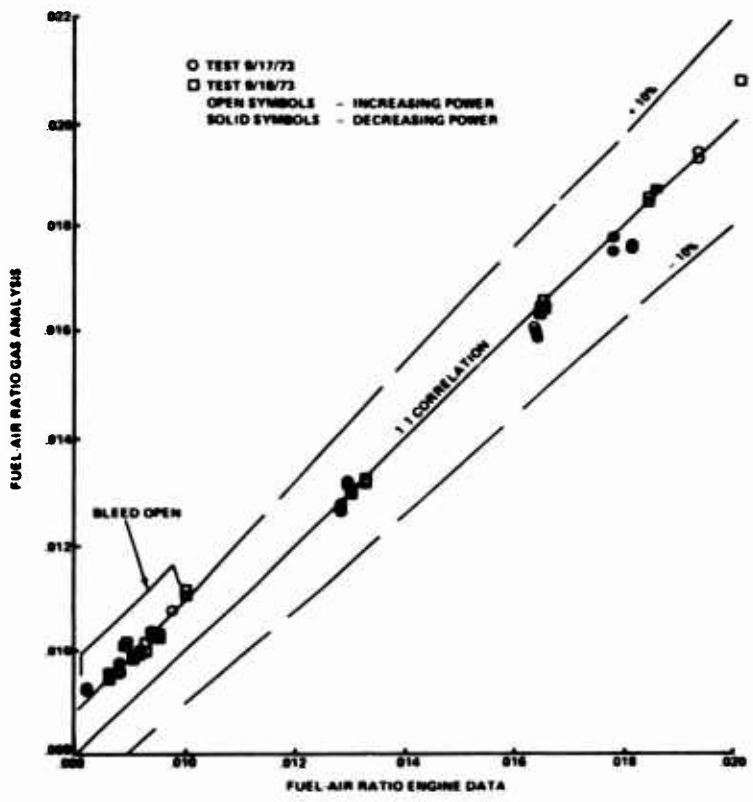

Figure 15. Comparison of Fuel-Air Ratio, Engine Data With Fuel-Air Ratio, Gas Analysis for Engine P2-J, Manifold 2.

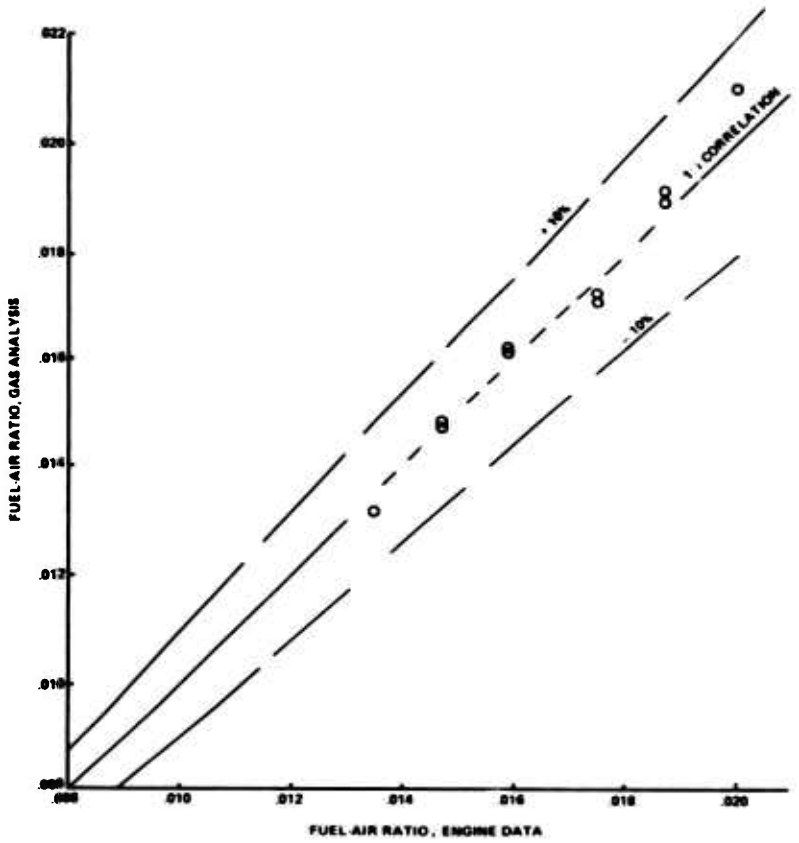

Figure 16. Comparison of Fuel-Air Ratio, Engine Data With Fuel-Air Ratio, Gas Analysis for Engine P2-K, Manifold 2.

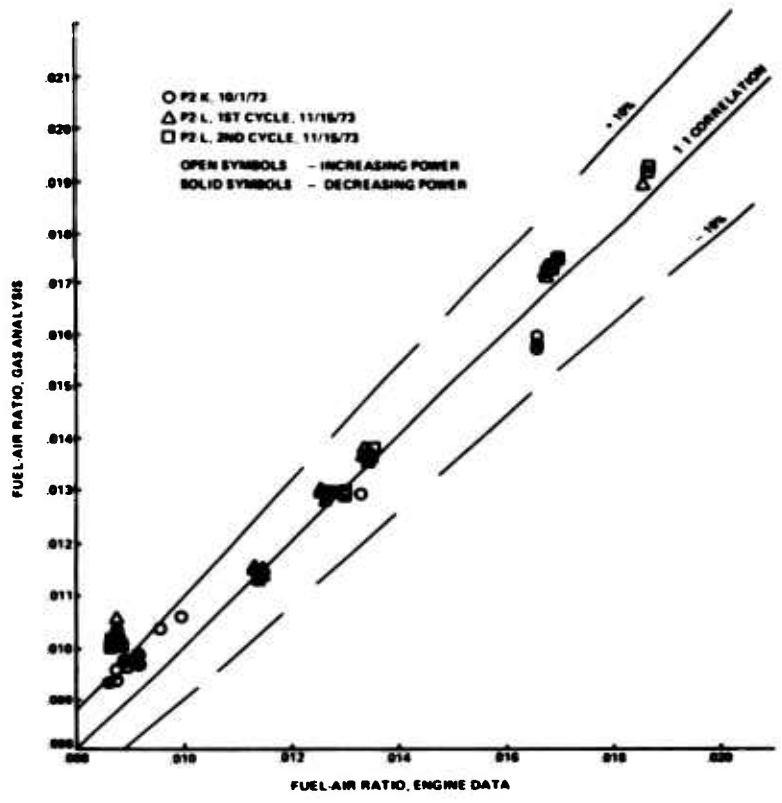

Figure 17. Comparison of Fuel-Air Ratio, Engine Data With Fuel-Air Ratio, Gas Analysis for Engines P2-K and P2-L, Manifold 3.

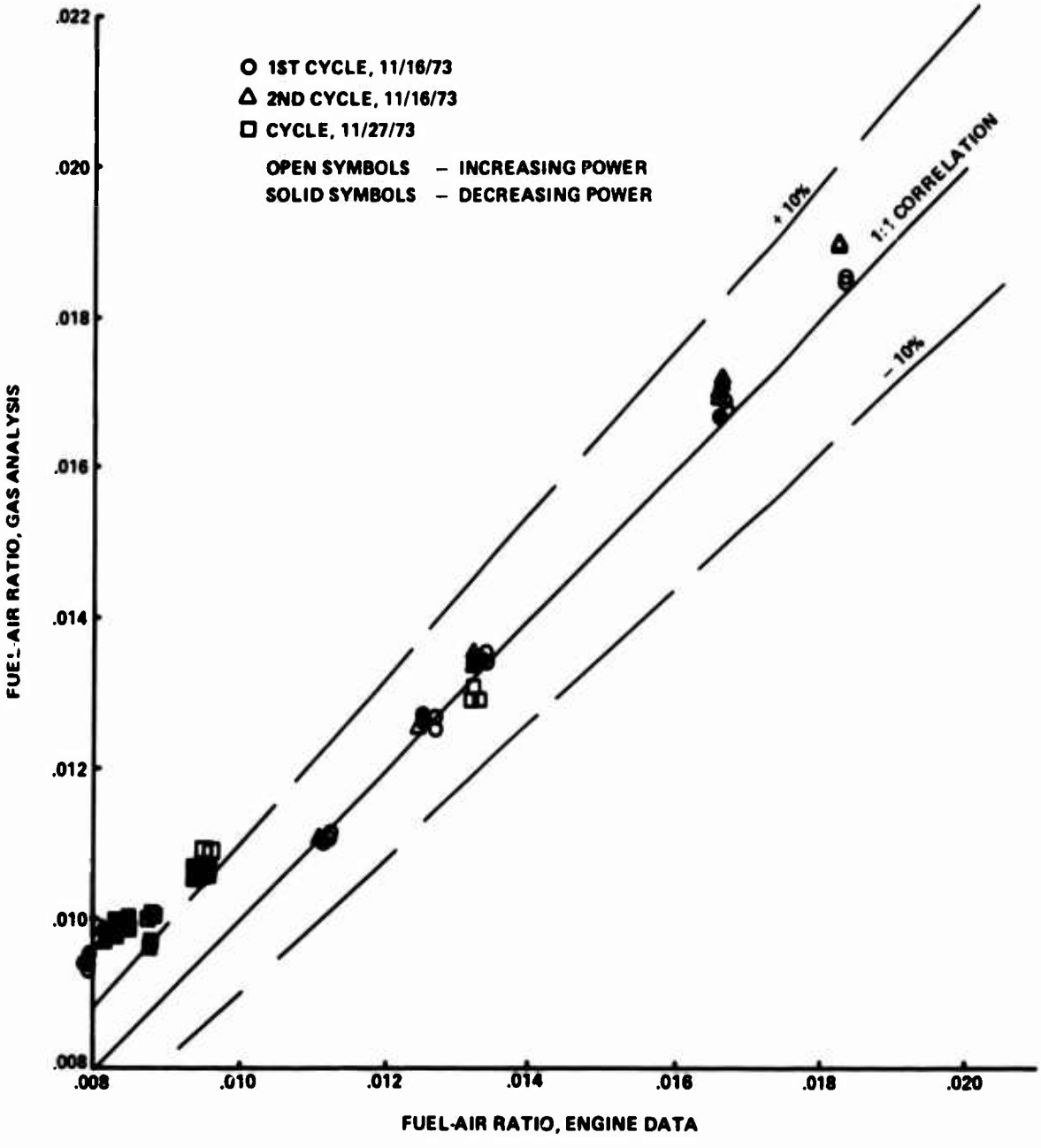

Figure 18. Comparison of Fuel-Air Ratio, Engine Data With Fuel-Air Ratio, Gas Analysis for Engine P2-L, Manifold 1 Repeat (Test 4).

Effect of Measurement Precision on Emission Determination

Good agreement between engine F/A and sampling F/A is evidence that the sample is representative of the engine exhaust and that leaks are negligible. Since the total difference between the two methods of F/A determination is for most cases ± 3 to 4% or less, it follows that the exhaust composition sample accuracy is within 3 to 4%. Therefore, if each gas component is measured by the detecting instrument with equal precision, its accuracy could be better than 3 to 4%. Thus the major source of error will be the individual detectors other than CO_2, specifically, the CO, NO_x, NO, and HC detectors. The problems of measurement of the individual instruments will be discussed as they occur in the analysis of the data.

In addition, 3 to 4% is a relatively small error for most emission measurements. For example, when measuring hydrocarbons in the range of 100 ppmC, an error of 3 to 4 ppmC, the probable limit on sampling accuracy, is just about on the limit of reliable repeatability for the detecting instrument. When measuring in the range of 10 ppmC, with instrument reliability of 3 to 4 ppmC, an error of .3 to .4 ppmC has no significance. Large changes in emission index will become obvious, and our main concern is to find significant improvements in pollution reduction; minute improvements are inconsequential.

A similar evaluation can be applied to CO and NO_x measurement. The principal difference in measuring CO is that, because of its heavier molecular weight, an equal ppm volume produces about twice the emission index value. Likewise, NO_x (as NO_2) produces about three times the emission index value for equal hydrocarbon ppmC.

Analysis of Data

A summary of the tests is shown in Table 3. The data will be discussed first in the following groupings:

Test 1 - Manifold 1 - Parker-Hannifin air-blast fuel injectors

Test 2 - Manifold 2 - T53 dual-orifice fuel injectors, Parker-Hannifin

Test 3 - Manifold 3 - Delavan air-blast injectors

Test 4 - Repeat of Manifold 1

TABLE 3. PLT 27 EMISSIONS TEST SUMMARY

Test Date	Ambient Temp. Humidity (°F/%)	Engine Build	Fuel Manifold	Runs	Comments
8/23/73	-	P2-J	1	19-23	Test to decide on intermediate points. Set at 130 and 200 lb/hr.
8/31/73	83/68 88/70	P2-J	1	36-61	Max. power 1470 and 1478 SHP. At one point there are short term large transients in HC and CO, possibly from exhaust of nearby engines. Sluggish HC response.
9/6/73	-	P2-J	2	62-68	Preliminary test. Intermediate points selected at 150 and 200 lb/hr.
9/17/73	63/40	P2-J	2	84-96	Performance test, one cycle, max. power data at 1651 SHP. Max. power limited by peak T_7. HC response sluggish.
9/18/73	71/67	P2-J	2	97-110	Performance test, one cycle, max. power data at 1654 SHP. Some HC response sluggishness.
9/27/73	70/68	P2-K	2	1-6	Engine rebuilt. Check test. Emission levels similar to previous test. (Some hysteresis shows on HC data.) Max. 1753 SHP permitted.
10/1/73	65/54 69/57	P2-K	3	7-10 11-16	Preliminary test. Engine malfunction above 75% power.
11/15/73	61/65 65/54	P2-L	3	9-11 12-32	Preliminary test (a.m.) Test recorded with 1500 SHP max. Smooth operation. Two complete cycles recorded.
11/16/73	53/49 49/44	P2-L	1	33-54	Repeat test of Manifold 1. Fuel setting similar to 11/15/73 test. Smooth operation throughout range. Two cycles recorded.
11/27/73	52/71	P2-L	1	61-74	Retest of Manifold 1 to fill in lower power fuel points. Idle to 30% and return, twice.
12/14/73	52/83	P3-C	3	7-32	Recheck of emissions with engine P3-C to 2000 SHP. Flow divider used. Two full cycles (0-100%SHP). Oil leak.
12/14/73	52/83	P3-C	3	33-38	Recheck of lower power points with secondary fuel flow only. Oil leak.

Test 5 - Verification of 2000 SHP emission levels in a second engine, Manifold 3

Comparisons of the three manifold configurations will then follow, including comparisons of emissions with Lycoming T53 and T55 engines.

Manifold 1 - Parker-Hannifin Air-Blast Injectors

The precision of data correlated between the F/A from the engine and from gas analysis is shown in Figure 14. At the low-power end, interstage bleed quantity is indicated by the 12% higher airflow entering the engine than leaving the exhaust. The F/A from gas analysis appears lower than the F/A from the engine by as much as 4% in some cases, but yet within the probable experimental error of about 6%, and well within the SAE ARP 1256 stipulated value of 15%. Possible causes are:

1. Sample line leaks.

2. Error in gas analysis, engine fuel flow, or engine airflow.

The sample line was pressure-checked before and after the test. Other possible errors were investigated, but none were found. It was decided to use the data as recorded.

Plots of the HC, CO, and NO_x emissions are shown in Figure 19. We find that the NO_x and CO data are closely grouped, while there is extensive spread in the HC data, with the appearance of "hysteresis" between increasing power and decreasing power of the engine.

The reason for this "hysteresis" was discovered in another concurrent program in time for remedial action to be taken during the test of Manifold 3. It is discussed there.

A comparison of NDIR (MSA) and chemiluminescent (Scott) data for NO is shown in Figure 20. There is a tendency for the chemiluminescence detector to indicate somewhat lower values at low concentrations of NO compared to NDIR. In these cases, the NO_x values from the Scott are very close to the NO from the MSA. At higher concentrations (10 lb/1000 lb fuel and greater), the two instruments agree quite well, and the difference between NO_x and NO (as NO_2) on the Scott is practically zero.

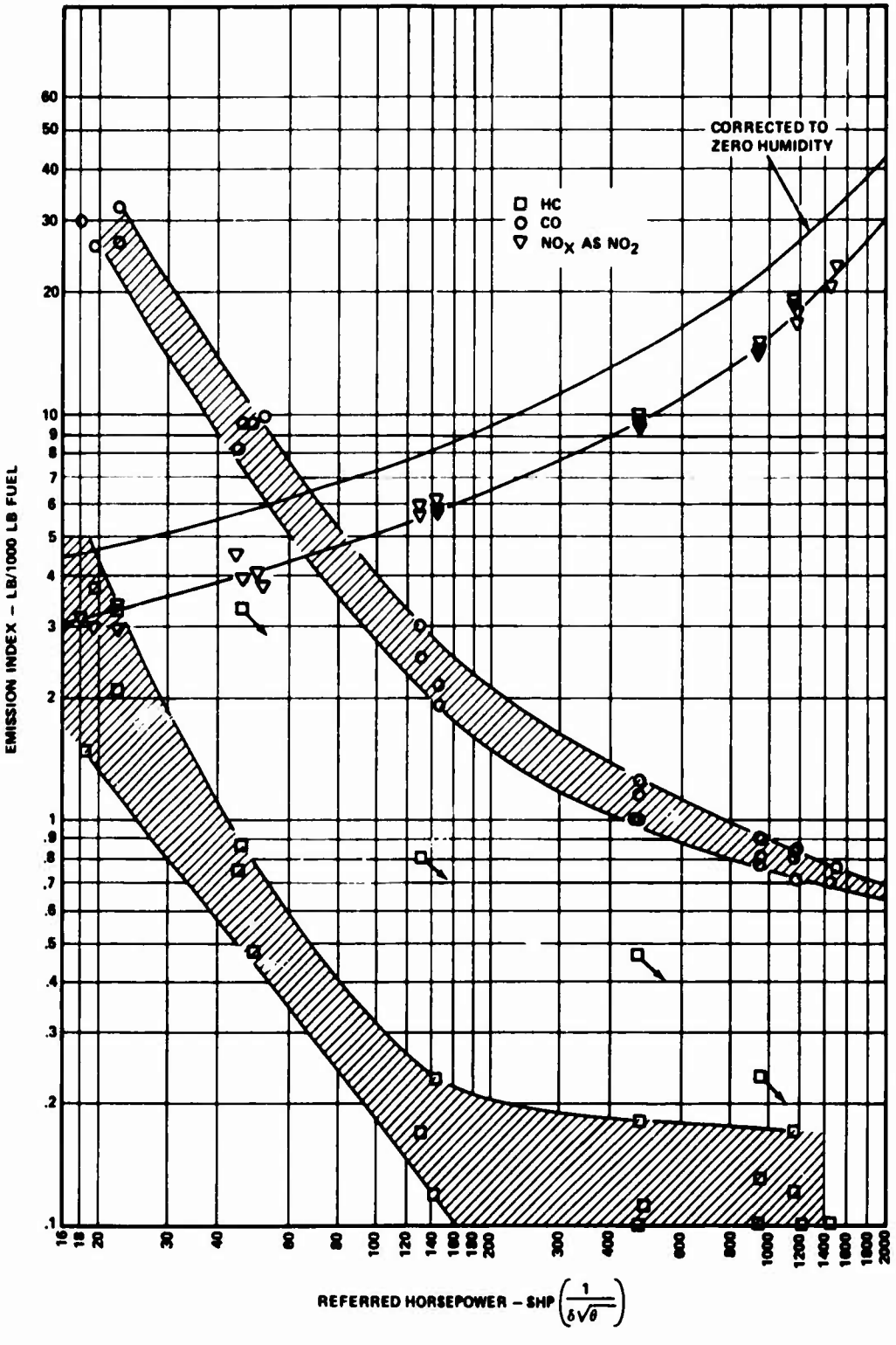

Figure 19. Emission Index Versus Referred Horsepower for Manifold 1 (P-H Air-Blast).

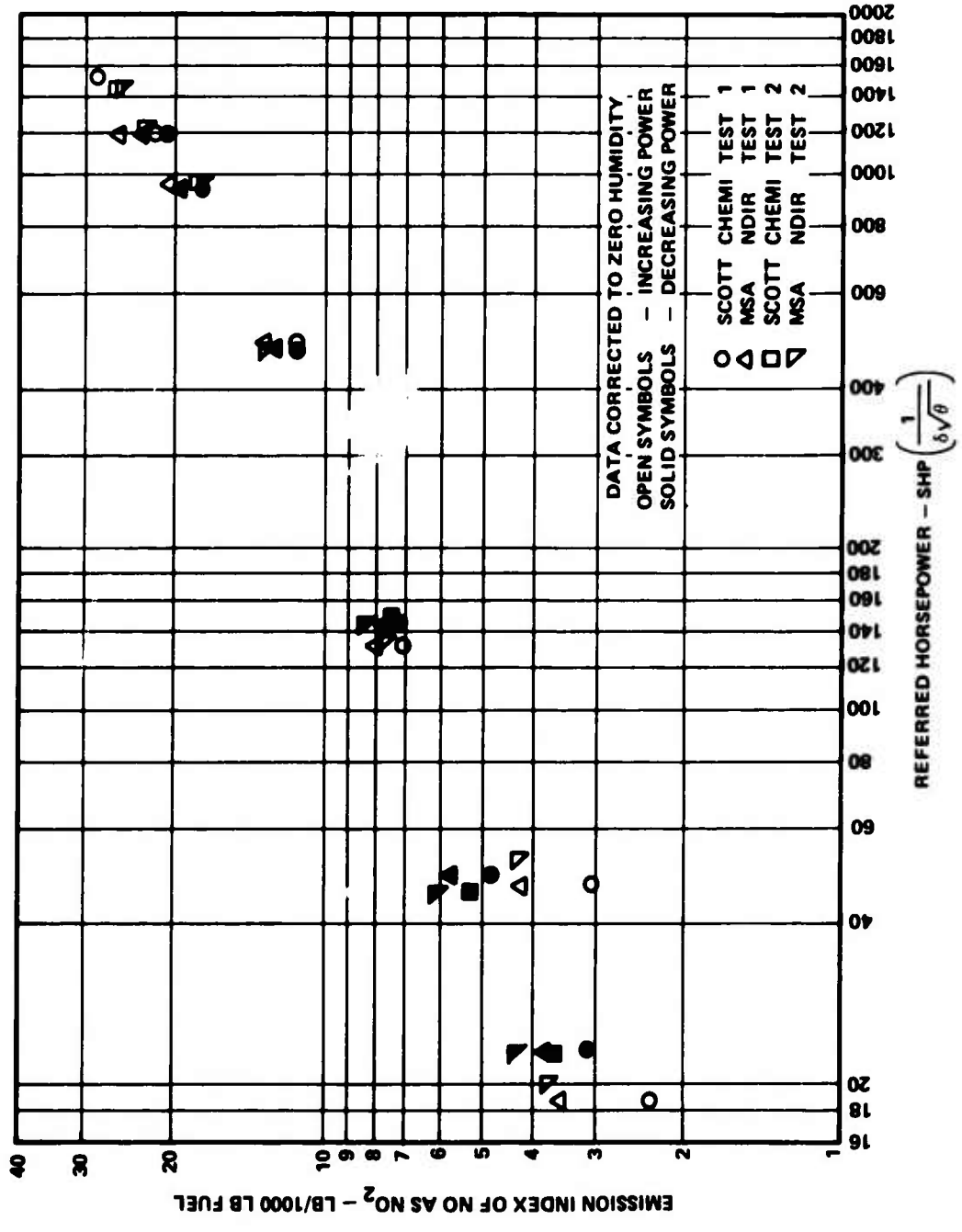

Figure 20. Comparison of MSA and Scott NO Analyzer, Referred Horsepower Versus Emission Index for Manifold 1 (P-H Air-Blast).

A comparison of the NO_x emission index with combustor inlet temperature is shown in Figure 21 and compared to the group of gas turbine data analyzed by Lipfert (Reference 13). The PLT 27 data all lie on the upper edge of the Lipfert band of data. Both NDIR (MSA) and chemiluminescence data (Scott) are plotted. The band width, as a percent of concentration, is nearly constant for the entire range of combustor inlet temperature (T_3).

It is of interest to separate the NO_2 from the NO_x by subtracting the NO from NO_x value, as is done in Figure 22, where NO_2 and NO_x are plotted against referred horsepower. The NO_2 trend appears haphazard, with higher concentrations at low horsepower. No conclusions can be drawn from this plot, except that the NO_2 values may be questionable because we do not know precisely where the NO_2 was formed. Above 100 horsepower, all the concentrations are 3 ppm or less, a value within the expected accuracy of measurement. The data spread at high power is higher than this.

Engine and combustor fuel-air ratio are plotted versus referred horsepower in Figure 23 for the Manifold 1 test. Turbine cooling air that bypasses the combustor was deducted from the engine exhaust air to determine combustor air and compressor bleed air. Engine airflow was measured at the engine bellmouth inlet.

Manifold 2 - Dual-Orifice Fuel Injectors

The correlation of F/A (engine) versus F/A (gas analysis) is shown in Figure 15. Agreement between the two is within 2 to 3%, better than for Manifold 1. The correlation was equally good (Figure 16) after rebuilding the engine (Table 3, test 9/27), when a test was made to determine if the engine rebuild affected the emission level.

Emission levels were remarkably consistent for test on two different days, as shown in Figures 24 and 25. Even the HC "hysteresis" seemed to be reproducible.

A plot of NO_x versus combustor inlet temperature is shown in Figure 26. The data lie in an almost identical position to those from Manifold 1, at the upper edge of the Lipfert data band, and appear to have less scatter.

A plot of the NO_2 values is shown in Figure 27. While the total NO_x values are quite consistent, the NO_2 (difference between NO_x and NO), as measured by the chemiluminescent method, is rather

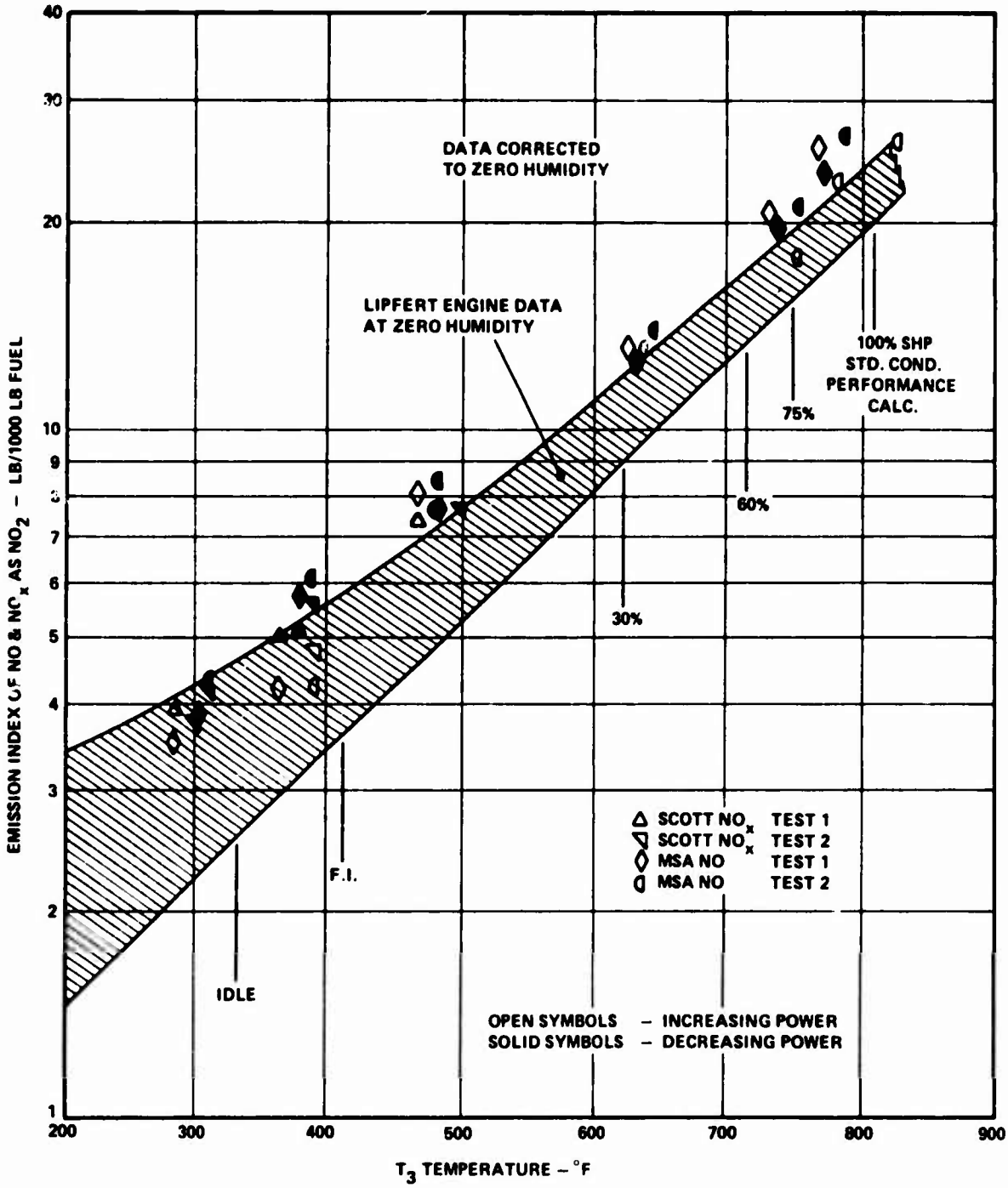

Figure 21. Emission Index of NO and NO_x As NO_2 Versus T_3 Temperature for Manifold 1.

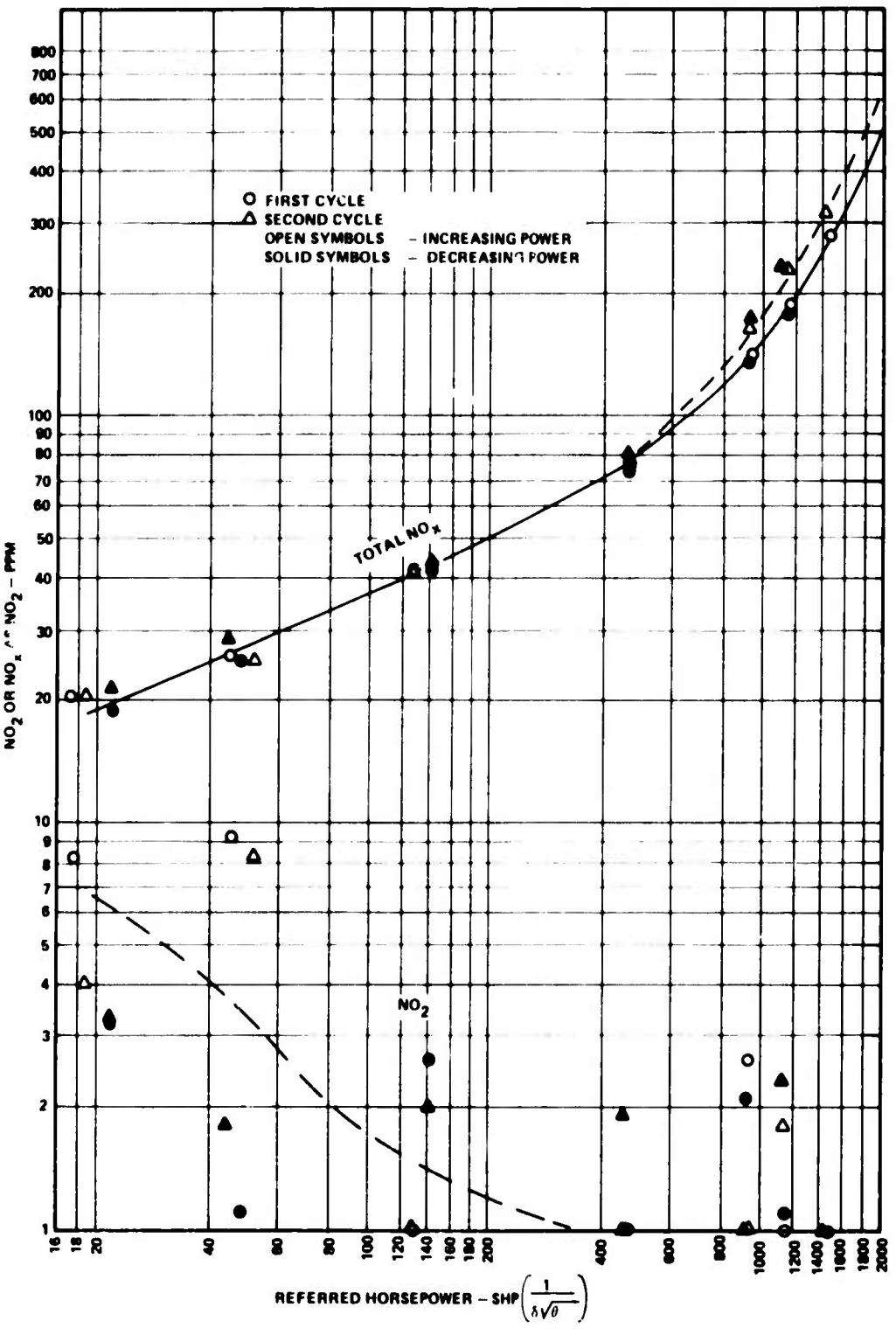

Figure 22. NO_2 or NO_x As NO_2 Versus Referred Horsepower for Engine P2, Manifold 1 (Test 1).

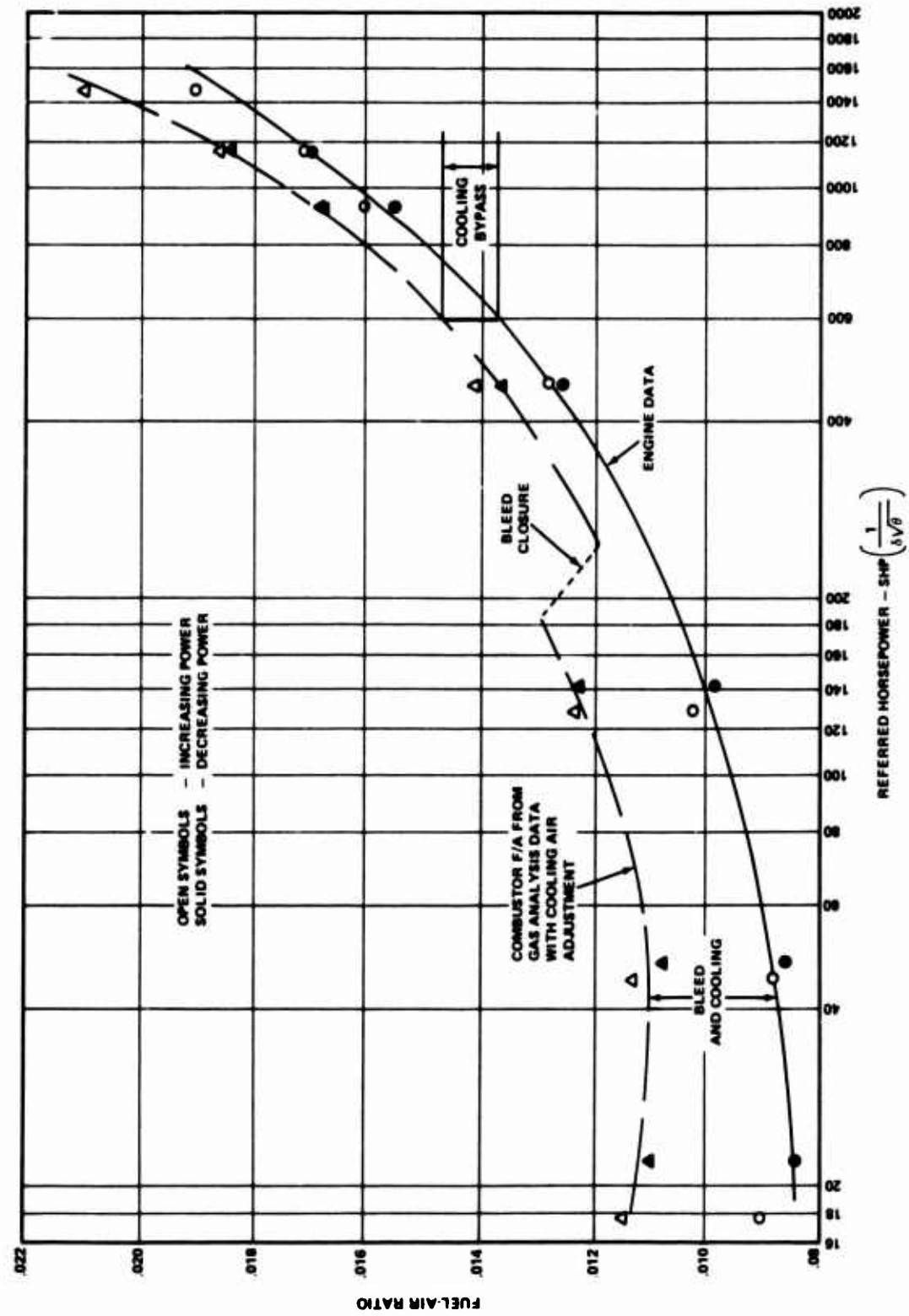

Figure 23. Fuel-Air Ratio Versus Referred Horsepower for Engine Data and Exhaust Gas Analysis for Manifold 1 (Test 1).

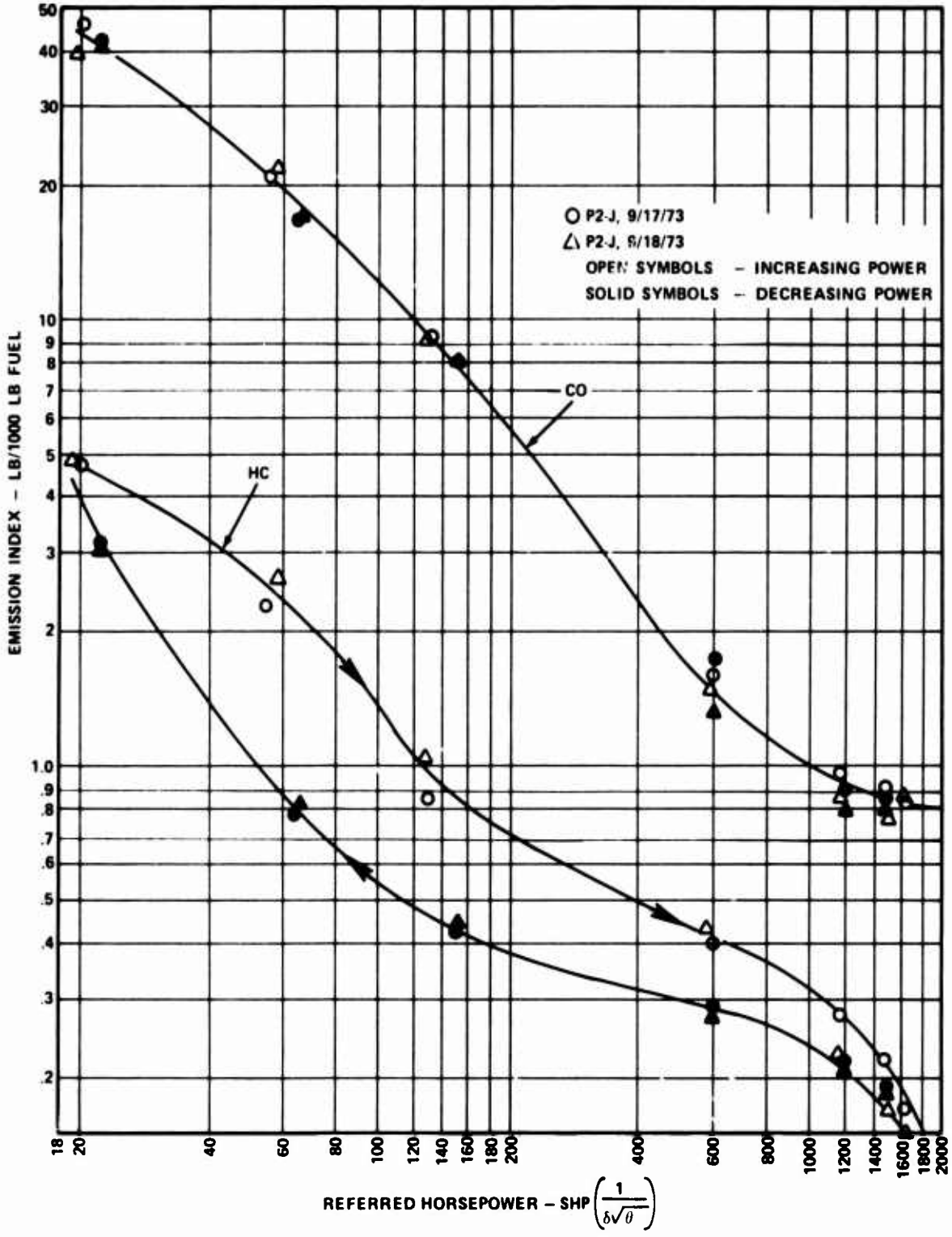

Figure 24. Emission Index of CO and HC Versus Referred Horsepower for Engine P2-J, Manifold 2.

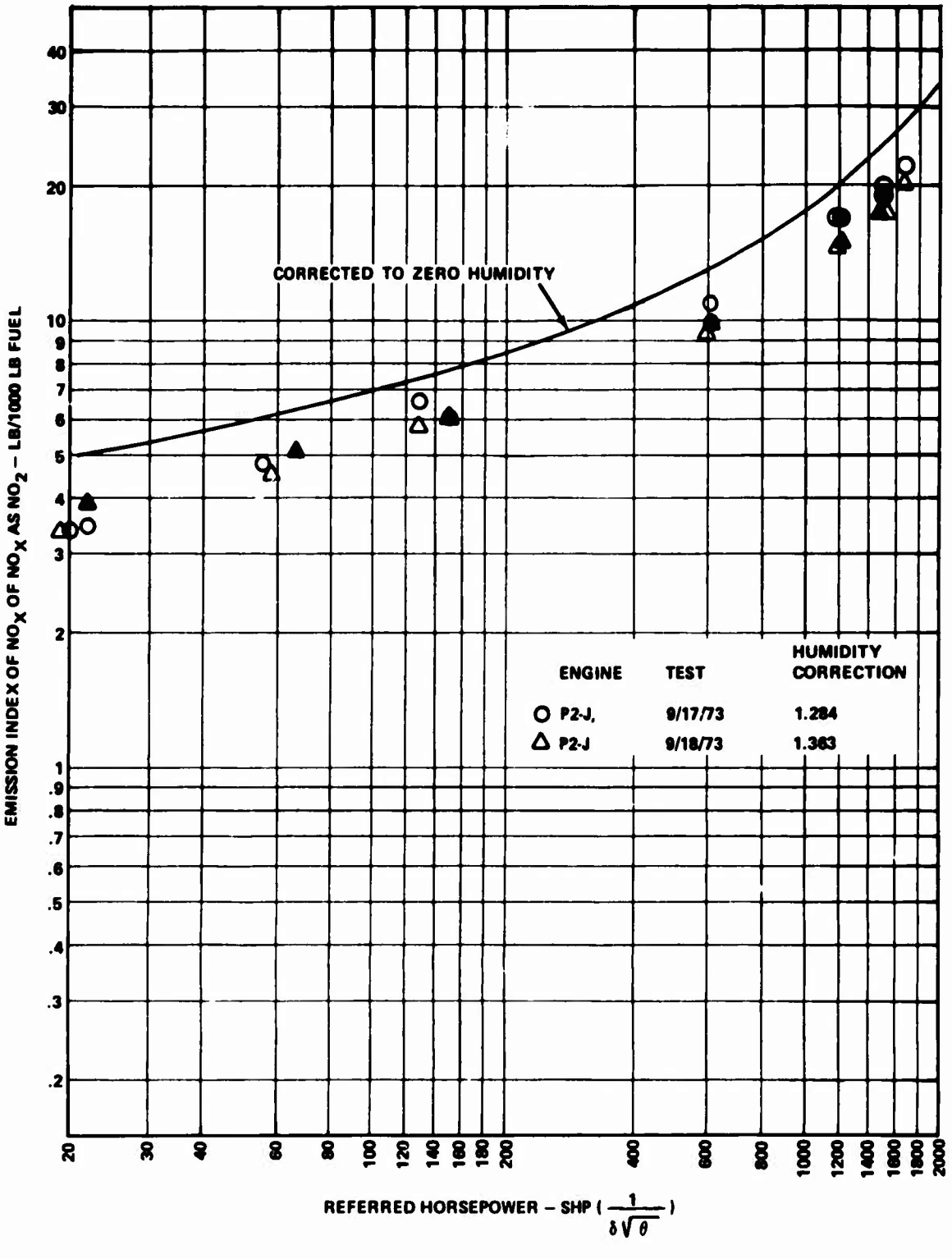

Figure 25. Emission Index of NO_x As NO_2 Versus Referred Horsepower for Engine P2-J, Manifold 2.

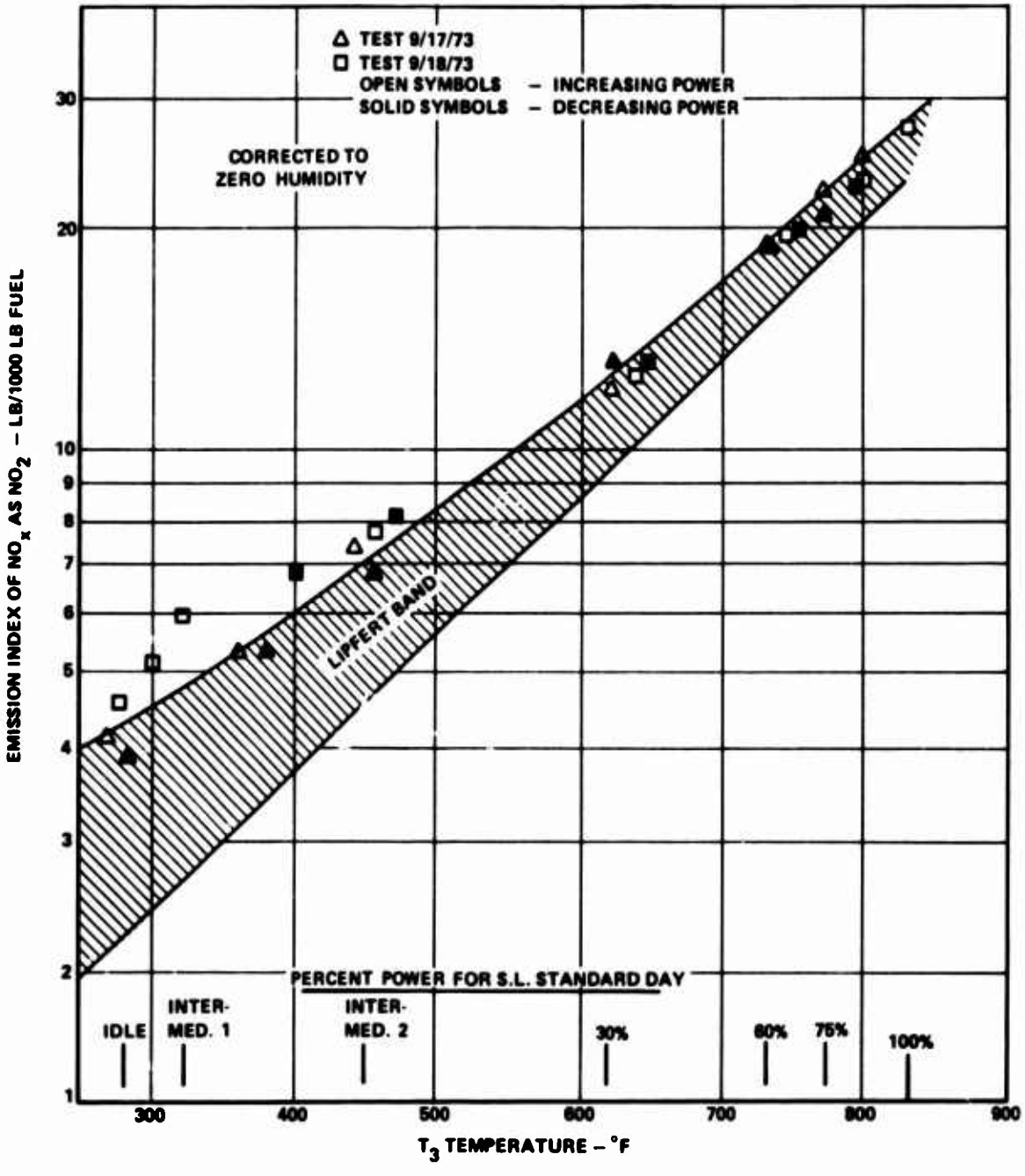

Figure 26. Emission Index of NO_x As NO_2 Versus T_3 Temperature for Engine P2-J, Manifold 2 (Data Corrected to Zero Humidity).

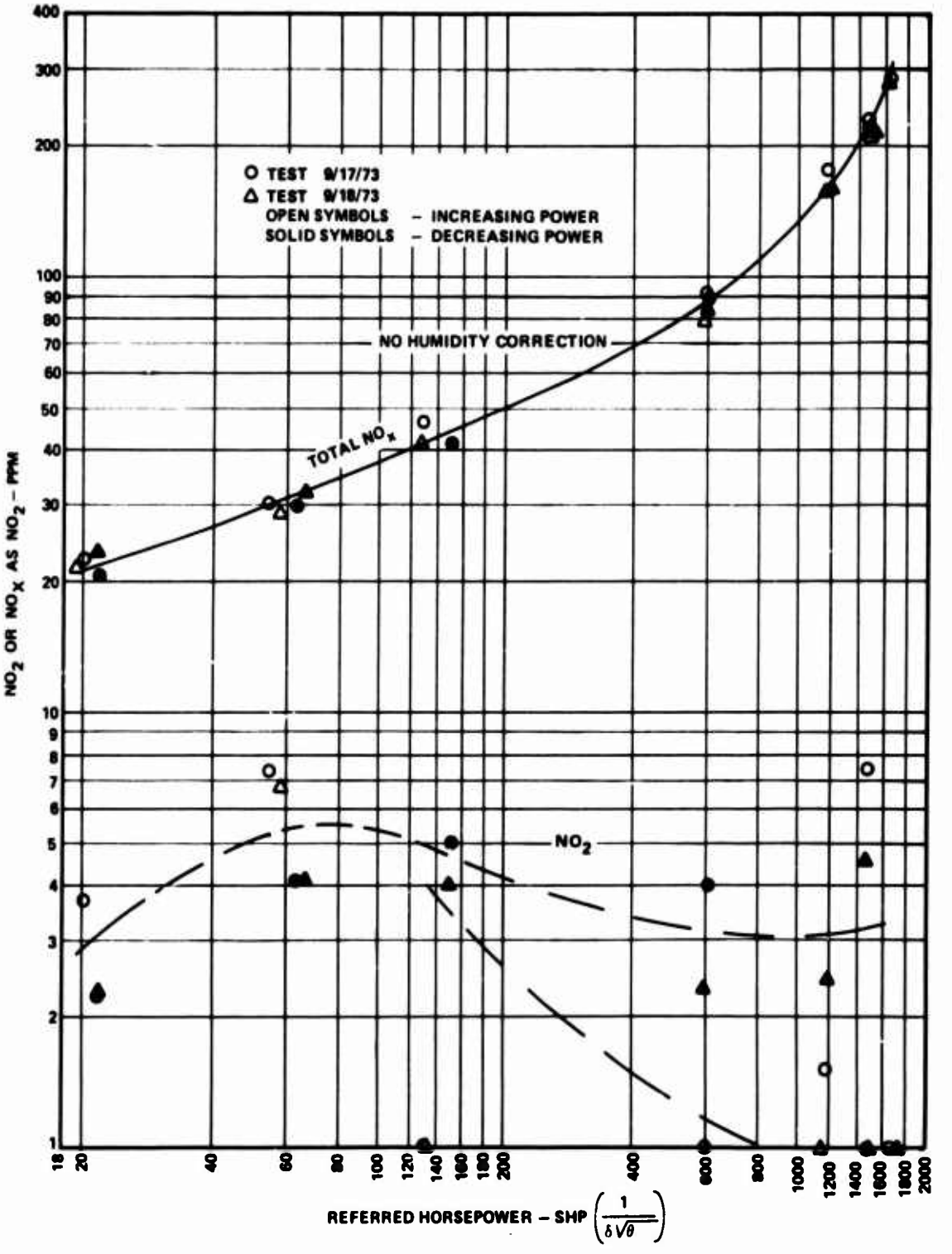

Figure 27. NO_2 and NO_x As NO_2 Versus Referred Horsepower for Engine P2, Manifold 2 (Data Not Corrected for Humidity).

haphazard and scattered. Some values as high as 7 ppm are indicated at low power. No strong conclusions can be drawn, other than that the NO_2 quantity must be quite small, of the order of 7 ppm or less, which is less than the data scatter above 50 horsepower.

Figure 28 shows the fuel-air ratio as a function of SHP for engine and combustor. Again, data were taken from engine fuel and air measurements and gas analysis. Values are similar to those for Manifold 1 and are reasonable.

Manifold 3 - Delavan Air-Blast Injectors

The F/A correlation data are plotted on Figure 17. For the preliminary test (10/1/73), the F/A correlation is as much as 5% low on the gas analysis, compared to 3% high on the 11/15/73 test, but both are within the ARP 1256 stipulated accuracy. For these tests, the interstage bleed air is indicated to be between 10 and 18% of the total flow, from gas analysis. Bleed flow was independently measured and agreed within 1 to 5% of these values.

Emission data from Manifold 3 are shown in Figure 29. The so-called HC "hysteresis" does not appear on this plot because the HC zero reference was recorded quite often when low concentrations were present. The sample flow rate was also increased to purge the sample line more rapidly. Some increase in HC concentration is found for the preliminary test at low power, but there is considerable scatter also, indicating scatter from an unknown cause.

An explanation of the large HC spread "hysteresis" was found during tests on a T53 engine run during this time period. At low-power points with high hydrocarbon content, the sample lines collected hydrocarbon concentrations on the interior walls. As power increased and HC concentration dropped, the deposits on the walls were gradually purged. It is likely that the sampling flow rate for the T53-test was somewhat low also, thus extending the purge time. However, when "zero gas" checks were made immediately after each data point, this scatter disappeared. This procedure was used on the later PLT 27 tests with similar results, thus demonstrating that the HC "hysteresis" is not an engine or combustor effect, but a "chromatographic" effect resulting from slow purge of heavy hydrocarbon components from the sample lines.

The conclusions reached from the "hysteresis" shape of the data plots are (1) that it is desirable to install monitoring gages to insure

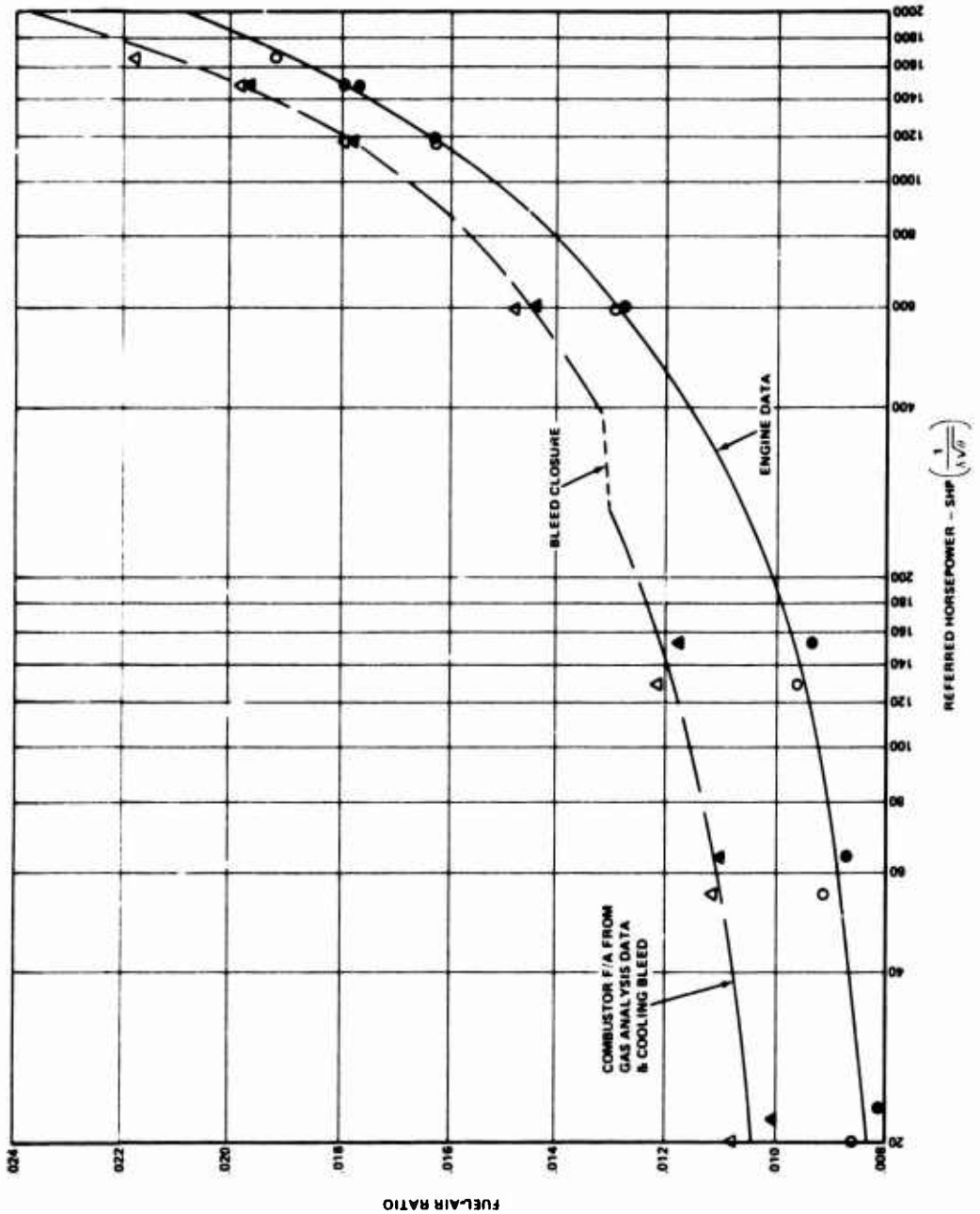

Figure 28. Fuel-Air Ratio Versus Referred Horsepower for Engine Data and Exhaust Gas Analysis for Manifold 2 (Test 2).

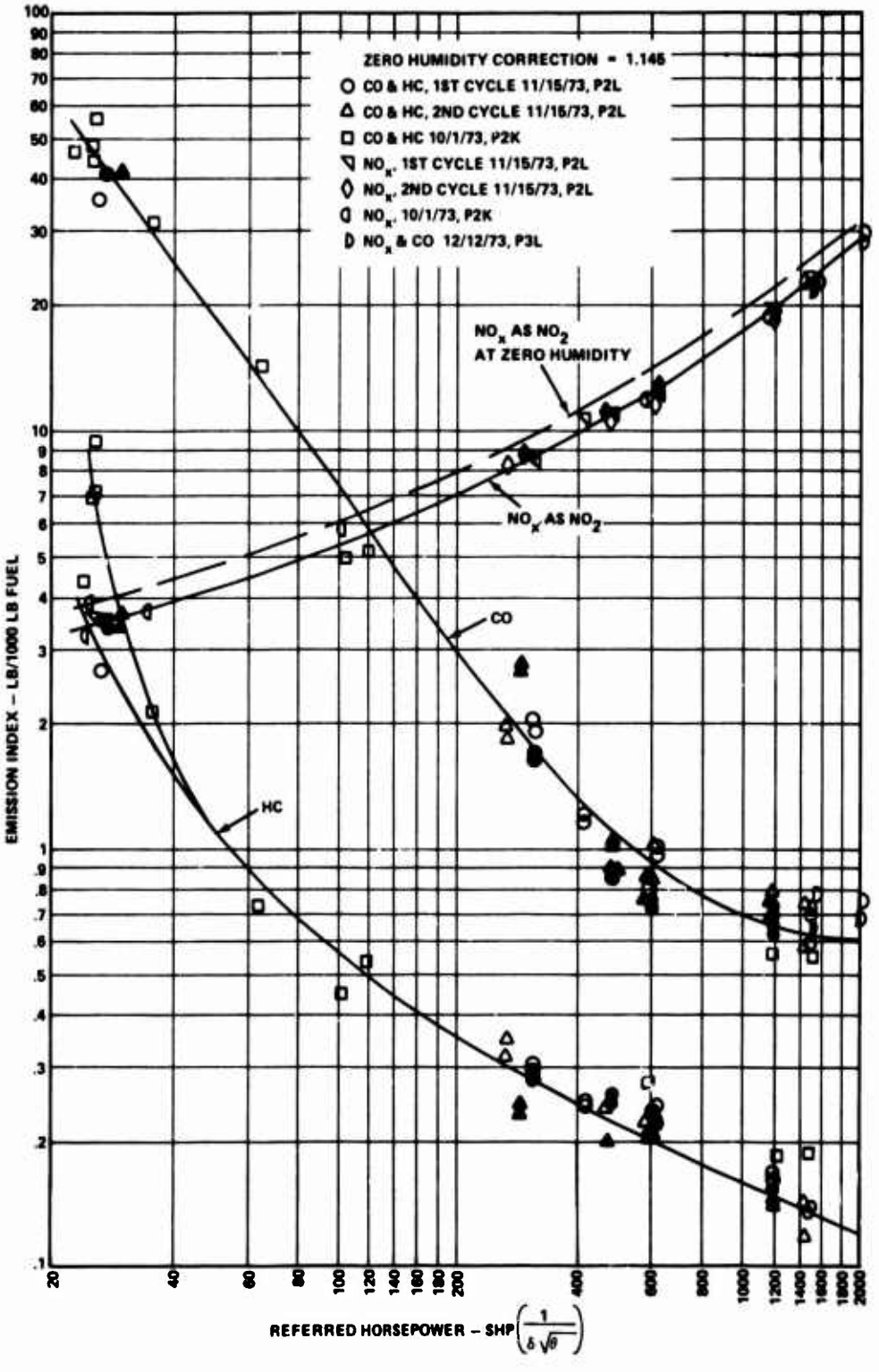

Figure 29. Emission Index of CO, HC, and NO_x Versus Referred Horsepower for Engine P2-L, Manifold 3.

that the desired sample line pressures and velocity are maintained, and (2) that when the sample lines are saturated with hydrocarbons and low concentrations are being measured, an immediate zero reference point is necessary.

The NO_x (Figure 30) values are similar to those from Manifolds 1 and 2, on a combustor inlet temperature abscissa, and compared with the Lipfert data band.

A third attempt to correlate NO_2 with NO_x is shown in Figure 31. At first glance, there appears to be a real trend of NO_2 concentration. The NO_2 values at low power (5 to 9 ppm) show a similar trend to the previous data, but with not so much scatter. At higher power, the NO_2 is about 4% of the total NO_x, with much less scatter than the previous data from Manifolds 1 and 2. An attempt to tie this trend to a change in converter efficiency was unsuccessful. For example, if the converter is 98% efficient, some NO_2 would be converted to NO, but 2% of the NO_x could be NO_2 and not be detected. Therefore, a low converter efficiency would produce less NO_2, rather than more. This raises the possibility that the converter was operating poorly for Manifolds 1 and 2. If this were the case, we could obtain negative values of NO_2; however, negative values were not observed. An explanation for the trend in Figure 50 is not obvious.

The F/A analysis from engine and combustor is shown in Figure 32. The trends are similar to those of Manifolds 1 and 2.

Manifold 1 Repeat

The F/A correlation for this test is shown in Figure 18, and the agreement between the two F/A measurements is within $\pm 4\%$, well within the specification of SAE ARP 1256.

Plots of the retested (Test 4) Manifold 1 data are shown in Figure 33 compared to the original Manifold 1 test. Agreement is close enough to state that there were no serious changes in emissions between tests. The HC values for the Test 4 are somewhat lower at low power; but at higher power, the two sets of data overlap. CO and NO_x data agreement are within the data scatter or a few percent of each other.

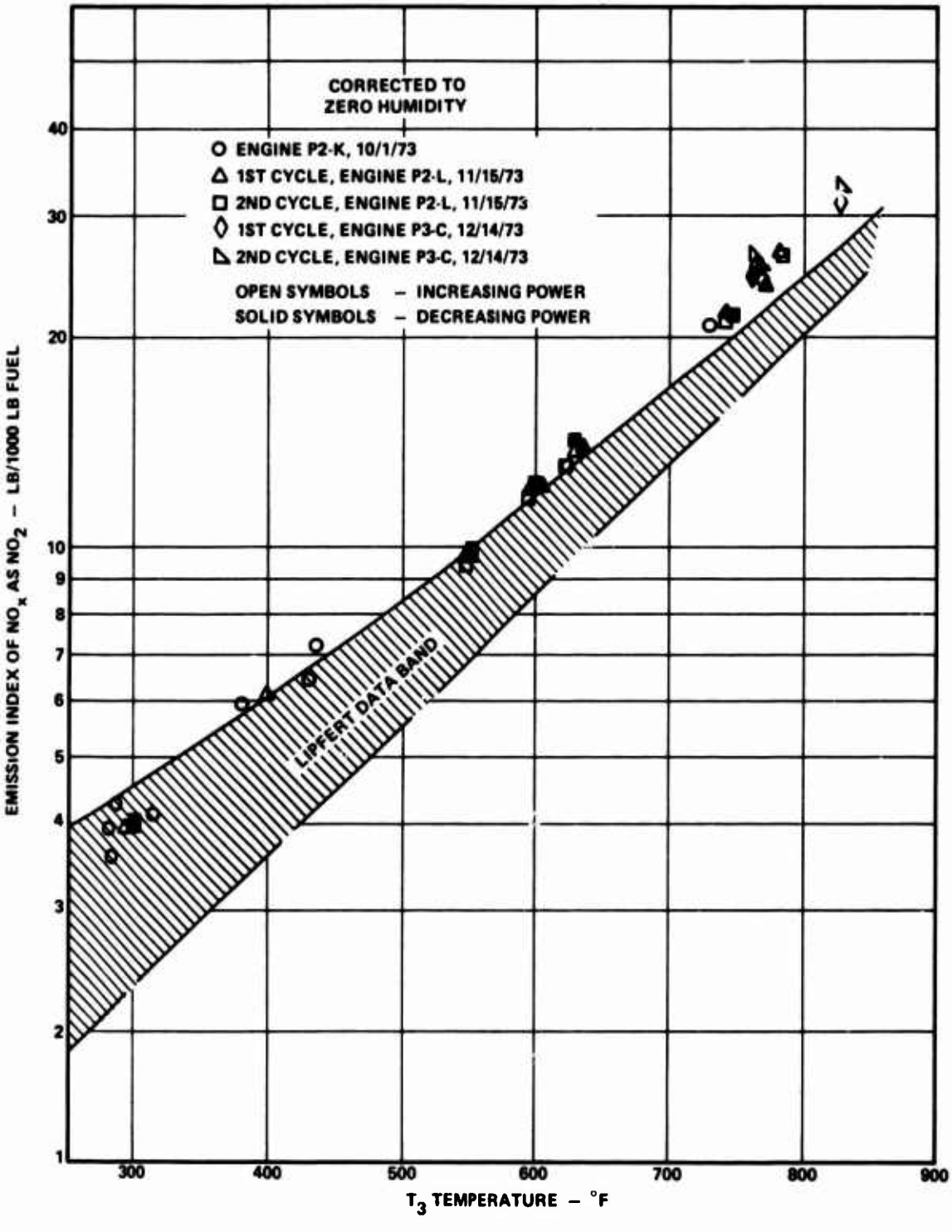

Figure 30. Emission Index of NO_x As NO_2 Versus T_3 Temperature for Engine P2-K, Manifold 3.

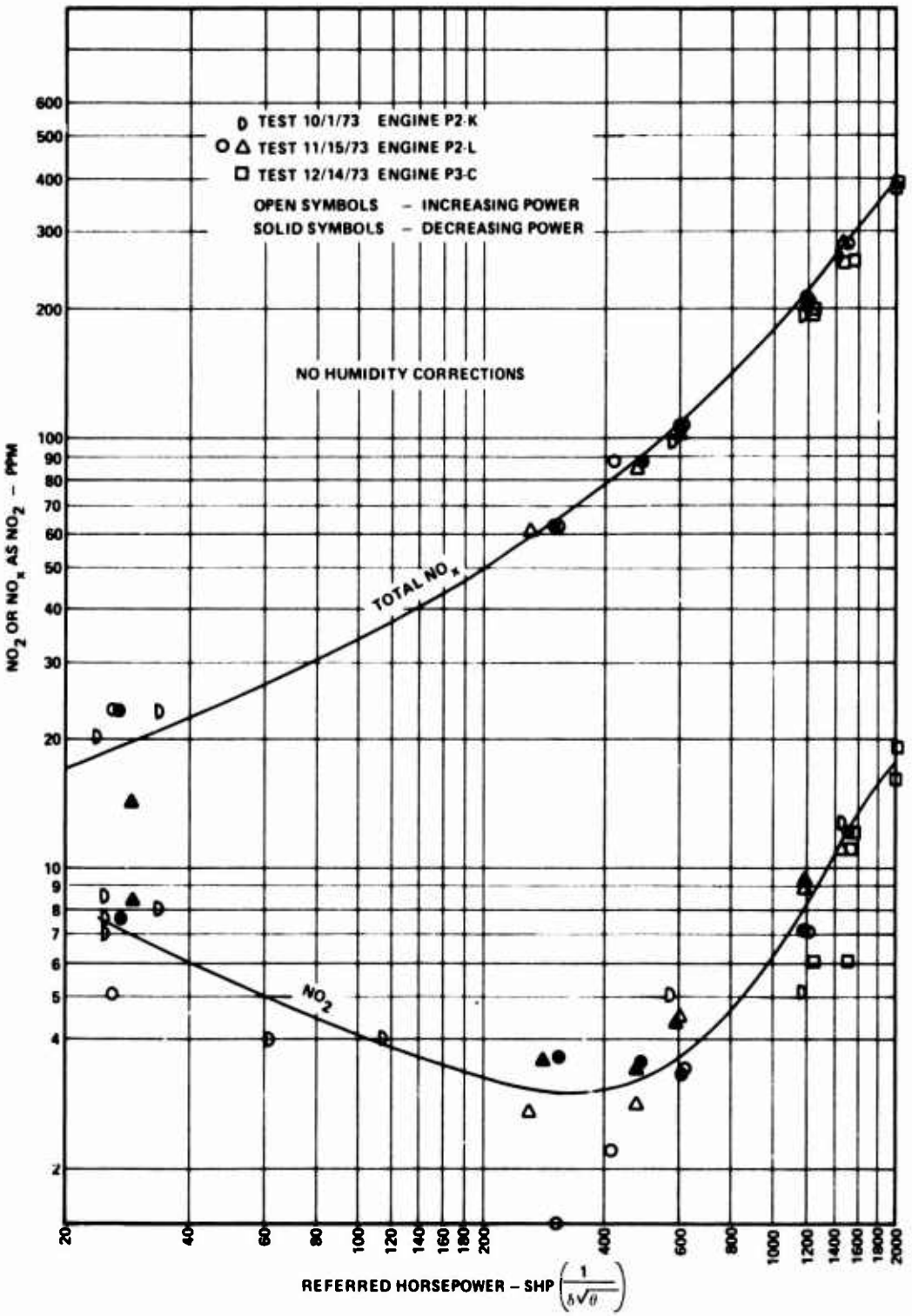

Figure 31. NO_2 or NO_x As NO_2 Versus Referred Horsepower for Engines P2-K, P2-L, and P3-C, Manifold 3 (Test 3).

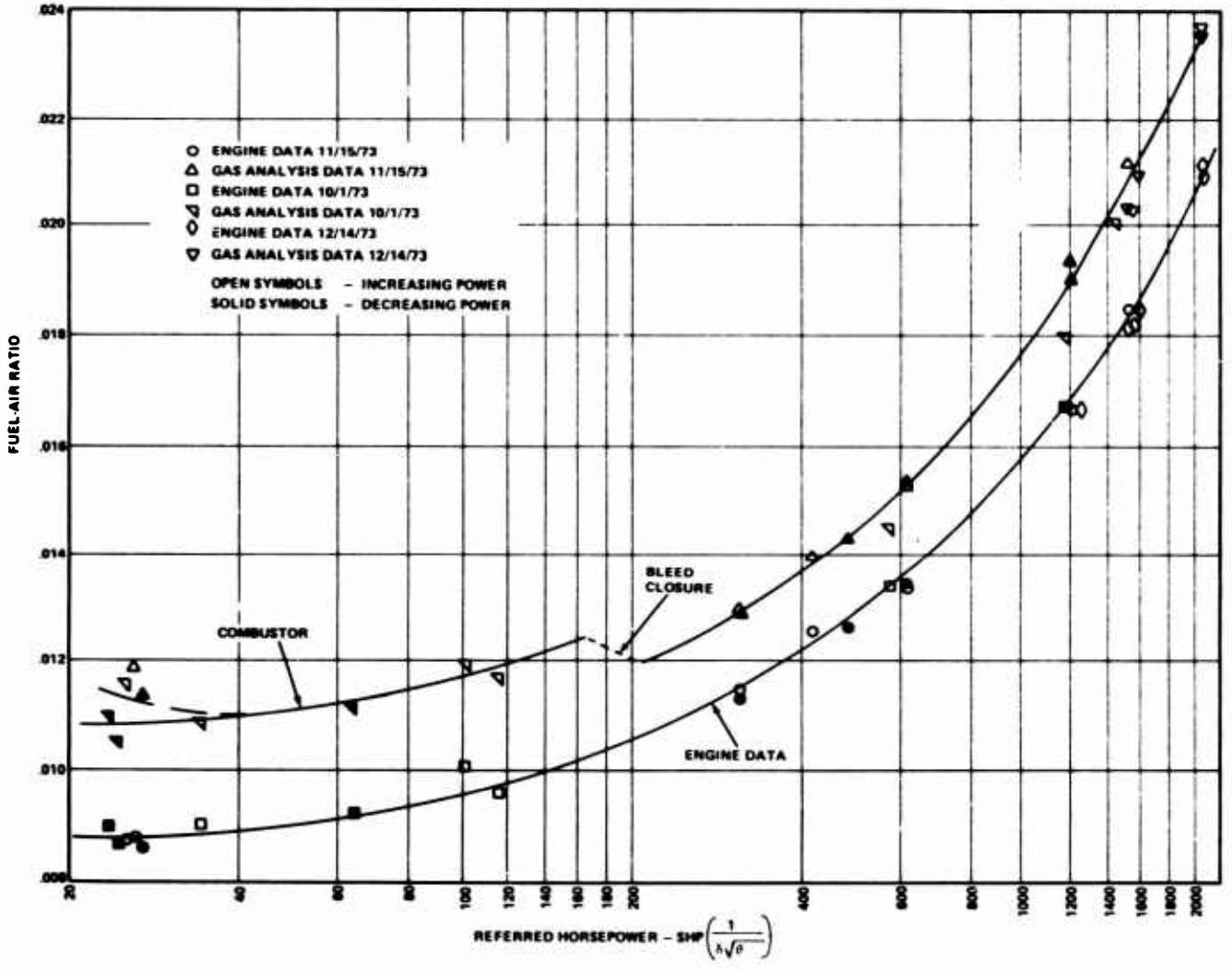

Figure 32. Fuel-Air Ratio Versus Referred Horsepower for Engine Data and Exhaust Gas Analysis for Manifold 3.

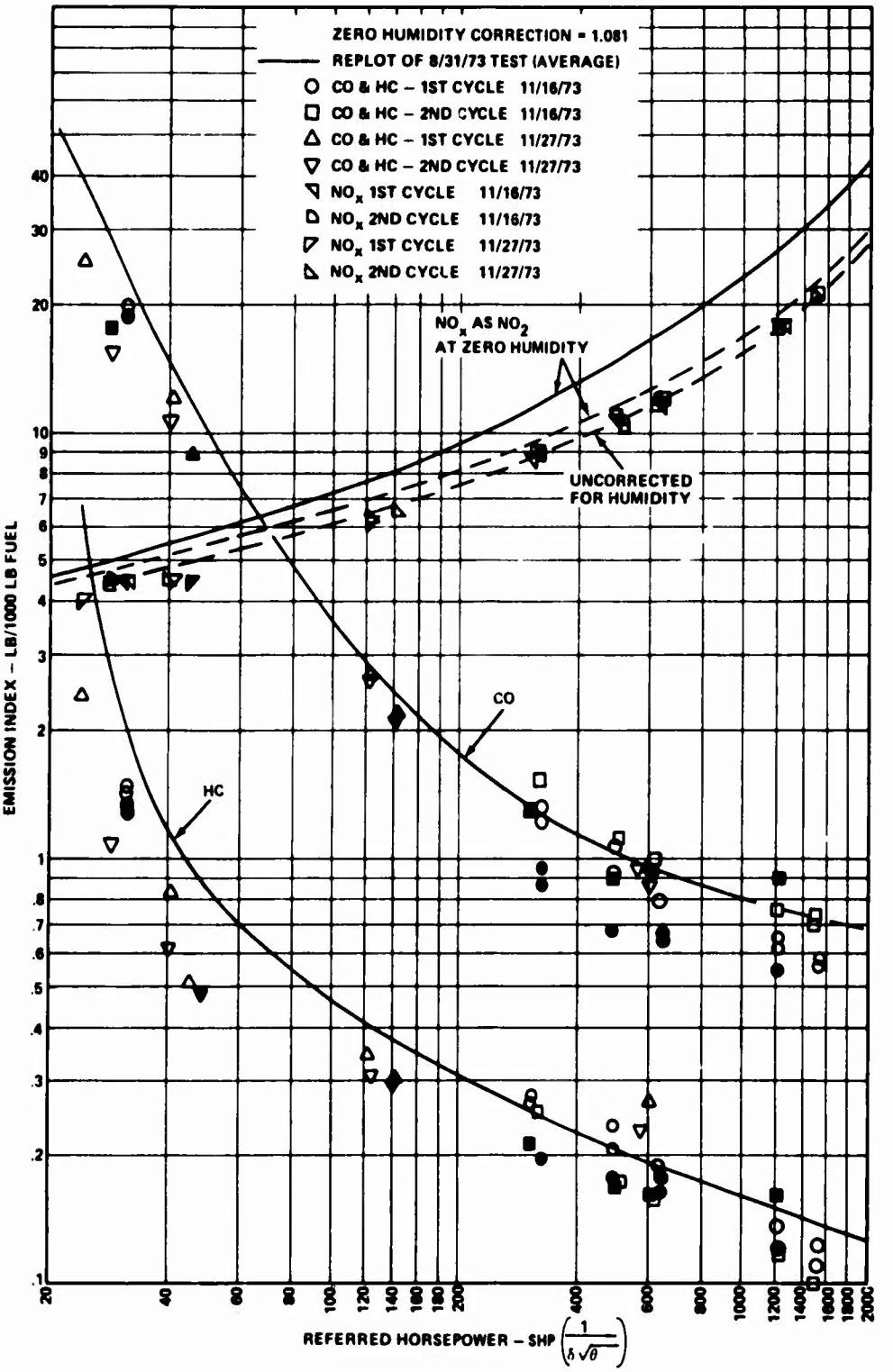

Figure 33. Comparison of Emission Index Versus Referred Horsepower for Manifold 1 at the Start (Test 1) and End (Test 4) of the Test Period.

Comparisons and Correlations of Three Fuel Injection Systems

Several comparisons were made to determine if any of the fuel injector designs were measurably better in performance or emission production. Combustion efficiency for the three manifolds as a function of SHP is shown in Figure 34. The Parker-Hannifin air-blast (Manifold 1) shows some superiority.

Although NO_x can be correlated nicely as a function of combustor inlet temperature and humidity, the CO and HC emission data have no obvious simple theoretical correlations based on combustor operating conditions.

An attempt was made to correct the CO and HC emissions to a common basis by using the θ parameter originally proposed by Herbert and discussed in Reference 14:

$$\theta = \left(P_3^{1.75} A_{ref.} e^{T_3/b} \right) / W_{ap}$$

$$\text{where } b = 396 \left(1.414 + \ln \frac{\phi_p}{1.03} \right)$$

The parameter θ is shown plotted against referred SHP and fuel flow at optimum N_2 (Figure 35), both taken from the computer representation of the engine model, for reference purposes. The value of θ was also calculated for actual combustor operating conditions, P_3, T_3, W_a, and ϕ_p in the primary zone, at which data were recorded.

Combustor efficiency for each test point was then plotted against θ for each injector configuration in Figure 36. This shows that Manifold 1, the Parker-Hannifin air-blast style, is best at all values of θ less than 1×10^6. The dual-orifice injectors in Manifold 2 give the worst result except at very low power levels where dual-orifice fuel flow is from the primary swirl slots alone. All manifolds give about the same performance at high powers, where $\theta > 30 \times 10^6$.

The relative CO and HC combustion inefficiency split is plotted in Figure 37, and shows that all injector styles had the same inefficiency characteristic, i.e., more CO than HC inefficiency, particularly above 99% efficiency.

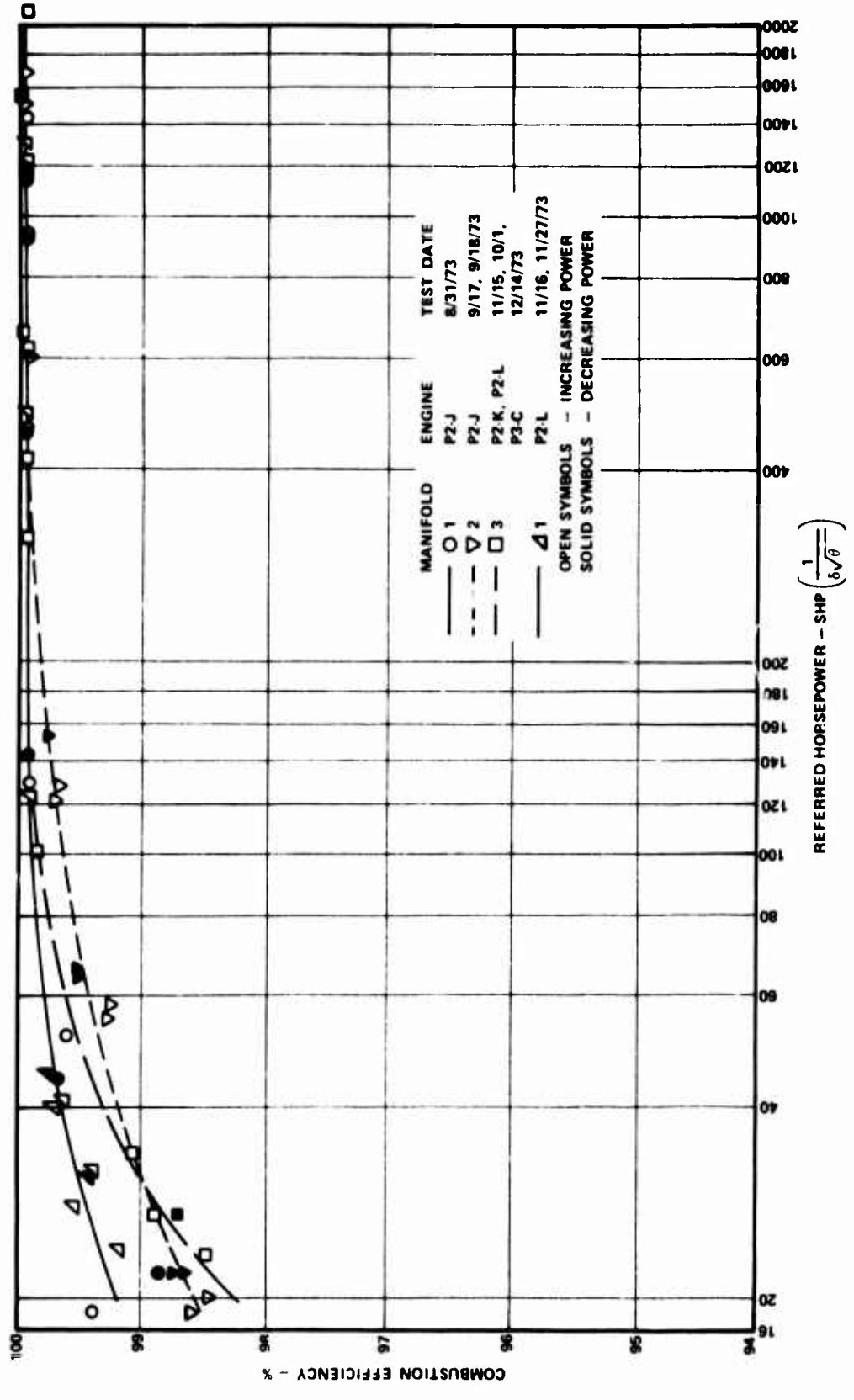

Figure 34. Referred Horsepower Versus Combustion Efficiency for Three Manifolds.

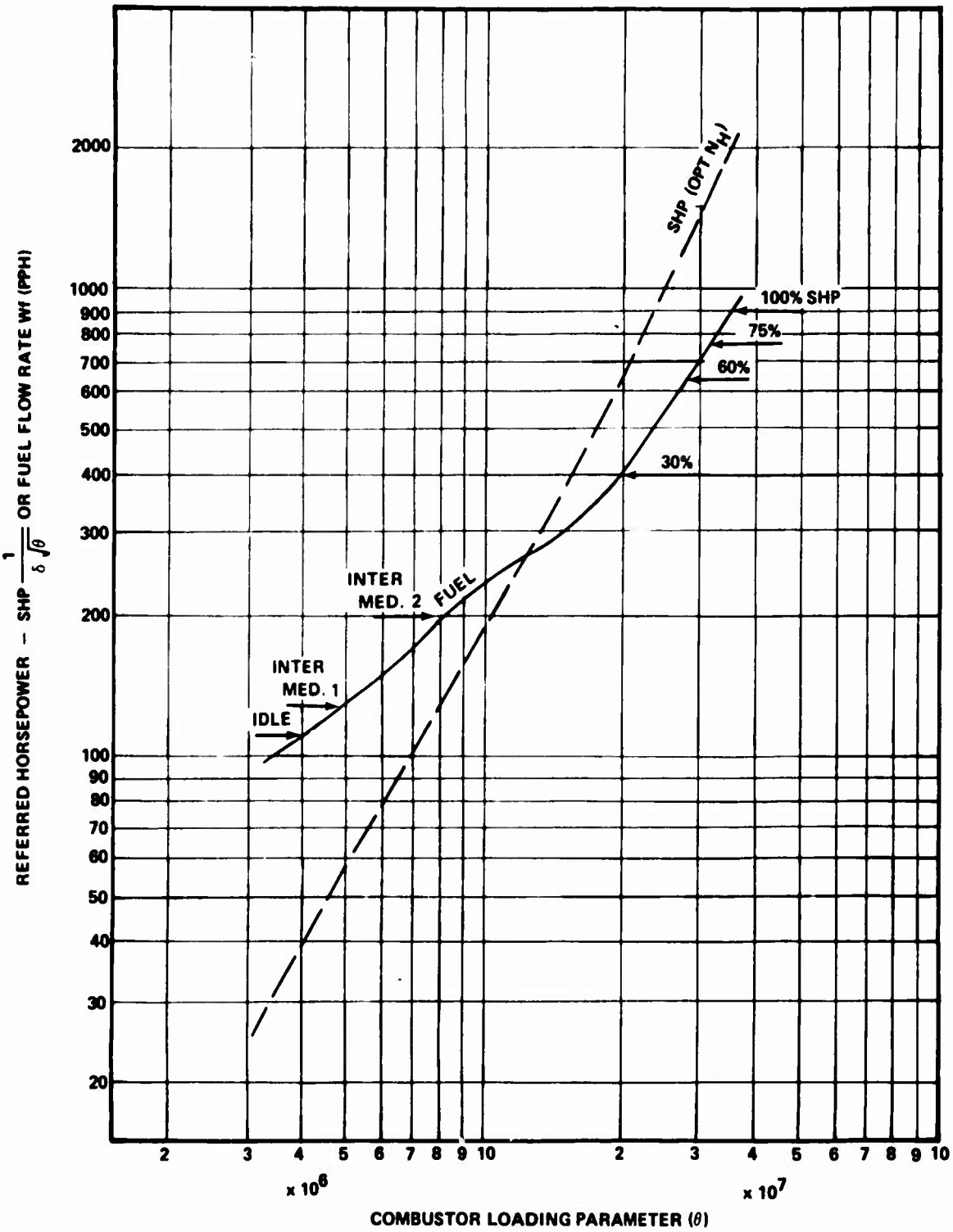

Figure 35. Referred Horsepower and Fuel Flow (Sea Level, Standard Day) Versus Combustor Loading Parameter (θ).

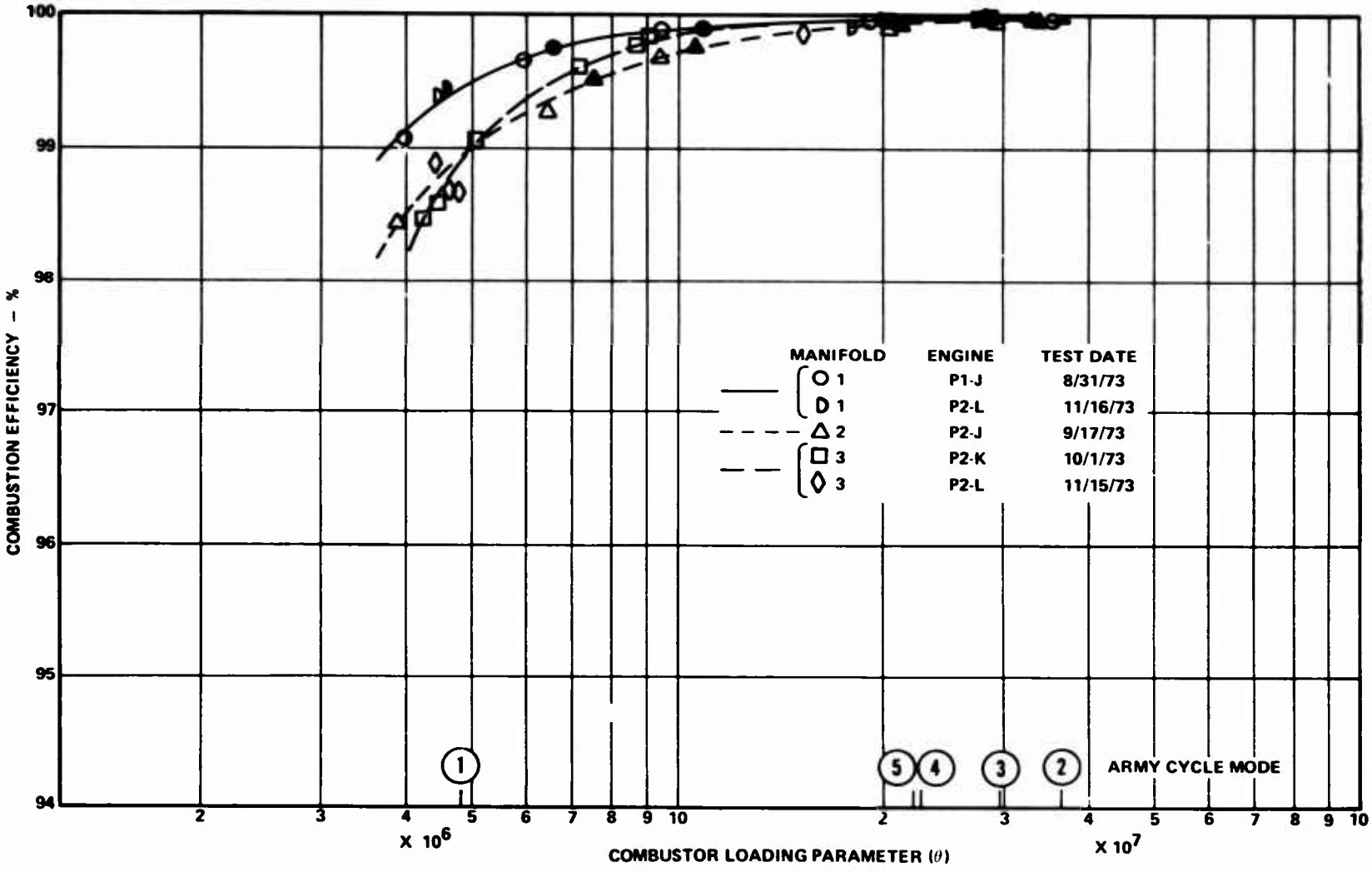

Figure 36. Combustion Efficiency Versus Combustor Loading Parameter (θ).

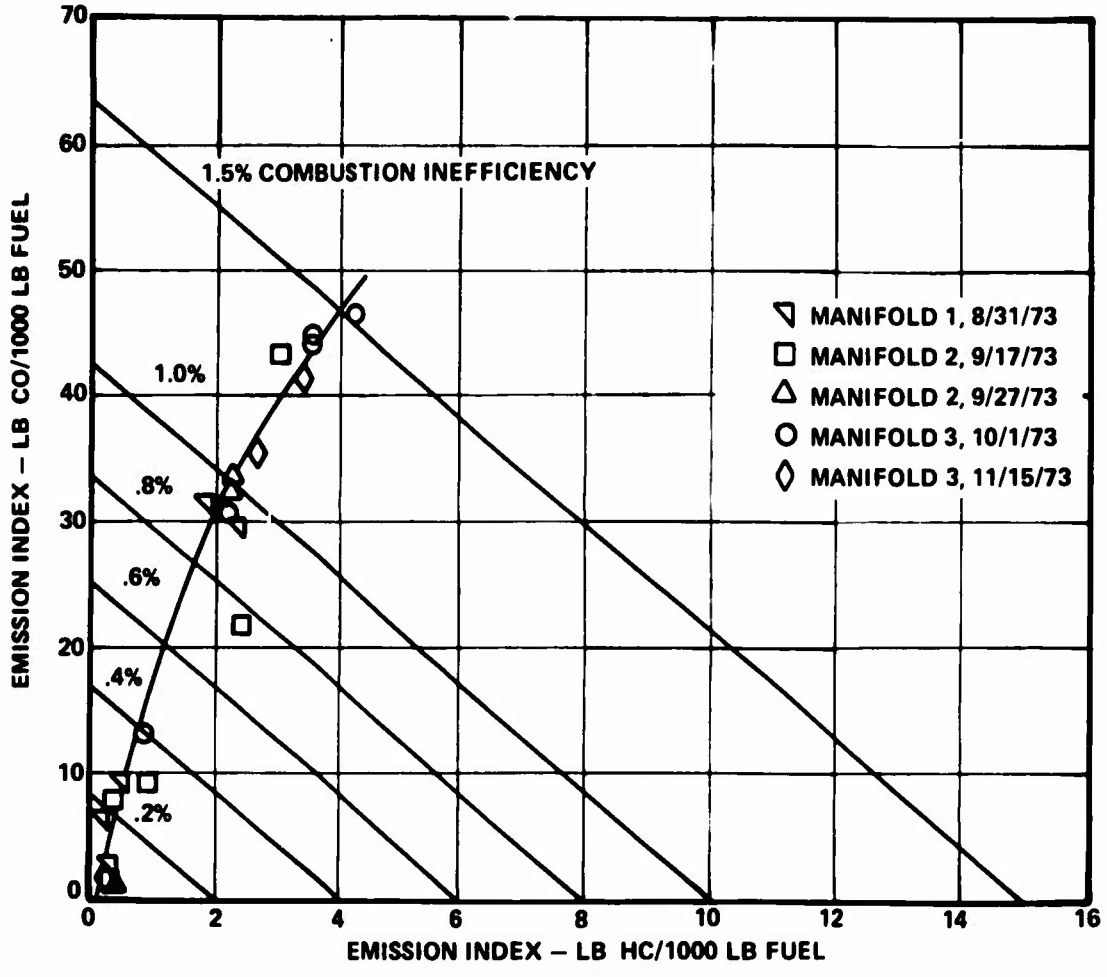

Figure 37. Emission Index of HC and CO Versus Combustion Efficiency Loss.

By using the curves in Figures 35 through 37, predictions of emission performance can be made by choosing θ for any operating condition, determining η_b for any injector style (Figure 36), then picking off the CO and HC emission index for that combustor efficiency (Figure 37).

NO_x emission indices are taken from the plot of emission index versus T_3 (Figure 38). It should be noted that the repeat of Manifold 1 did not conform exactly with original test, and the rerun of Manifold 3 in engine P3-C did not conform identically with the data taken in engine P2-K. (See Figure 39 for the plotted data.)

An Army helicopter duty cycle, listed in Table 4, was chosen as an example of the application of this prediction method.

TABLE 4. ARMY HELICOPTER DUTY CYCLE

Cycle Point	Mode	Power (%)	PLT 27 SHP	Weighting Factor
1	Idle	2.8	57	.15
2	Takeoff	100	2018	.05
3	Climb/Hover	75	1514	.20
4	Cruise	55	1110	.45
5	Descent	40	807	.15

This cycle was applied to the computer representation of the PLT 27 cycle. The resulting combustor operating conditions are shown in Table 5. A value of θ was obtained from Figure 35 after finding the combustor efficiency from Figure 36. The emission index of NO_x was obtained from Figure 38 and correlations of T_3 and SHP, as shown in Table 5. This permits the configurations to be compared under identical operating conditions.

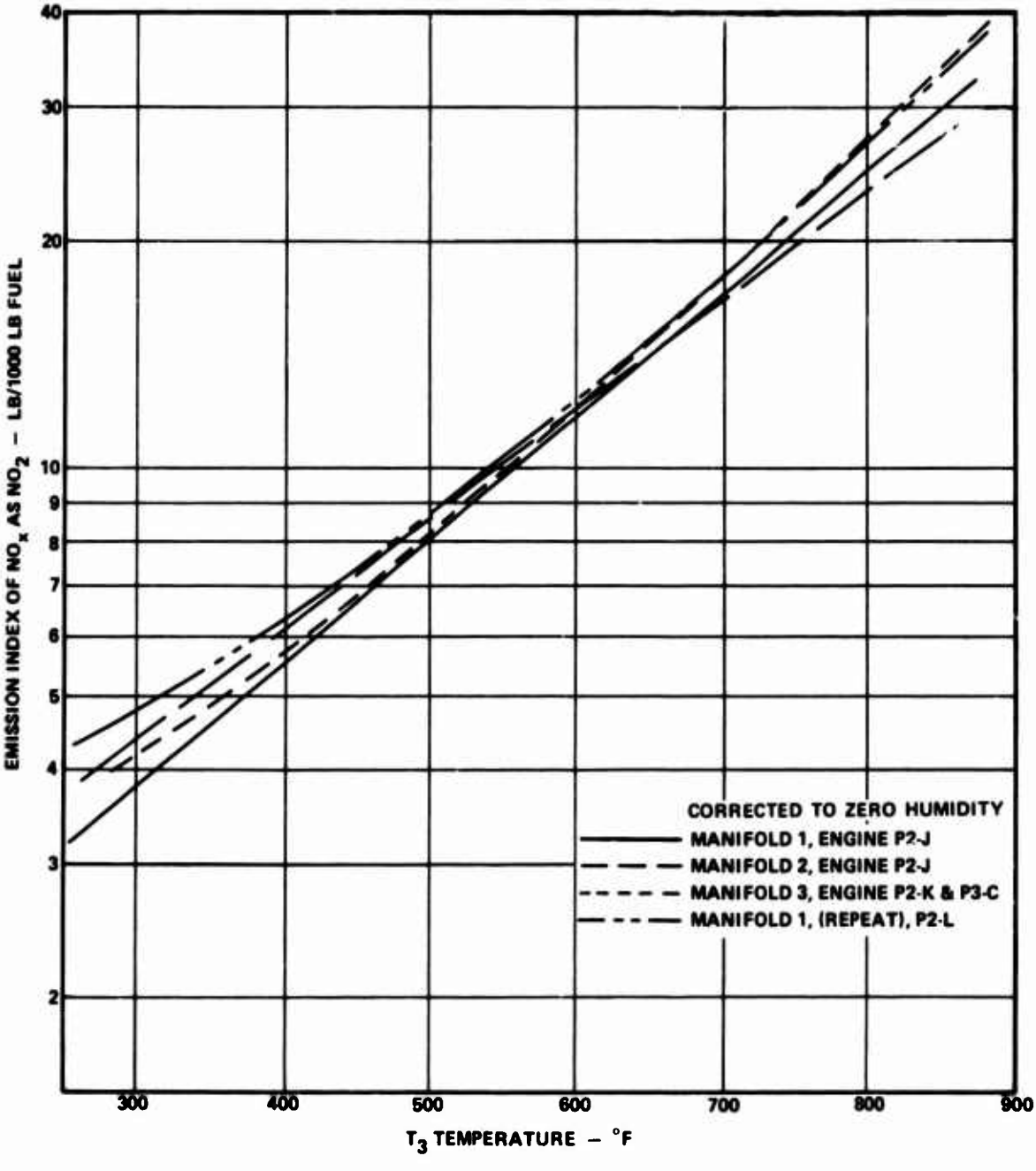

Figure 38. Comparison of Emission Index Versus T_3 Temperature for Engines P2-J, P2-K, and P2-L, Manifolds 1, 2, and 3.

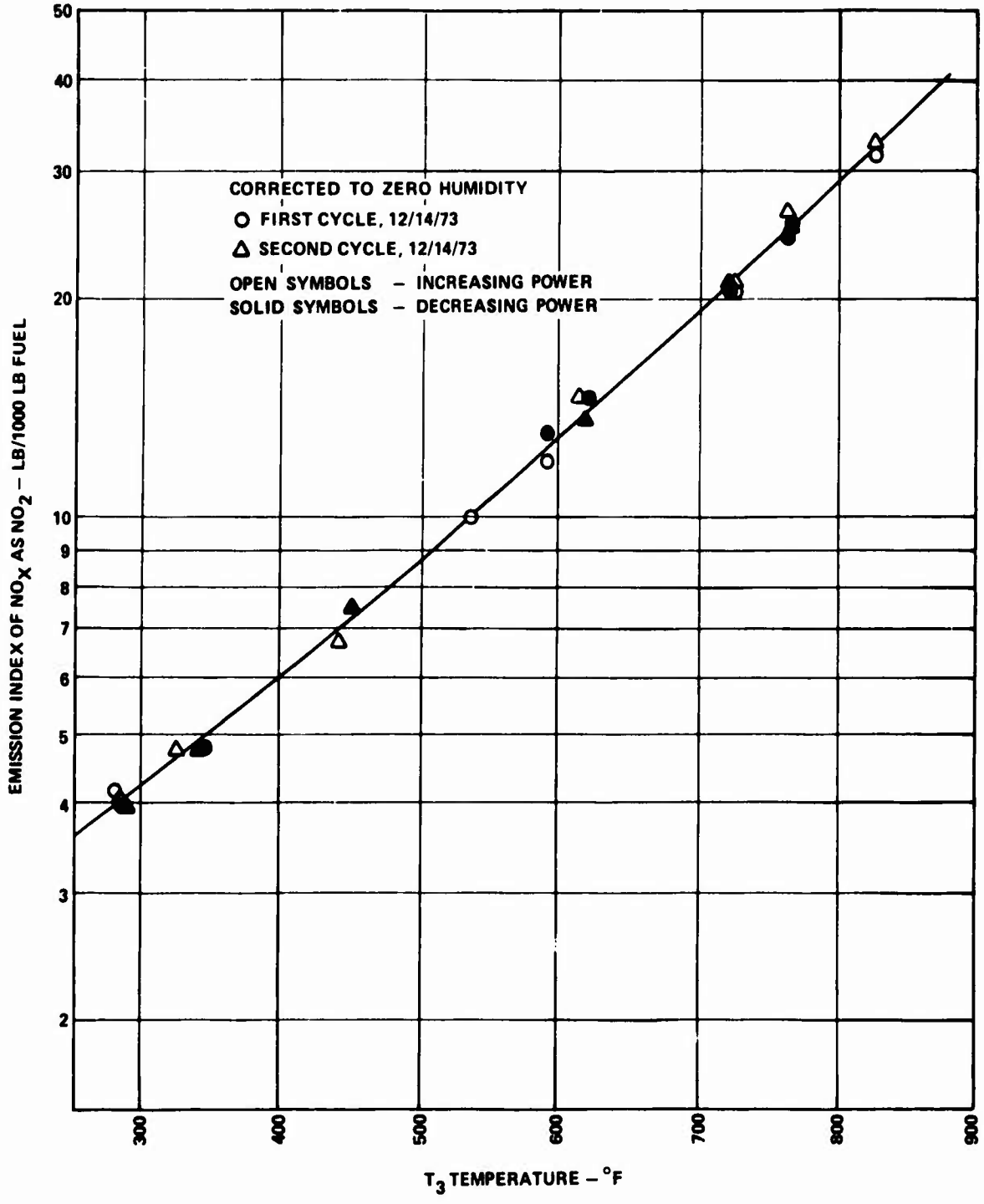

Figure 39. Comparison of Emission Index Versus T_3 Temperature for Engine P3-C, Manifold 3.

TABLE 5. PLT 27 COMBUSTOR OPERATING CONDITIONS FOR ARMY HELICOPTER DUTY CYCLE

Cycle Point	SHP at Opt. N_H	P_3 (Atm.)	T_3 (°F)	W_a Combustor (lb/sec)	W_f (lb/hr)	θ
1	57	3.2	330	3.02	130	4.9×10^6
2	2018	15.9	825	11.5	965	36.3×10^6
3	1514	13.5	750	10.4	730	29.9×10^6
4	1110	11.1	700	9.3	595	26.8×10^6
5	807	10.3	665	8.3	480	22.6×10^6

The results are given in terms of idle emission index, average emission index per cycle, and pounds of pollutant emitted per hour per cycle, and are shown in Table 6.

It is clear that the differences between configurations are small, and NO_x contributes the overwhelming proportion of the total pollutant. Smoke is always below the value of 36 allowed by the EPA for this size engine in the P-2 class; and, for the air-blast configurations, smoke is nearly nonexistent. The combustor efficiency at idle varies from 98.9% for Manifolds 2 and 3 to 99.5% for Manifold 1.

The repeatability of the smoke, hydrocarbon, and carbon monoxide data is good, and the values are so small that a 10% variation is of little consequence.

The NO_x data repeatability of cyclic emission index is about 8% for Manifold 1 and 6% for Manifold 3. These repeatability ranges can be considered to be, roughly, probable error, and to include instrument repeatability, calibration gas accuracy, instrument operating range readout error, and variations in engine emissions themselves from ambient causes and unknown causes. The total spread of data for all manifolds at maximum power is approximately 30%, with a spread in the average data of 20%. Therefore, we conclude that there are real differences between NO_x production between the manifold configurations tested. However, because of the crossover of the NO_x emission index for the manifolds tested (Figure 38), and the observed difference in NO_x produced from Manifold 1 and the repeat test of Manifold 1

TABLE 6. PLT 27 CUMULATIVE EXHAUST EMISSIONS FROM ARMY HELICOPTER DUTY CYCLE

Manifold Description		Gaseous Emissions HC	CO	NO_x	Maximum Smoke Number
P/H Air-Blast					
Manifold 1 Test 1	Idle EI	1.1	18.5	4.3	2.5
	Cyclic EI	0.3	4.2	16.0	2.5
	Pollutant/Cycle (lbm)	0.10	0.87	10.0	-
Test 4	Idle EI	1.1	18.5	5.3	0
	Cyclic EI	0.3	4.2	17.2	2
	Pollutant/Cycle (lbm)	0.10	0.87	10.8	-
DLN Air-Blast					
Manifold 3 Test 3	Idle EI	2.3	33.5	4.6	2
	Cyclic EI	0.5	5.6	17.2	2
	Pollutant/Cycle (lbm)	0.12	1.02	10.8	-
Test 5	Idle EI	N/A	N/A	4.7	3
	Cyclic EI	N/A	N/A	18.3	3
	Pollutant/Cycle (lbm)	N/A	N/A	11.6	-
Dual-Orifice					
Manifold 2 Test 2	Idle EI	2.4	35.0	4.9	10
	Cyclic EI	.6	6.0	15.6	19
	Pollutant/Cycle (lbm)	0.16	1.15	9.7	-

N/A - Not available

at the end of the series, the value of judging the relative merit of the manifolds from one test only is subject to question. In making the calculations for total cycle emissions (Table 6), small differences in NO_x can cause larger (factor of 2) changes in the cumulative emissions. Therefore, the data suggest that multiple additional tests are needed to resolve the fine line question of which fuel manifold really produces less pollution.

Considering the data repeatability listed, we conclude from the preceding analysis that:

1. Both air-blast configurations produce essentially zero smoke, much lower than the dual-orifice injector style.

2. The combustor efficiency is highest (or CO and HC is lowest) with the Parker-Hannifin air-blast injector style.

3. The oxides of nitrogen are indicated to be lower with the dual-orifice injector. However, the results are relatively close, and should be verified by further repeated tests to be conclusive.

Another method of comparing the emission performance of the three injector configurations is to apply the criteria issued by the E. P. A. in Title 40, Part 87 of the Code of Federal Regulation, assuming a turboprop application of the PLT 27 engine.

For the taxi idle power, which was assumed to be 5 percent of maximum power (100 shp), and the 30 percent maximum power condition, the combustor efficiencies (Figure 36), the emission indices for CO, HC (Figure 37), and NO_x (Figure 38) were obtained as functions of the combustor loading factor θ which was calculated from the average engine performance. For the 90 percent and 100 percent power conditions, the emission indices were determined directly from the emission index versus power curves.

The results are tabulated below and show that the engine meets the class P-2 requirements with the three tested injector configurations.

	EPAP VALUES			
	HC	CO	NO_x	SMOKE NUMBER
EPA 1979 P-2 Standard	4.9	26.8	12.9	36
Manifold 1 (Test 1 and 4 Average)	.5	6.3	12.0	3
Manifold 2	.7	11.0	10.8	24
Manifold 3	.7	10.4	12.2	4

Comparisons of all three manifolds and their emissions, plus data from Lycoming T53 and T55 engines, are shown in Figures 40 through 42. For CO, the Parker-Hannifin air-blast has a slight edge at low power, a definite advantage (by a factor of 2 to 3) in the range of 3 to 10% of full power, with average emissions observed up to full power. By contrast, the T53 produces nearly 10 times as much CO in the low power region, approaching the average at full power. The T55 CO emissions are still higher, with five times as much produced at full power.

The trends for HC production (Figure 41) are somewhat similar to the CO, with the Parker-Hannifin air-blast showing an edge over the others, and dual-orifice producing higher HC quantities. The T53 produces several times as much HC over most of the range, compared to the Parker-Hannifin air-blast. The T55 does somewhat better, and reaches the PLT 27 average at high power.

In Figure 42 the variation in NO_x produced is shown for the four PLT 27 tests, and the values are high compared to the T53 or T55 engines. This is the result of the higher compression ratio in the PLT 27 resulting in higher combustor inlet and flame temperatures.

Smoke Measurement

The AIA smoke number was calculated through use of the SAE ARP 1179 procedure. Smoke is usually visible at AIA values of over 50 for this engine size. Smoke number has been plotted against percent of full power for the three manifolds and for the repeat of Manifold 1 in Figures 43 through 46.

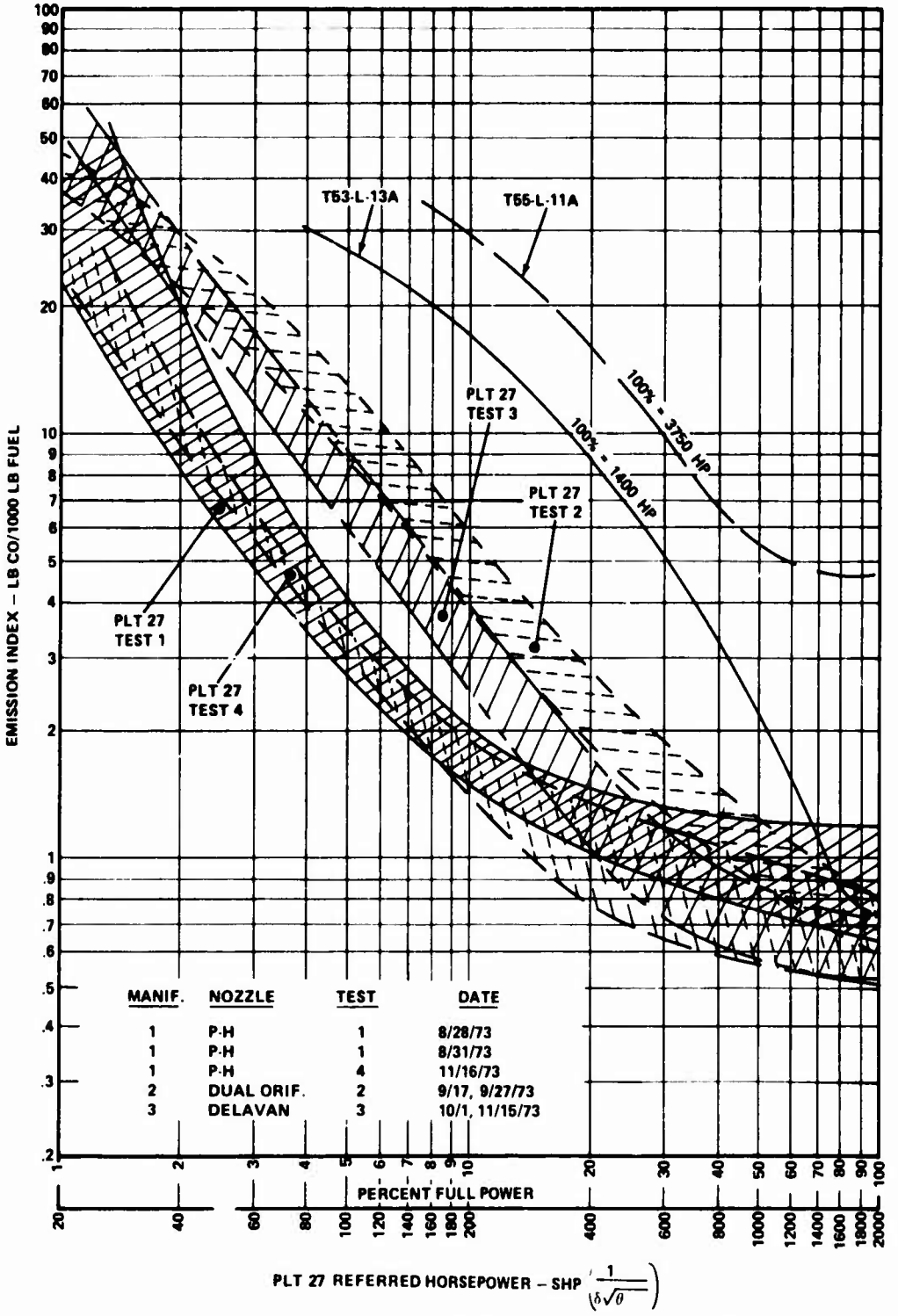

Figure 40. Emission Index of CO Versus Referred Horsepower for Three Fuel Nozzles (Four Tests) and Compared With T53 and T55 Engines.

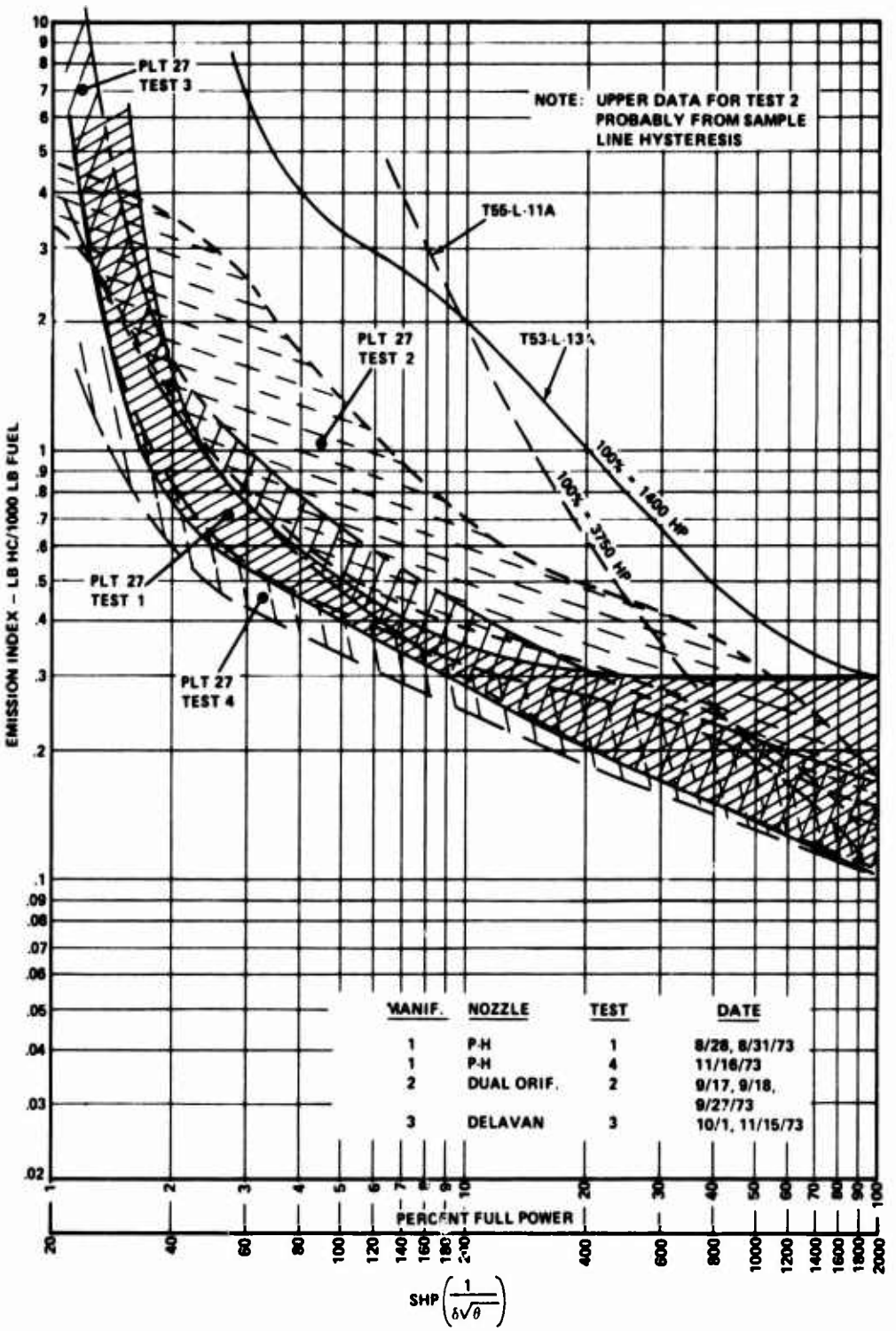

Figure 41. Emission Index of Hydrocarbons Versus Referred Horsepower for Three Nozzles (Four Tests) and Compared With T53 and T55 Engines.

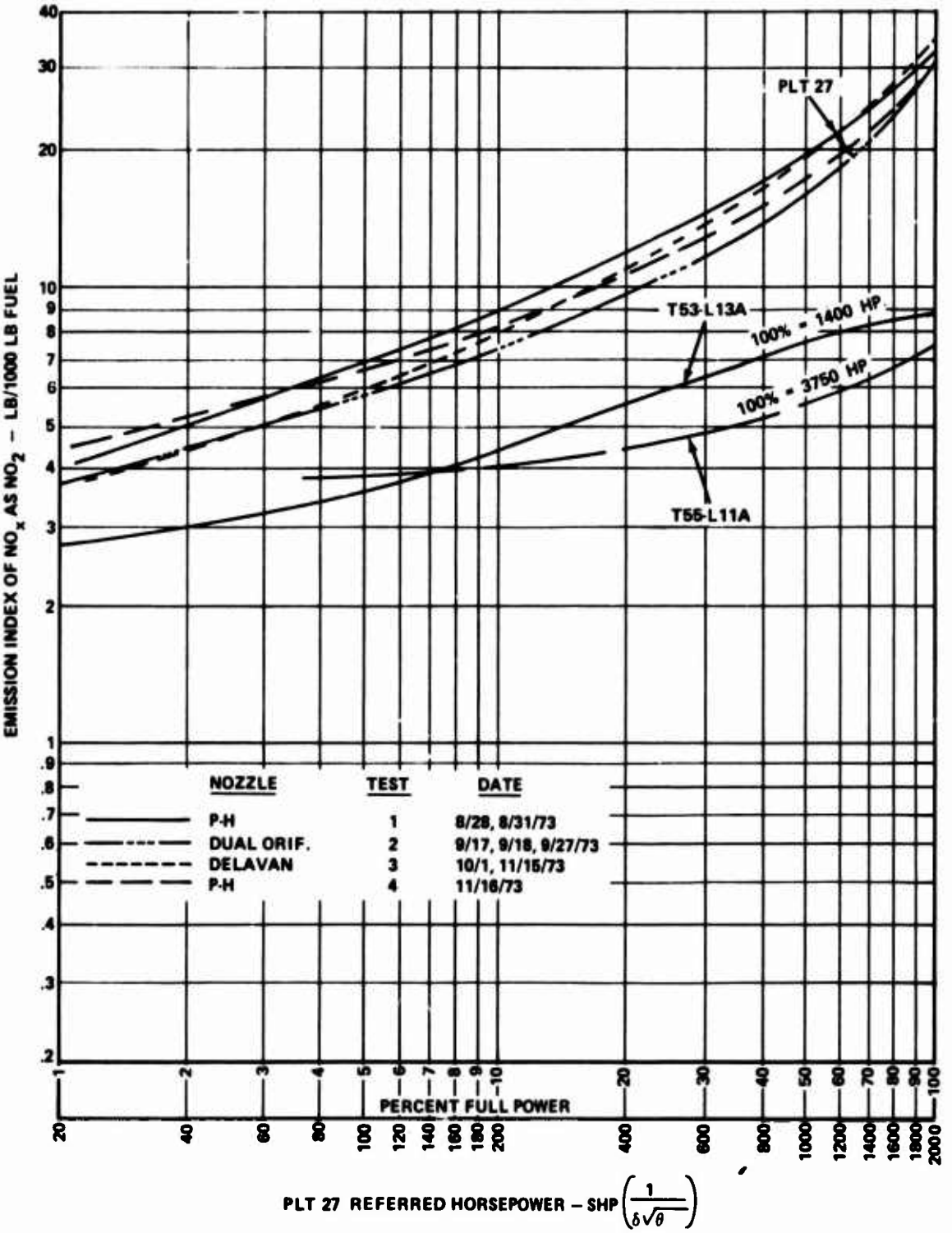

Figure 42. Emission Index of NO_x As NO_2 Versus Referred Horsepower for Three Nozzles (Four Tests) and Compared With T53 and T55 Engines.

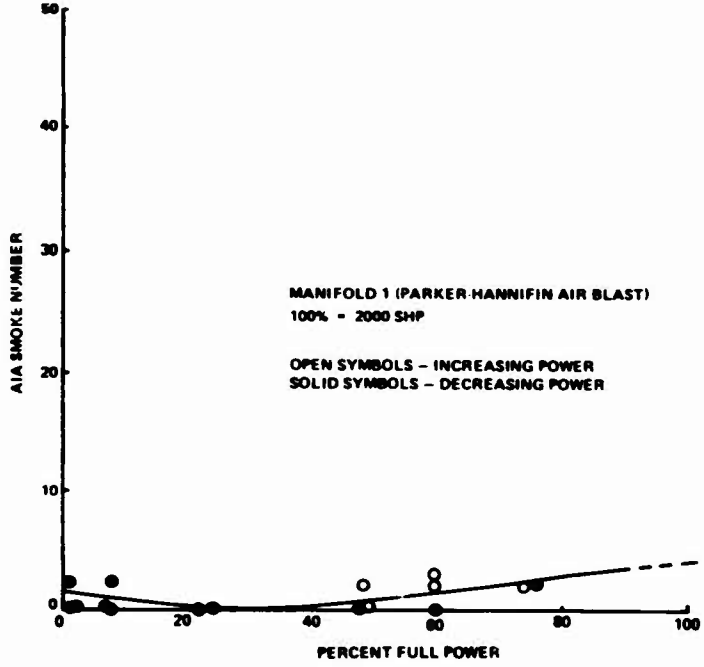

Figure 43. AIA Smoke Number Versus Percent Full Power for Engine P2-J, Manifold 1.

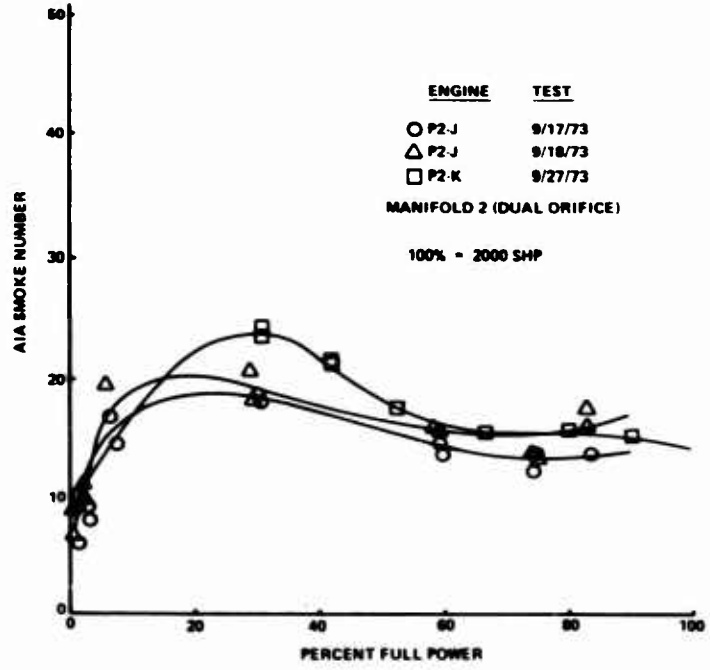

Figure 44. AIA Smoke Number Versus Percent Full Power for Engines P2-J and P3-K, Manifold 2.

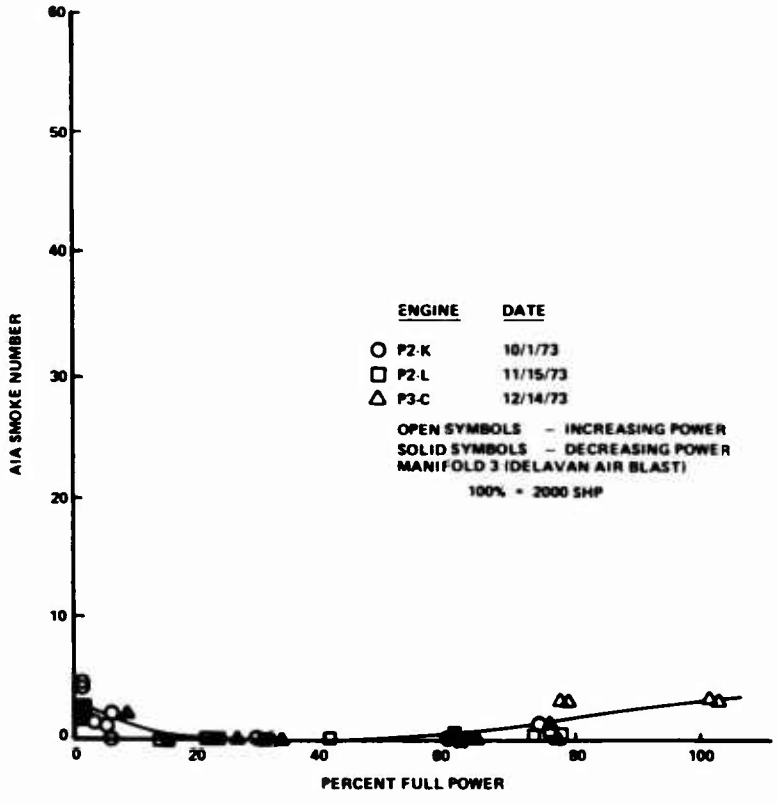

Figure 45. AIA Smoke Number Versus Percent Full Power for Engines P2-K, P2-L, and P3-C, Manifold 3.

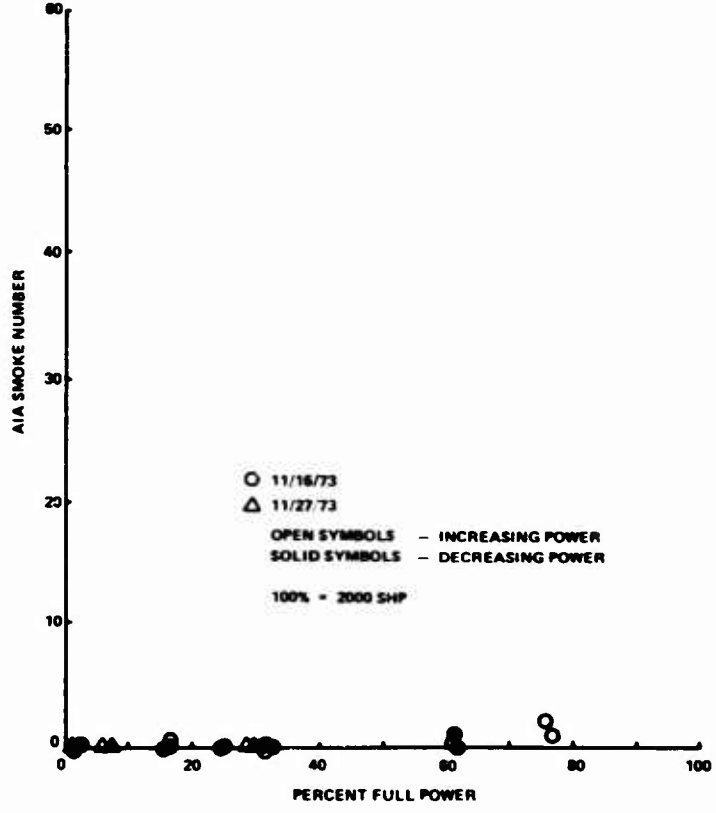

Figure 46. AIA Smoke Number Versus Percent Full Power for Engine P2-L, Manifold 1 Repeat (Test 4).

The results show that:

1. Manifold 1 (Parker-Hannifin air-blast) produces a smoke number of 3 or less in both Test 1 and Test 4, 2-1/2 months later.

2. Manifold 3 (Delavan air-blast) produces smoke numbers less than 5 in the operating range.

3. Manifold 2 (Parker-Hannifin dual-orifice) produces a smoke number in the range of 19 to 24 at 20 to 30 percent of full power, possibly visible, but not observed. At 50 to 100 percent of full power, the smoke number is 12 to 17, not visible.

Obviously, the air-blast fuel injectors (Manifolds 1 and 3) are much superior to the dual-orifice injector in producing low smoke emission.

Based on known characteristics of dual-orifice and air-blast injectors, it is probable that the air-blast injector produces better fuel and air mixing than the dual-orifice injector does, plus the reduction of high local fuel concentrations. Both of these factors tend to reduce smoke.

Engine Operational Limits

A combination of circumstances prevented the recording of emission data at the PLT 27 maximum power for all the configurations. Emission measurement evaluation was not affected, however, for two reasons. First, the combustor inlet temperature associated with maximum power was always reached, making is possible to compare NO_x values. Secondly, at high power, CO and HC values are both small and nearly invariant with power, making extrapolation easy.

An important limitation in engine maximum power occurred with Manifold 2, the dual-orifice configuration. Previous engine test experience had indicated the advisability of limiting the gas temperature spread at Station 7, just forward of the power turbine. The maximum allowable local temperature was reached with Manifold 2 before maximum power was reached. This would imply a poor circumferential temperature distribution with this combustor configuration which would require additional development before it would be suitable for extended engine operation. Both of the air-blast configurations were satisfactory, suggesting that combustor pattern factor is naturally better than with dual-orifice injectors, which are subject to carbon fouling, as discussed next.

Effect of Fuel Nozzle Characteristics on Power Turbine Inlet Peak Temperature

Measured peak T_7 temperatures showed that the Parker-Hannifin air-blast injector produces appreciably lower peak temperatures than either of the other two injectors (Figure 47). The Delavan is next, and the dual-orifice produced T_7 temperatures high enough to preclude operation at full engine power. Functional testing of the fuel injectors both before and after engine test resulted as follows (Reference 15):

1. Manifold 1 - Parker-Hannifin Air-Blast.
   First Test: ± 3% flow variation between nozzles. (11/16/73)

   Second Test: Two nozzles 8% low flow at positions 15 and 16. Remainder ± 3% from average.

2. Manifold 2 - Parker-Hannifin Dual-Orifice.
   First Test: Spray quality good. Primary flow variation ± 5%. (6/1/73) Secondary flow variation -3 to +4%.

   Second Test: Typical deterioration of spray quality. (11/27/73) Primary flow variation -13 to +6%. Nozzles at positions 8, 14, and 16 are low on flow. Secondary flow variation was -24 to +6%. Nozzles at positions 8, 13, and 14 were deviant. No mechanical damage - deviation was caused by carbon fouling.

3. Manifold 3 - Delavan Air-Blast.
   First Test: Flow variation was -2 to +3.5%. (9/18/73)

   Second Test: Performance was the same as for the (10/16/73) First Test (9/18/73).

   Third Test: Flow variation was insignificant from First (11/12/73) Test.

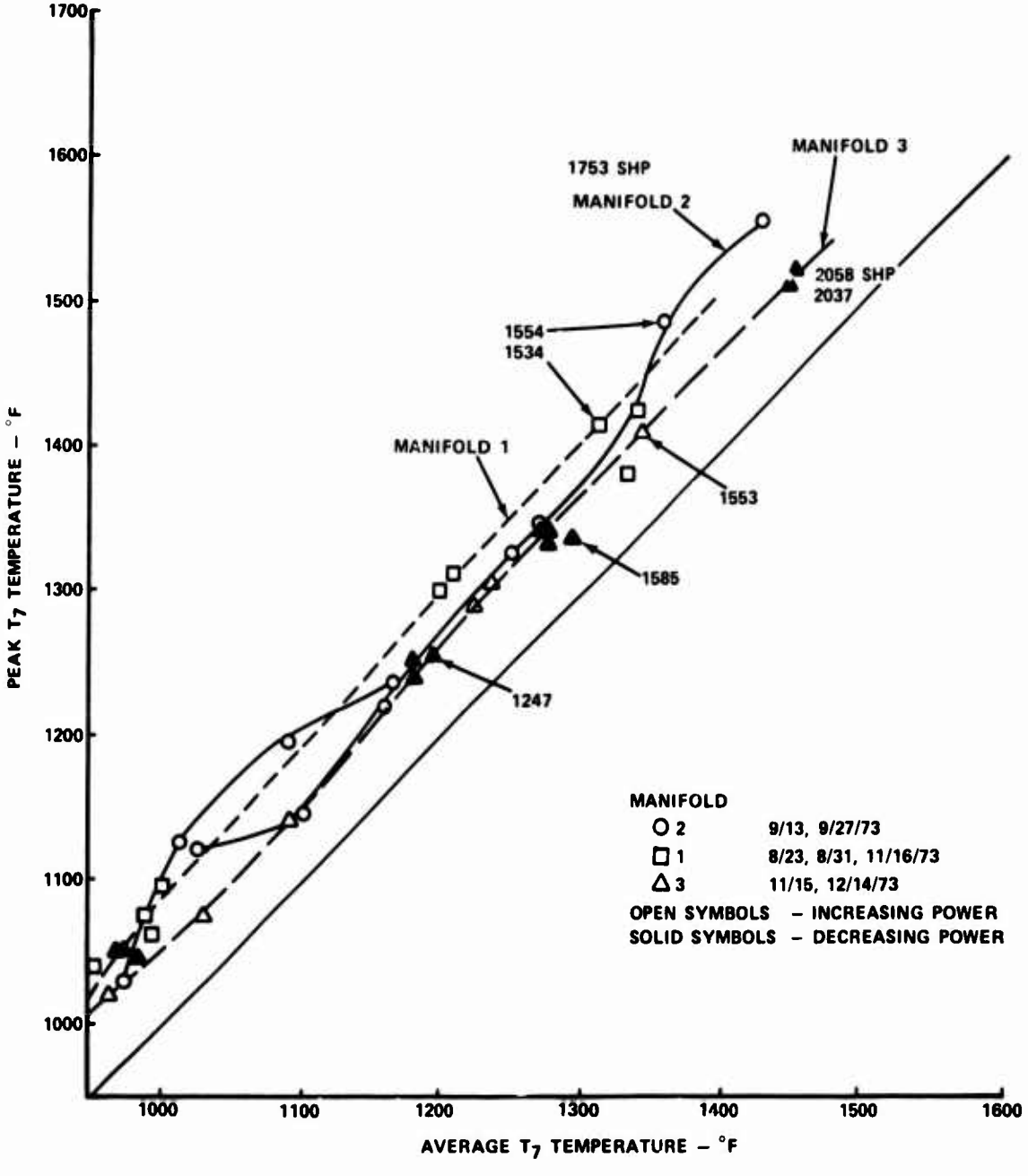

Figure 47. Comparison of Average and Peak T_7 Temperatures for Three Manifolds.

From these tests, we conclude that:

1. The changes in performance of the air-blast nozzles were not large enough to affect T_7 temperature appreciably.

2. The three deviant dual-orifice nozzles may have contributed to the high peak T_7, but it is not known to what extent. However, these nozzles are more susceptible to carbon fouling than air-blast nozzles, and the flow variation was obviously caused by carbon fouling.

CONCLUSIONS AND RECOMMENDATIONS

Conclusions reached from analyzing these data are divided into categories, as follows:

Engine and Combustor Emission Performance

1. The PLT 27 is a low emission producing engine in its present stage of development, particularly with respect to CO and HC emissions, using any of the three fuel injectors tested. It produces somewhat more NO_x than the average of a group of gas turbine engines investigated and reported by Lipfert, but still mostly within the band spread of these engines.

2. All three of the fuel manifolds tested produced less CO and HC pollutants, but more NO_x, than the T53 and T55 engines in tests recently reported.

3. Both the Delavan and Parker-Hannifin air-blast fuel injectors produced significantly less smoke than the dual-orifice injector, which was still well below the threshhold of visibility. Both air-blast injectors produced AIA smoke numbers of the order of 0 to 5.

4. The Parker-Hannifin air-blast injector produced slightly lower emissions than the Delavan air-blast for a portion of the low power operating range, or 2 to 15% of full power. Both air-blast injectors produced similar NO_x values, slightly higher than the dual-orifice injectors.

5. The Parker-Hannifin air-blast injector produced a lower peak temperature at the power turbine inlet than the other two injectors. The dual-orifice peak temperature was excessive

and limited the peak power that could be obtained from this engine. Therefore, air-blast injection appears preferable for this combustor configuration from the standpoint of turbine temperature.

Reliability and Repeatability of Data

1. Emission levels from engine tests on different days were remarkably consistent. This demonstrates the consistency of operation of the engine, combustion system, and of the measurement system.

2. Variations in emission levels produced during repeat runs were well within the experimental error. This indicates that the effect of engine build variation on emission generation was too small to be firmly detected with existing methods of measurement.

Corrections and Correlations

1. Corrections for NO_x measurements to a reference humidity level were easily applied, and can be adopted as standard practice. NO_x data for a specific engine was successfully correlated against combustor inlet temperature.

2. Exhaust gas analysis was used to obtain a measure of the interstage bleed, and to check the air-bleed flowmeter.

3. The combustor loading parameter, θ, was used to relate to a corresponding combustion efficiency and CO-HC concentrations. These concentrations, plus NO_x values, were then used with an Army helicopter duty cycle to arrive at a "cumulative cycle emissions value" for this engine.

Measurement Observations

1. Accuracy of the complete sample was determined by comparing the F/A from engine input measurements to F/A calculated from gas analysis. In many cases, agreement between the two was of the order of 0 to 3%, and in no case higher than 5%. Calculated probable error between the two measurements was $\pm 6\%$. These results are well within the SAE ARP 1256 specifications of +15%.

2. Good agreement was obtained between NO measurements from the chemiluminescence (Scott) and NDIR (MSA) instruments at the high power range. However, at low power, the MSA readings were usually higher by 2 to 5 ppm, and in some cases up to 9 ppm. A physical reason for the difference has not been determined.

3. The data indicated low values of NO_2. Attempts to separate NO_2 from the NO_x data produced mostly random values of 0 to 8 ppm of NO_2 for Manifolds 1 and 2. More definite trends were observed for Manifold 3, with no explanation available. The total concentrations ranged from 1 to 13 ppm, while NO_x varied from 20 to 300 ppm. The only conclusion we can draw is that NO_2 never exceeded a value of about 13 ppm. Considering that there is, as yet, no accepted chemical kinetic sequence developed to account for NO_2 production in a gas turbine engine, the justification of any NO_2 measurements may be only a quirk of the sampling and measurement system, and may not be significant, even then, from a pollution standpoint.

4. An apparent "hysteresis" of the hydrocarbon content was observed during cyclic engine operation. The cause was found to be residual hydrocarbons in the sample line, which required time to purge. The effect was measured by frequent zero reference procedures. The problem is that <u>any</u> sample line length will collect unburned hydrocarbon residuals. When hydrocarbons are increasing, equilibrium is quickly established. However, when hydrocarbons are decreasing, the walls of the sample line reluctantly part with the large hydrocarbon molecule residents. The residuals can be reduced, but not eliminated, by

    a. Keeping the sample lines short

    b. Maintaining a higher sample line temperature

    c Maintaining a high sample flow velocity

    The method used in these tests, frequent zero reference recording, is a good method of eliminating the effect of sample line residuals. There is no quantitative check for hydrocarbon residuals now specified in SAE ARP 1256 or EPA regulations known at this time. Perhaps a check method of this type is needed.

Recommendations

In view of the data, analysis, and conclusions, recommendations can be made as a result of this work. Some are specific as regards the engine, and other pertain to procedures and improved methods of analysis:

1. The PLT 27 engine exhibits excellent low pollution generation qualities. As a turboprop, it will meet the 1979 EPA requirements for P-2 class engines.

2. Air-blast injection should be further investigated to capitalize on the low pollution and low turbine peak temperature properties of these injectors.

3. The sample line design method should be specified such that design pressures and temperatures are maintained at specified parts of the sample line in order to ensure that sample line velocity does not vary. This is primarily to reduce HC absorption and "chromatographic" effects. Frequent zero references should be recorded to eliminate the effect of any sample line residual hydrocarbons.

4. The discrepancy between NO from chemiluminescence measurements and NO from NDIR should be investigated to determine whether it is a chemical, sampling line, or detection problem. In addition, a serious effort to pinpoint any possible NO_2 formation mechanisms would be useful.

NOISE MEASUREMENT AND ANALYSIS

TEST SETUP

Test Arrangement

The PLT 27 engine noise measurements were performed on the Lycoming acoustical test site. This test site provides a large level and clear acoustically reflecting asphalt surface and service buildings for engine operation and data acquisition.

The engine was installed on an elevating and rotating platform as shown in Figure 48.

An array of five microphones was first positioned on a 200-foot radius arc, centered on the engine center of gravity, and then on an arc having a 100-foot radius. The microphones were spaced at 10-degree intervals, thus subtending a total angle of 40 degrees. In addition, a near-field microphone was placed 10 feet away from the engine centerline.

In order to obtain full polar measurements of 180 degrees with one microphone overlapping in each engine position for data validation, the engine was rotated in five separate 40-degree intervals relative to the fixed microphone positions.

The engine centerline and the microphones were placed 7-1/2 feet above the asphalt surface.

A diagram of the test arrangement is given in Figure 49.

Test Equipment

The noise measurement was performed with PLT 27 engines, P2 and P3, equipped with the calibration bellmouth and the reference tail pipe.

Engine power was absorbed by a Lycoming waterbrake supported from the engine by four calibrated strain-gaged beams to provide the output torque indication.

The noise data acquistion equipment consisted of:

a) Six B and K Model 4131 microphones with B and K Model 2619 microphone preamplifiers for the primary sound signal acquisition.

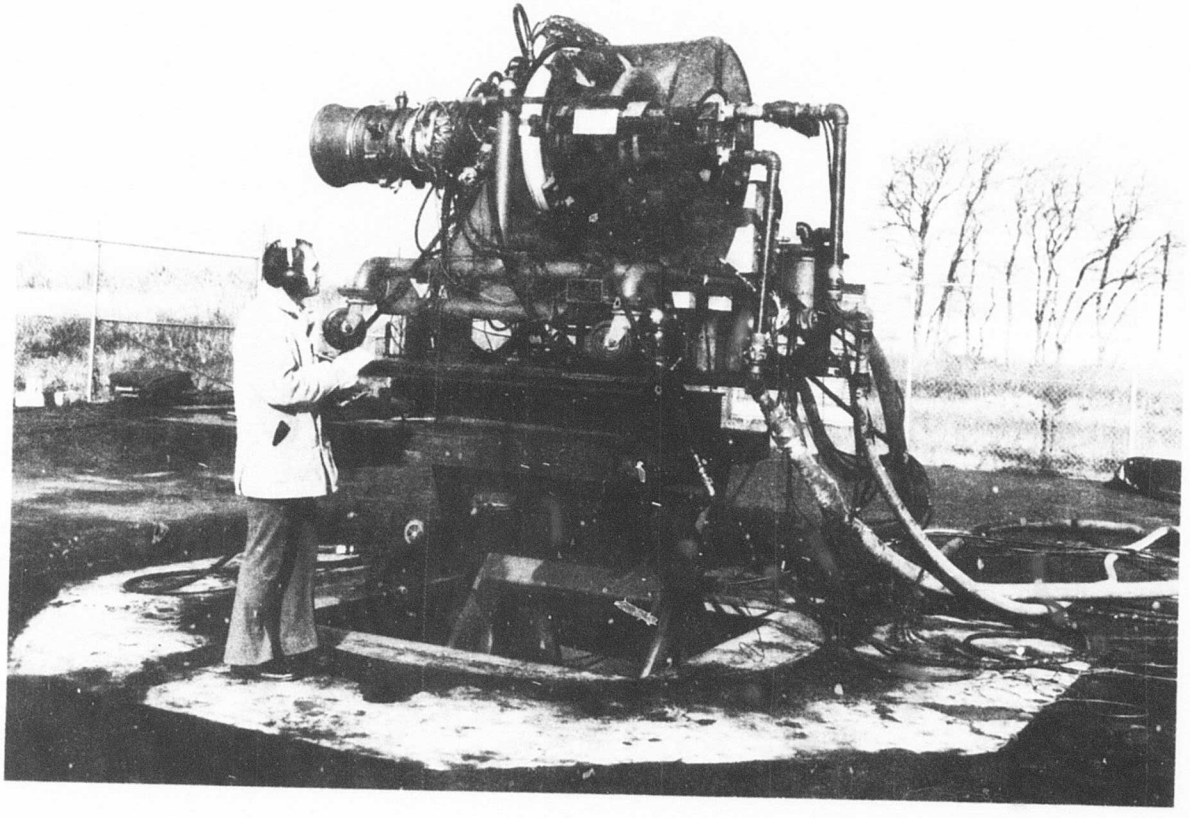

Figure 48. PLT 27 Engine Installed for Noise Measurement Test.

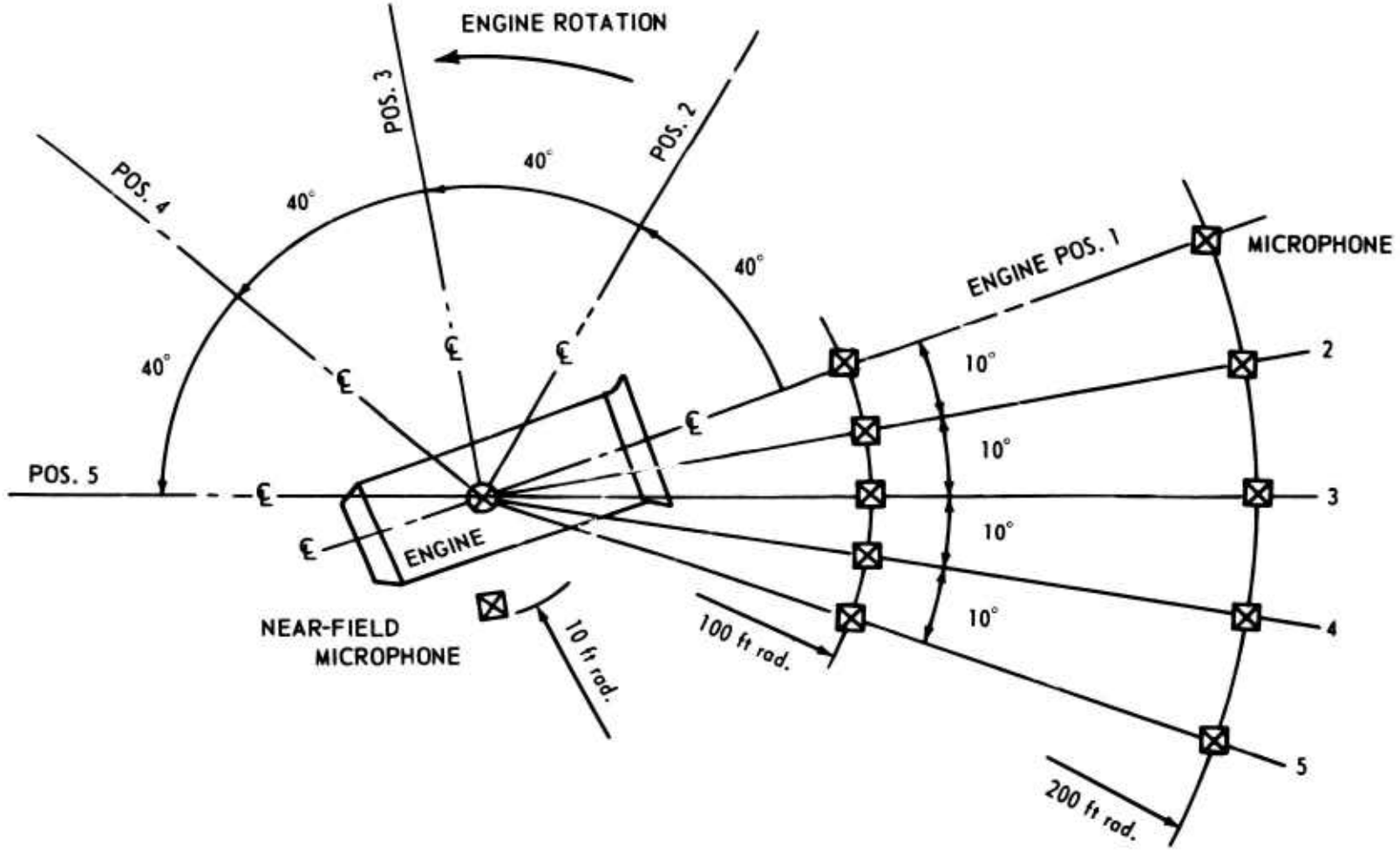

Figure 49. Noise Measurement Test Arrangement.

b) Four B and K Model 2803 microphone power supplies for delivering power to the preamplifiers, polarizing voltage to the condenser microphones, and converting the output impedance of the preamplifiers to a much lower impedance to accommodate the use of long cables.

c) Six B and K Model 2203 precision sound level meters acting as decade attenuators to the incoming signal and for instantaneous monitoring of the engine noise level.

d) A Sangamo Model 3500 14-channel instrumentation tape recorder for acquistion and storage of the analog noise signal. The taped information was used for the further analysis of the noise characteristics.

e) A dual-beam oscilloscope for immediate on-site monitoring of the input and output sound signal quality of the Sangamo Model 3500 tape recorder.

The microphones were calibrated before and after each test run with a B and K Model 4220 pistonphone.

The overall accuracy of the acquisition system is ± 0.5 dB. Figure 50 is a schematic of the noise measurement and data acquisition system.

Test Procedures

The noise produced by the engine at idle, 30, 60, 75, and 100 percent of maximum rated power was measured and recorded on the Sangamo Model 3500 tape recorder for a time period of 2 minutes at each power setting. The input signals to the tape recorder were continually monitored by the sound level meters and by the oscilloscope. The initial noise measurements were made with the engine centerline lined up with microphone No. 1. Then the engine was rotated through four 40-degree intervals to accomplish full polar measurement of the noise. The power series from idle to maximum power was run at each of the resulting five engine positions. (See Figure 49.)

The full far-field polar noise measurements were conducted with the array of microphones first placed at 200 feet and then at 100 feet away from the engine's center of gravity. Measurements at 100 feet were made to provide a check on the attenuation of the engine noise levels with distance. One microphone was placed 10 feet away from the engine center to measure near-field noise.

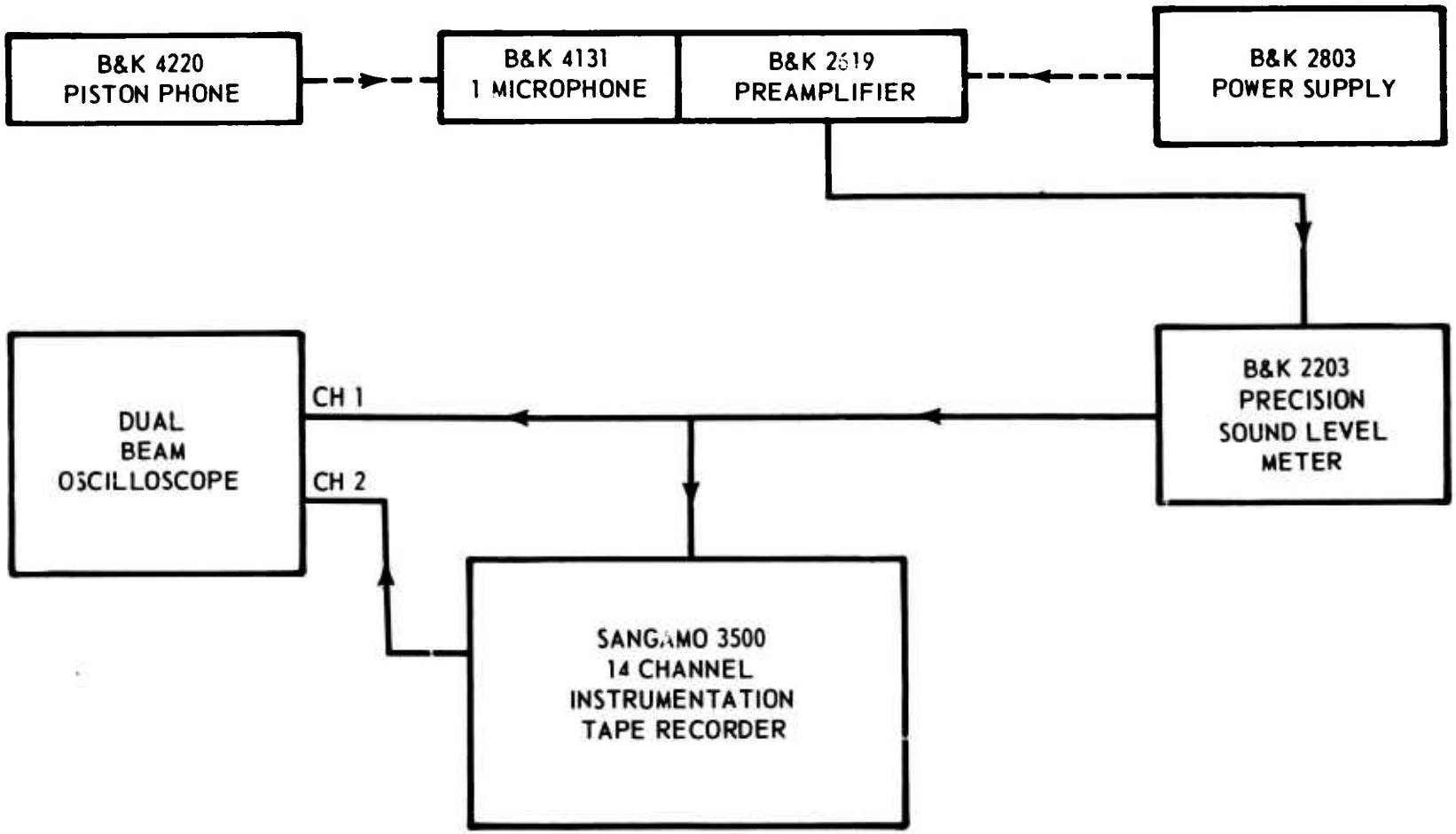

Figure 50. Schematic of Noise Acquistion System.

In addition to the acoustic data, the ambient temperature, the atmospheric humidity, and the wind velocity and direction were recorded to determine the correction for the atmospheric attenuation of the acoustic signal traveling from the engine to the microphones. The engine rotor speeds at the prescribed power setting were recorded to permit identification of the engine noise sources.

No noise measurements were made if any of the following atmospheric conditions existed: (a) ambient temperature was below 41°F or exceeded 90°F, (b) wind velocity exceeded 10 mph, and (c) relative humidity was below 10 percent or exceeded 90 percent.

This test procedure complies with MIL-E-5007D (Section 4.6.4.10) with the exception of the maximum allowable wind velocity and the minimum allowable relative humidity.

ANALYSIS

To determine the acoustic characteristics of the engine, the data recorded during the engine test were subjected to a 1/3-octave band spectrum analysis and a narrow-band (40 Hz) width spectrum analysis.

The 1/3-octave band analysis yields the engine sound pressure levels in the particular frequency bands of 1/3-octave width within a frequency range from 22.4 to 11200 Hz. The 1/3-octave band sound pressure levels are used to compute the perceived noise levels (PNL), the tone corrected perceived noise levels (PNLT), and the overall "A" weighted sound pressure level (dBA).

This analysis was performed by feeding the tape recorded noise information into a real time 1/3-octave band spectrum analyzer yielding the 1/3-octave band sound pressure levels. These pressure levels were averaged over time to ensure their stability and repeatability. The time averaged sound pressures were then used to calculate PNL, PNLT, and dBA, using an acoustical computer program.

The analyzing system is presented schematically in Figure 51.

The narrow-band analysis of the noise signal identifies the sources of the engine noise.

The narrow-band analysis was conducted by putting the tape recorded noise data through a real time spectrum analyzer and time averaging the sound pressure between zero and 20 KHz, using a 40-Hz bandwidth. The results were plotted as sound pressure versus frequency.

The narrow-band analyzer system is also shown schematically in Figure 51.

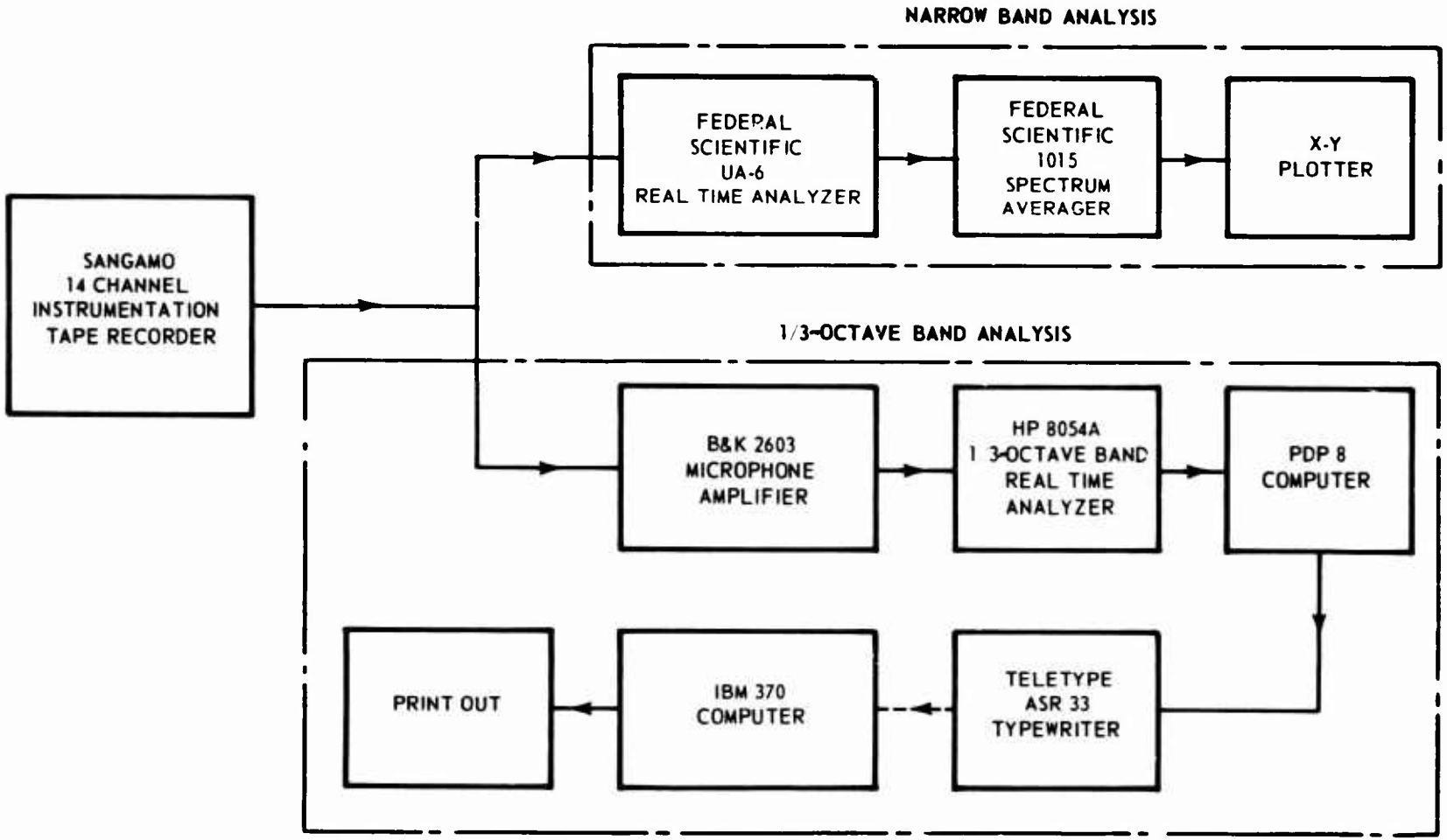

Figure 51. Schematic Analysis System.

RESULTS

The far-field (200-foot radius) 1/3-octave band and dBA noise levels are given in Tables 7 through 11. The sound pressure levels at polar locations around the engine are shown for the tested engine power levels in Figures 52 through 56. These plots indicate an overall sound pressure level peak in the 115-degree position for all engine power settings.

The narrow-band characteristics identify discrete sources of noise, such as the blade passage frequency of the first compressor rotor and the last power turbine rotor.

The sources of the discrete tone peaks were identified by using the equation

$$M = \frac{F}{N}$$

where M = integer order of shaft speed

F = discrete tone frequency, Hz

N = shaft speed, cps

If M = 1, 2, 3, ... (an integer order of engine speed), when N = low pressure compressor shaft speed, this indicates the presence of multiple pure tones caused by a transonic tip velocity on the first compressor rotor.

If M = nB, where n = 1, 2, 3, ... (harmonic integer) and B = number of rotor blades, then F = NM = NnB; this indicates the presence of a multiple of the blade passage frequency.

The tabulation below shows how the blade passage frequencies of the compressor rotor and second power turbine rotor were derived by using B and N.

	SHP	B	N	F
First-Stage Compressor Rotor	1500	26	4960	12900
	2000	26	5320	13820
Second-Stage Power Turbine Rotor	1500	56	2990	16750
	2000	56	3240	18200

TABLE 7. FAR-FIELD (200 FT RADIUS) ONE-THIRD OCTAVE BAND AND dBA NOISE LEVELS - IDLE

MICROPHONE RADIUS = 200. FEET, TEST TEMPERATURE = 41. F, TEST RELATIVE HUMIDITY = 65. PCT
DATA IS CORRECTED TO 59. F AND 70. PCT RELATIVE HUMIDITY ATMOSPHERIC ABSORPTION

FREQ HZ	SPL AT AZIMUTH ANGLE (DEG) AND RADIUS OF 200. FEET																	PNL RE 10**-12 W
	0.	10.	20.	30.	40.	50.	60.	70.	80.	90.	100.	110.	120.	130.	140.	150.	160.	170.	180.	
25.	66.0	65.0	65.0	63.0	64.0	70.5	69.0	68.0	67.0	62.0	61.0	62.0	60.0	64.0	61.5	58.5	61.0	73.0	71.0	111.5
32.	63.0	62.0	62.0	59.5	60.5	65.0	64.5	63.0	62.5	59.5	59.0	60.0	58.5	61.5	59.0	57.0	59.5	66.5	64.5	107.8
40.	61.0	58.5	59.5	56.5	58.0	58.5	59.5	59.0	58.0	57.5	57.5	58.0	57.5	60.5	60.5	58.0	61.0	61.0	60.0	105.8
50.	58.5	56.0	58.0	56.0	54.5	60.5	61.0	60.0	59.0	59.0	58.5	60.0	57.5	60.0	60.0	59.0	61.5	61.0	60.0	105.9
63.	62.0	59.0	65.0	65.0	60.0	60.0	65.0	65.5	59.0	58.5	64.5	65.5	57.0	57.5	62.0	63.5	58.5	59.5	62.0	108.9
80.	70.0	70.0	71.0	70.0	70.0	60.5	61.0	60.0	59.0	59.5	59.0	59.0	57.0	60.0	59.5	58.0	60.5	64.0	67.5	111.7
100.	60.0	60.5	61.0	60.5	61.0	58.0	58.5	57.5	57.0	58.5	57.0	57.5	55.0	61.0	61.0	59.5	62.0	61.0	64.0	106.3
125.	60.0	60.0	60.5	59.5	60.0	60.0	59.5	59.5	59.5	59.0	58.5	58.0	57.0	58.5	59.5	56.5	61.0	60.5	61.0	105.9
160.	63.5	64.0	65.0	64.0	63.5	62.0	62.5	62.5	61.0	62.0	63.5	64.0	63.5	62.5	62.0	60.5	63.5	63.5	65.5	109.6
200.	60.5	61.0	62.0	61.0	60.5	60.0	61.5	61.5	60.0	62.5	64.0	63.5	61.0	60.5	60.5	59.5	62.0	61.5	63.5	108.0
250.	58.5	65.5	70.0	71.0	71.5	65.0	64.0	60.5	59.5	59.5	60.0	59.5	59.5	56.5	56.0	53.5	57.5	62.0	65.0	111.3
315.	57.0	62.0	66.0	66.5	67.0	53.5	55.0	56.5	55.5	53.5	55.0	56.5	54.0	55.5	55.5	55.5	57.0	55.0	60.5	107.0
400.	55.3	56.0	56.0	56.0	56.5	52.5	51.5	54.0	53.5	52.5	53.0	54.5	54.0	56.0	56.5	54.5	57.5	58.0	62.0	101.7
500.	54.0	54.5	55.5	55.5	55.5	52.0	52.0	52.5	52.0	51.0	52.5	53.0	52.0	54.0	54.0	52.5	55.5	57.5	60.0	100.3
630.	55.0	55.0	55.0	54.0	54.0	52.5	52.0	51.5	50.5	54.0	55.5	57.5	56.5	56.5	55.0	50.5	52.5	54.0	57.5	100.7
800.	58.5	58.0	58.0	56.0	55.5	56.0	55.0	53.5	53.0	58.0	60.0	61.0	61.0	60.0	58.0	51.5	53.0	54.0	57.0	103.9
1000.	59.5	59.5	60.0	59.0	57.0	60.5	58.5	57.0	57.0	59.5	61.5	63.5	63.5	63.0	60.0	53.5	54.0	53.0	57.0	106.3
1250.	59.5	59.0	59.0	59.5	59.0	60.5	58.0	58.5	59.0	58.5	59.5	62.0	63.0	61.0	58.0	52.5	53.5	52.0	55.5	105.7
1600.	58.6	58.1	58.6	59.6	60.6	59.1	59.1	60.1	59.1	59.6	56.1	58.6	59.1	57.1	55.6	51.1	52.6	50.6	54.6	104.4
2000.	62.8	62.3	60.3	59.8	57.8	57.8	56.8	56.3	55.3	56.3	57.3	59.3	59.8	57.8	55.3	51.8	52.8	50.8	53.8	104.5
2500.	64.5	63.5	61.4	60.9	59.4	58.9	55.9	54.9	55.4	55.9	55.4	59.4	60.4	57.4	54.9	51.9	52.5	51.4	52.9	105.3
3150.	63.7	62.2	58.7	59.2	58.2	57.7	52.7	54.2	53.2	56.2	54.2	58.7	59.2	57.7	55.2	51.2	52.2	50.7	51.2	103.9
4000.	65.1	62.1	56.1	56.6	56.1	57.6	51.1	51.6	50.6	55.6	52.1	56.1	57.1	55.6	53.6	49.1	50.1	48.1	49.1	102.9
5000.	61.8	56.8	52.3	53.8	58.3	52.3	45.8	46.8	51.3	49.3	47.3	51.8	58.3	50.3	47.8	52.3	46.3	42.3	41.3	100.1
6300.	60.8	59.8	57.3	59.8	62.3	59.3	54.8	54.8	58.8	55.8	55.8	59.8	65.8	59.8	53.8	60.8	48.8	47.3	44.8	105.7
8000.	66.5	63.5	62.0	66.5	64.0	60.5	53.5	54.5	55.5	54.5	53.0	57.0	60.0	56.0	53.0	57.0	50.0	47.5	47.0	106.6
10000.	70.3	64.3	58.3	61.8	66.3	61.3	53.8	54.3	54.3	57.3	53.3	57.3	58.8	59.3	58.3	60.3	48.8	45.8	50.3	108.8
CASPL	77.1	76.0	76.8	77.0	76.8	73.0	72.3	72.0	70.7	71.3	72.4	73.7	73.7	72.4	71.5	71.7	70.9	71.5	74.3	120.3
DB(A)	74.5	72.5	71.3	72.3	71.8	70.3	67.7	67.6	67.7	68.1	68.5	71.0	72.5	70.2	67.7	67.2	64.7	64.3	67.1	
PNL	78.8	87.3	85.7	86.5	85.5	83.8	81.1	81.1	81.6	81.8	81.3	84.3	86.6	83.4	81.3	81.6	78.8	78.1	80.1	
PNLT	89.3	87.9	86.7	87.7	87.2	85.1	82.0	81.8	82.5	82.5	82.2	85.2	87.7	84.5	81.9	82.5	78.8	78.8	80.7	
THE FOLLOWING TWO LINES ARE FOR A 200. FOOT SIDELINE RATHER THAN A CONSTANT 200. FOOT RADIUS																				
PNL		87.1	74.3	78.8	81.1	81.1	79.6	80.5	81.4	81.8	81.1	83.6	85.1	80.6	76.9	73.7	67.4	61.5		
PNLT		87.7	75.3	80.0	82.4	82.4	80.6	81.2	82.2	82.5	82.1	84.6	86.2	81.8	77.4	74.6	67.4	62.6		

TABLE 8. FAR-FIELD (200 FT RADIUS) ONE-THIRD OCTAVE BAND AND dBA NOISE LEVELS - 600 SHP

MICROPHONE RADIUS = 200. FEET, TEST TEMPERATURE = 41. F, TEST RELATIVE HUMIDITY = 65. PCT
DATA IS CORRECTED TO 59. F AND 70. PCT RELATIVE HUMIDITY ATMOSPHERIC ABSORPTION

FREQ HZ	SPL AT AZIMUTH ANGLE (DEG) AND RADIUS OF 200. FEET																		PWL RE 10^{**-12} W
	C.	10.	20.	30.	40.	50.	60.	70.	80.	90.	100.	110.	120.	130.	140.	150.	160.	170.	180.	
25.	63.0	62.5	64.0	62.5	63.0	71.5	70.5	69.5	67.5	61.5	61.5	60.5	60.0	63.5	65.5	61.5	63.0	72.0	70.5	112.1
32.	61.5	60.5	62.5	60.5	61.5	66.5	65.5	65.0	63.0	58.5	59.0	58.0	58.0	62.0	63.0	59.5	61.0	67.0	65.5	108.7
40.	61.5	59.5	61.5	59.0	61.5	59.0	59.5	59.0	57.0	55.0	58.0	58.0	61.0	62.5	59.0	61.5	62.0	62.0	62.0	106.6
50.	60.5	59.5	61.5	60.5	61.0	60.5	61.5	61.0	59.5	60.0	61.5	61.5	61.0	62.0	63.5	60.5	63.0	63.5	63.5	107.9
63.	61.5	61.0	66.0	66.0	63.0	62.0	66.5	66.5	63.5	64.5	68.0	67.5	65.0	64.5	64.0	62.0	64.5	66.5	67.0	111.5
80.	66.0	65.5	67.0	66.0	67.0	63.0	64.5	64.0	63.5	66.5	68.0	68.5	67.0	65.5	64.5	62.0	65.5	63.5	63.5	112.5
100.	62.5	63.5	64.0	64.5	64.0	64.0	65.0	64.5	64.0	66.5	67.0	67.0	66.5	65.5	64.0	61.5	65.5	64.0	64.5	111.4
125.	65.5	66.0	66.5	66.0	66.0	66.0	66.0	66.0	65.5	67.0	67.5	67.0	67.5	67.0	65.0	62.0	65.5	65.5	65.5	112.6
160.	68.5	7.5	70.0	69.0	68.5	69.5	69.0	68.5	68.0	69.0	70.5	71.5	72.0	72.0	69.0	65.5	66.5	66.5	67.0	115.8
200.	68.0	68.5	70.0	68.5	68.5	68.0	69.0	69.0	69.0	72.5	73.5	72.5	72.0	72.5	69.0	64.5	64.0	63.5	64.0	116.2
250.	64.5	65.5	66.0	65.0	65.5	64.5	65.5	65.5	66.0	66.5	67.5	68.5	69.0	70.0	67.0	61.5	61.0	61.5	61.5	112.6
315.	63.5	63.0	64.5	66.0	68.0	67.5	67.0	63.5	64.0	61.5	64.5	64.5	65.5	67.0	65.0	59.5	59.5	58.5	63.0	111.2
400.	64.0	61.5	62.5	64.0	66.0	64.5	63.0	63.5	59.0	63.5	63.0	62.5	66.0	63.5	62.0	63.5	59.5	59.5	62.0	109.8
500.	63.0	58.5	62.0	63.5	66.0	63.0	60.5	61.5	55.0	57.5	62.5	61.5	58.5	64.5	60.5	59.5	61.5	58.5	61.0	108.3
630.	55.0	56.5	56.0	55.5	56.5	57.0	59.0	56.0	55.5	58.5	59.0	59.0	59.5	64.5	60.0	55.5	56.0	58.0	56.5	104.2
800.	60.5	60.5	62.0	63.0	62.5	63.0	62.0	60.0	60.5	63.5	66.5	67.0	68.0	68.5	62.5	57.5	57.0	56.5	56.0	110.1
1000.	62.0	62.0	63.5	64.5	64.5	64.5	63.5	63.5	64.5	65.5	68.5	70.5	71.5	70.0	66.0	58.5	57.5	56.5	56.5	112.5
1250.	58.5	59.5	59.0	61.0	63.0	61.5	60.0	61.0	60.5	61.0	63.5	68.0	69.0	65.5	61.0	56.5	55.5	55.5	56.0	109.3
1600.	56.1	55.6	56.6	57.6	58.6	57.6	56.1	56.6	56.6	57.1	58.1	62.1	63.1	62.1	57.1	53.6	53.1	52.1	53.1	104.7
2000.	55.8	5.8	62.8	62.3	59.8	60.8	59.8	57.8	57.8	60.3	60.3	62.8	63.8	62.8	57.8	54.8	54.3	54.3	55.3	106.8
2500.	61.4	6.4	60.9	60.9	61.5	61.4	58.5	57.5	58.4	58.9	58.4	62.4	63.9	61.9	57.4	54.4	53.9	55.4	57.5	106.5
3150.	61.7	60.2	57.7	60.2	58.2	58.2	54.7	55.7	55.7	58.7	57.7	61.7	63.2	62.2	57.7	54.2	54.7	56.7	59.7	105.4
4000.	64.1	60.6	56.6	58.1	58.1	63.1	54.1	55.1	54.1	58.6	56.6	60.6	61.6	61.1	58.1	53.6	54.6	58.6	62.1	103.3
5000.	60.3	55.8	51.8	54.3	57.8	54.3	47.8	49.3	54.8	52.8	52.3	56.3	62.8	54.3	49.8	53.8	47.8	50.8	53.3	101.8
6300.	59.3	58.8	55.8	57.8	61.3	55.8	52.3	52.8	57.8	54.8	56.3	55.8	65.3	56.8	49.8	57.8	46.3	52.8	52.3	104.4
8000.	63.5	60.0	58.0	59.5	60.5	58.5	53.5	55.0	57.0	58.0	58.5	62.5	64.5	60.0	54.5	58.5	50.0	55.5	56.0	103.6
10000.	65.8	59.3	55.8	58.8	58.3	57.3	51.3	53.3	54.3	56.8	55.8	70.8	61.3	59.8	55.3	56.8	51.3	53.3	55.3	107.4
CASPL	77.2	76.7	77.6	77.5	77.8	77.1	77.0	76.6	76.2	78.2	79.5	80.6	80.5	80.2	76.9	73.5	74.7	74.5	75.3	124.2
CB(A)	73.4	71.9	72.0	72.5	73.5	73.1	71.1	70.8	71.0	72.3	74.0	76.8	77.5	76.2	71.5	68.5	67.7	68.1	69.8	
PNL	86.5	86.5	86.2	86.8	87.4	87.7	84.6	84.3	84.5	85.9	86.9	89.7	90.3	89.1	85.0	82.7	81.7	83.4	85.6	
PNLT	89.5	86.5	87.5	86.8	88.5	89.8	84.6	85.3	85.8	86.9	88.4	90.5	91.6	89.1	86.5	82.7	81.7	85.1	87.4	
THE FOLLOWING LINES ARE FOR A 200. FOOT SIDELINE RATHER THAN A CONSTANT 200. FOOT RADIUS																				
PNL		86.3	74.9	79.6	82.0	84.5	83.2	83.1	84.3	85.9	86.7	89.0	88.8	86.5	80.5	75.0	70.3	64.6		
PNLT		86.3	76.3	80.6	84.0	87.0	83.2	84.7	85.7	86.9	88.2	90.2	90.1	86.5	81.9	75.0	70.8	66.4		

TABLE 9. FAR-FIELD (200 FT RADIUS) ONE-THIRD OCTAVE BAND AND dBA NOISE LEVELS - 1150 SHP

MICROPHONE RADIUS = 200. FEET, TEST TEMPERATURE = 41. F, TEST RELATIVE HUMIDITY = 65. PCT
DATA IS CORRECTED TO 59. F AND 70. PCT RELATIVE HUMIDITY ATMOSPHERIC ABSORPTION

FREQ HZ	SPL AT AZIMUTH ANGLE (DEG) AND RADIUS OF 200. FEET																		PWL RE 10**-12 W
	0.	10.	20.	30.	40.	50.	60.	70.	80.	90.	100.	110.	120.	130.	140.	150.	160.	170.	180.	
25.	70.5	71.0	71.0	69.0	67.5	62.0	62.5	60.5	70.5	71.5	70.5	70.0	69.0	62.0	60.0	58.0	59.0	68.5	66.5	114.3
32.	66.5	67.0	67.0	65.5	64.0	59.5	60.0	58.5	65.5	66.0	64.5	64.5	64.0	60.0	58.5	57.0	59.0	64.0	63.0	110.0
40.	62.0	60.5	62.5	60.5	60.5	57.0	58.5	57.0	65.5	66.0	66.0	66.0	66.0	67.5	59.0	58.5	57.0	60.0	61.5	62.0	109.2
50.	61.5	61.0	62.0	61.0	59.5	57.0	58.5	58.5	65.5	66.5	66.0	67.5	66.5	60.0	60.0	58.5	61.5	63.0	63.0	109.5
63.	61.0	60.5	66.0	66.5	60.5	59.5	65.0	66.0	65.0	66.5	68.5	69.5	67.5	62.0	63.0	62.0	62.5	63.0	63.5	111.6
80.	62.0	63.0	63.0	62.5	61.5	63.0	63.0	62.5	66.5	68.0	68.5	70.0	69.5	64.0	63.5	61.0	63.0	66.0	66.0	111.8
100.	63.5	64.5	65.0	65.0	64.5	64.0	65.5	64.5	67.0	68.5	68.5	70.5	70.5	65.5	64.5	61.5	63.0	67.0	67.0	112.8
125.	66.5	67.5	67.5	67.5	67.0	66.0	66.5	66.0	68.0	69.5	69.5	70.5	71.0	69.5	67.5	63.0	63.5	65.5	66.0	114.2
160.	70.5	72.0	71.5	71.0	70.5	70.0	71.0	70.5	71.0	72.0	72.0	74.5	75.5	75.5	73.5	68.5	66.5	70.0	70.0	118.2
200.	71.5	72.5	73.0	72.0	72.0	70.5	71.0	71.5	72.0	75.5	75.5	76.5	76.5	77.0	74.0	69.0	65.5	68.5	69.5	119.8
250.	68.0	69.0	69.5	68.0	68.0	66.5	68.5	68.5	69.5	70.5	70.5	72.0	73.0	74.0	72.5	66.5	63.0	68.0	68.5	116.2
315.	69.5	68.0	66.0	67.0	69.5	67.5	65.0	65.5	66.5	67.0	67.0	68.0	68.5	70.0	67.5	62.0	58.5	64.0	66.0	113.8
400.	63.5	63.0	61.0	60.5	62.0	60.5	60.0	62.0	61.5	63.0	62.5	64.5	65.0	66.5	65.5	61.5	58.5	62.0	63.0	109.1
500.	65.5	65.0	66.5	65.5	65.5	66.0	65.5	65.0	62.5	62.0	64.0	66.0	65.5	68.0	64.5	63.0	64.5	64.0	64.5	112.2
630.	57.5	58.5	57.5	59.0	59.5	62.0	62.0	56.5	59.0	60.0	62.0	64.0	64.5	64.5	59.5	55.0	54.5	61.0	60.5	107.0
800.	59.5	59.5	59.5	60.5	59.5	62.5	61.5	59.5	64.0	65.0	65.5	69.0	69.0	66.0	60.0	55.0	53.0	60.5	60.0	109.9
1000.	64.0	63.5	66.0	68.0	67.5	65.5	67.0	65.0	66.5	68.0	69.0	72.5	72.0	68.5	64.0	58.5	56.0	60.5	60.5	114.0
1250.	61.0	62.0	62.0	65.5	65.5	63.5	62.5	63.5	62.5	64.5	65.5	71.0	71.0	68.0	63.5	58.5	55.0	59.5	60.0	111.8
1600.	59.1	60.6	61.1	60.6	65.1	65.1	61.1	60.1	59.1	61.1	60.1	67.1	68.1	64.6	60.6	57.6	55.1	58.1	58.1	110.4
2000.	60.3	61.3	64.3	64.8	62.3	64.8	62.8	62.3	61.8	63.3	59.8	64.8	65.3	63.8	61.3	60.8	56.3	57.8	57.8	109.1
2500.	67.4	67.9	68.9	67.9	67.9	69.9	67.4	64.9	64.9	63.9	63.5	68.4	66.9	63.4	60.9	58.5	56.4	59.4	59.4	112.6
3150.	65.2	63.7	60.2	61.7	65.2	63.7	59.7	61.7	63.2	60.2	58.7	65.2	64.2	62.2	59.7	57.2	54.7	58.2	58.7	109.1
4000.	63.6	60.6	56.1	59.6	57.6	61.6	56.1	58.1	62.6	60.6	56.1	63.6	62.6	61.6	59.6	55.1	52.6	58.6	60.6	106.6
5000.	55.8	56.3	49.8	54.3	57.8	53.8	49.8	52.3	58.8	54.3	52.3	59.8	64.3	54.8	51.8	50.3	46.8	52.3	53.8	103.1
6300.	57.8	56.3	53.3	56.8	59.8	54.8	52.3	54.8	56.8	55.8	56.3	63.8	67.3	57.8	51.3	59.3	44.8	54.3	53.3	105.4
8000.	63.5	59.5	56.0	59.5	59.5	58.0	54.5	56.5	61.5	58.5	57.5	65.0	66.0	61.0	56.0	60.5	49.5	56.5	57.0	106.6
10000.	65.8	58.3	54.8	57.8	56.8	56.8	52.3	54.8	62.8	57.3	55.3	63.3	63.3	60.8	56.8	58.8	50.3	55.8	57.8	105.6
OASPL	79.1	79.3	79.5	80.1	79.5	79.1	79.0	78.7	79.3	80.7	81.0	83.3	83.5	82.6	80.1	75.9	74.0	77.3	77.8	126.5
DB(A)	75.4	74.8	75.1	77.2	76.9	76.7	74.9	74.0	74.8	75.2	75.3	75.4	79.5	77.2	73.8	71.0	67.8	71.4	72.0	
PWL	90.4	90..	0.0	91.2	90.8	91.2	89.5	88.2	89.4	89.0		93.1	93.0	90.4	87.3	85.0	81.6	85.6	86.6	
PWLT	92.1	91.5	92.5	94.5	93.7	93.2	91.7	90.3	90.6	90.	9.	.3	93.0	90.4	87.3	86.6	84.4	88.7	87.5	
THE FOLLOWING TWO LINES ARE FOR A 200. FOOT SIDELINE RATHER THAN A 200. FOOT RADIUS																				
PWL		70.6	78.9	84.1	86.4	88.6	88.1	87.7	89.2	89.0	88.7	92.5	91.6	87.5	82.9	77.8	70.4	66.5		
PWLT		72.5	81.3	87.4	85.2	90.7	90.2	89.1	90.4	90.2	90.3	93.7	91.6	87.9	82.9	79.4	73.1	69.5		

TABLE 10. FAR-FIELD (200 FT RADIUS) ONE-THIRD OCTAVE BAND AND dBA NOISE LEVELS - 1500 SHP

HELICOPTER RADIUS = 200. FEET, TEST TEMPERATURE = 41. F, TEST RELATIVE HUMIDITY = 65. PCT
DATA IS CORRECTED TO 59. F AND 70. PCT RELATIVE HUMIDITY ATMOSPHERIC ABSORPTION

FREQ HZ	SPL AT AZIMUTH ANGLE (DEG) AND RADIUS OF 200. FEET																		PNL RE 10**-12 W
	0.	10.	20.	30.	40.	50.	60.	70.	80.	90.	100.	110.	120.	130.	140.	150.	160.	170.	180.	
25.	73.5	72.0	70.5	69.5	68.0	63.0	63.5	62.0	60.5	61.5	61.0	61.5	61.0	73.0	70.5	67.5	68.0	69.5	66.0	114.5
32.	66.0	67.0	66.0	65.0	63.5	60.5	60.5	60.0	58.0	59.0	59.5	59.5	59.5	69.5	66.0	64.0	65.0	65.0	64.0	110.7
40.	60.5	60.0	60.5	59.5	59.0	58.0	58.0	57.5	57.0	58.0	58.5	59.5	59.5	65.0	61.5	60.0	62.5	63.0	63.5	107.9
50.	61.5	61.5	62.0	61.5	60.0	57.0	59.0	58.5	56.5	59.0	60.0	61.0	60.5	64.0	62.5	61.5	63.5	66.0	66.5	109.8
63.	62.5	63.0	63.0	63.0	62.5	58.5	65.0	76.0	58.5	61.5	66.0	67.5	63.5	64.5	65.5	66.0	65.5	65.5	67.5	113.6
80.	66.0	66.0	67.5	64.5	66.0	60.5	61.5	61.5	61.0	63.5	63.0	68.0	68.0	65.5	65.0	63.5	65.5	66.5	67.5	112.0
100.	63.5	64.0	64.5	64.5	64.5	63.5	64.5	64.5	64.5	66.5	66.5	68.0	68.0	66.0	65.0	62.5	64.5	67.0	67.5	111.7
125.	67.5	68.0	68.5	68.0	67.5	63.0	66.0	67.5	67.5	69.5	69.5	70.5	71.0	69.0	68.0	64.0	65.0	66.5	68.0	114.6
160.	71.0	72.5	72.5	71.5	71.0	71.5	72.0	72.5	71.5	72.5	73.5	76.0	76.5	75.0	73.5	68.0	66.5	78.0	76.5	119.1
200.	72.5	73.0	73.5	72.5	72.5	72.5	73.0	73.5	74.5	77.5	77.5	78.0	78.0	76.5	74.5	67.5	65.0	70.0	72.0	120.9
250.	69.5	70.5	71.0	69.5	70.0	65.0	71.0	71.0	72.0	72.5	73.0	74.5	75.5	74.5	73.0	64.5	64.5	68.0	70.5	118.0
315.	71.0	69.5	69.0	69.5	71.0	66.5	69.5	68.0	68.5	68.0	68.0	70.0	70.0	70.0	68.0	62.0	61.5	63.5	66.5	114.9
400.	65.0	64.5	62.5	62.0	63.0	62.5	62.5	64.0	63.5	63.0	63.0	65.5	66.5	67.5	66.5	60.0	59.5	62.0	63.5	110.3
500.	62.5	61.5	63.5	67.5	66.5	64.0	62.5	63.0	63.0	63.5	64.5	65.5	66.5	67.5	66.5	64.5	62.0	62.5	65.0	111.1
630.	59.0	60.5	60.5	60.5	59.0	61.5	62.0	59.0	59.0	65.5	64.0	66.5	68.0	66.5	62.5	57.5	57.0	59.0	59.0	109.2
800.	60.5	61.0	62.0	62.0	61.0	64.5	63.0	62.5	63.0	68.0	68.0	69.5	70.0	66.0	62.0	57.0	56.0	58.5	59.5	111.2
1000.	65.0	63.0	65.0	66.5	67.0	68.5	66.5	67.0	68.5	70.5	71.0	73.5	73.5	68.5	64.5	59.0	58.0	59.5	61.0	114.8
1250.	62.0	62.5	63.0	66.0	66.5	65.0	64.0	66.0	67.0	67.0	68.5	73.0	73.5	68.5	64.0	59.0	58.0	59.0	61.5	113.7
1600.	62.1	60.6	64.6	70.6	68.6	63.6	61.6	62.1	63.1	63.6	64.6	65.6	69.6	65.6	62.6	60.6	57.6	57.1	59.6	111.9
2000.	59.8	64.3	65.8	66.3	63.3	65.8	63.8	62.8	63.8	64.8	63.8	66.3	66.3	64.3	62.8	59.8	57.3	56.3	57.8	110.4
2500.	67.4	65.9	67.9	67.4	67.4	70.4	67.4	65.4	65.9	66.9	67.4	70.4	68.4	64.9	61.9	59.9	58.9	58.4	59.4	113.2
3150.	61.7	60.2	59.2	64.2	62.7	62.7	59.7	60.2	60.2	63.2	61.2	66.2	64.7	62.2	59.7	56.7	56.2	55.7	59.7	108.2
4000.	62.6	60.1	60.6	65.1	59.6	63.1	58.6	59.6	58.6	63.1	60.6	66.1	64.1	62.1	59.6	55.6	55.6	56.1	61.1	107.9
5000.	58.8	54.3	51.8	57.8	60.8	56.3	51.8	54.8	56.8	56.8	55.3	60.8	64.8	55.8	52.3	56.8	49.8	45.8	54.3	104.2
6300.	63.8	58.8	57.8	66.3	67.8	62.8	57.8	58.8	63.8	59.8	60.3	64.8	68.3	59.3	52.8	61.3	48.8	52.8	54.3	109.0
8000.	65.0	61.0	56.0	64.0	64.0	63.0	58.0	59.5	61.5	61.5	61.0	65.5	66.5	62.0	57.5	61.5	52.5	55.0	58.0	108.4
10000.	67.8	62.3	54.8	60.3	59.8	61.3	54.8	57.3	57.8	56.8	58.3	63.8	63.3	61.8	58.3	59.8	53.3	54.3	58.3	106.5
CASPL	80.0	79.9	80.4	80.8	80.6	76.5	79.9	81.3	80.4	82.2	82.5	84.4	84.7	82.6	80.8	76.2	75.2	80.4	80.6	127.5
CB(A)	75.7	76.7	75.6	77.5	77.3	77.2	75.3	75.2	76.2	77.6	77.8	80.9	81.0	77.6	74.8	71.6	69.2	71.3	73.0	
PNL	90.7	89.6	90.4	91.8	91.4	92.1	89.9	89.7	90.1	91.4	91.4	94.6	94.2	91.0	88.3	85.8	83.7	86.5	87.6	
PNLT	92.9	90.9	92.2	93.8	93.2	94.2	91.8	91.0	91.5	92.2	93.1	96.0	94.2	91.0	88.3	87.7	85.0	88.1	89.0	
THE FOLLOWING TWO LINES ARE FOR A 200. FOOT SIDELINE RATHER THAN A CONSTANT 200. FOOT RADIUS																				
PNL		76.1	79.3	84.7	86.5	85.4	88.5	89.1	90.0	91.4	91.3	94.0	92.7	88.4	83.9	78.8	72.4	68.6		
PNLT		71.5	81.1	86.8	88.8	91.5	90.4	90.4	91.3	92.2	93.0	95.4	92.7	88.4	83.9	80.5	73.7	69.5		

TABLE 11. FAR-FIELD (200 FT RADIUS) ONE-THIRD OCTAVE BAND AND dBA NOISE LEVELS - 2000 SHP

PICROPHONE RADIUS = 200. FEET, TEST TEMPERATURE = 41. F, TEST RELATIVE HUMIDITY = 65. PCT
DATA IS CORRECTED TO 59. F AND 70. PCT RELATIVE HUMIDITY ATMOSPHERIC ABSORPTION

FREQ	SPL AT AZIMUTH ANGLE (DEG) AND RADIUS OF 200. FEET																		PNL RE
HZ	0.	10.	20.	30.	40.	50.	60.	70.	80.	90.	100.	110.	120.	130.	140.	150.	160.	170.	180.	10**-12 W
25.	64.0	66.5	62.5	63.5	62.5	61.5	61.0	71.0	69.5	68.0	77.0	75.5	76.0	75.5	75.0	74.5	75.0	76.5	73.0	118.1
32.	62.5	63.5	61.0	61.5	62.0	60.0	60.5	66.5	65.5	64.0	74.5	72.5	73.0	72.5	72.0	72.0	73.0	73.0	73.0	115.3
40.	60.5	60.0	59.0	58.5	61.5	60.5	60.0	62.0	61.5	61.0	71.0	69.5	70.0	70.0	69.5	70.0	72.5	73.0	73.5	112.5
50.	61.0	60.0	60.5	59.5	62.5	62.5	62.5	64.0	64.0	64.0	69.0	68.0	68.5	69.0	68.5	69.5	71.5	74.0	74.5	111.8
63.	63.5	62.0	67.5	65.5	65.0	65.0	67.5	66.0	65.5	66.5	65.0	70.0	70.0	69.5	71.5	71.5	71.0	71.0	73.0	116.5
80.	66.0	64.5	64.0	64.0	66.5	67.0	66.5	67.5	68.0	68.0	76.5	76.5	76.5	73.5	73.5	74.0	76.0	77.0	78.0	115.6
100.	64.5	63.5	63.5	63.5	65.5	70.0	70.5	71.5	72.0	72.0	74.5	74.5	74.5	75.5	74.5	74.5	76.5	78.0	79.5	118.1
125.	68.5	67.0	67.5	67.0	73.5	72.5	74.5	76.5	77.0	77.5	75.0	79.0	78.5	77.5	75.0	75.0	76.0	77.5	79.0	121.7
160.	71.0	70.5	70.0	70.0	77.5	76.5	78.5	79.0	78.5	80.0	81.5	82.0	82.0	79.5	77.0	75.5	74.0	78.5	80.0	124.2
200.	73.0	72.5	73.0	72.5	77.5	76.5	78.5	79.5	80.0	81.5	81.5	82.0	81.5	78.5	76.5	75.0	72.5	77.5	80.0	124.5
250.	71.5	71.0	71.5	70.0	75.5	76.5	76.5	78.5	79.5	79.5	81.0	82.0	81.5	79.5	76.5	73.5	73.5	77.0	79.5	123.9
315.	70.0	68.5	68.5	69.0	73.5	73.5	74.5	76.5	77.0	77.5	78.5	80.0	78.5	77.0	74.5	70.5	70.0	73.0	78.0	121.6
400.	66.0	63.5	66.0	71.5	70.5	70.5	73.0	73.0	74.0	75.5	74.0	75.5	77.5	73.5	70.5	68.5	68.0	70.5	73.0	118.7
500.	61.5	62.0	63.0	63.5	69.5	70.0	71.5	71.5	72.0	74.0	73.0	73.5	75.5	71.5	68.5	66.0	65.5	66.0	66.5	116.9
630.	59.5	59.0	59.5	60.0	66.5	61.5	66.5	70.0	70.5	71.5	74.5	74.0	73.5	71.5	68.5	65.5	65.0	67.0	67.0	115.5
800.	63.0	61.0	60.5	60.0	65.0	65.0	65.5	66.0	66.5	68.5	76.0	75.0	73.0	71.5	68.5	64.5	63.5	66.5	66.5	115.7
1000.	65.0	63.5	65.5	66.5	70.0	68.0	66.5	69.0	70.0	69.5	78.0	77.0	76.0	73.5	69.0	65.0	64.0	65.5	65.0	117.6
1250.	63.5	63.5	65.0	67.0	71.5	68.5	65.5	71.0	70.5	72.5	78.0	77.0	75.5	73.5	68.0	65.5	64.5	65.5	69.0	118.2
1600.	64.1	64.6	66.1	72.6	73.6	71.1	71.1	72.1	71.6	74.1	76.6	75.6	75.1	72.1	68.1	66.1	63.1	62.6	65.1	118.3
2000.	61.3	62.8	65.8	66.3	70.3	68.8	68.8	69.8	69.3	71.8	75.3	73.3	71.8	70.8	66.3	63.8	61.3	63.3	61.8	115.5
2500.	62.9	65.9	63.4	66.9	67.4	66.9	66.5	66.5	66.4	70.4	74.4	72.5	71.9	69.4	64.4	63.9	62.9	62.4	63.4	116.8
3150.	61.2	62.7	61.2	66.7	69.7	65.2	68.2	66.7	65.2	70.7	73.2	69.7	71.2	68.7	62.7	63.7	63.2	63.7	64.7	114.0
4000.	58.6	61.1	62.1	67.1	68.1	62.6	66.6	65.1	64.1	70.1	72.1	68.6	70.1	67.6	62.1	63.6	63.6	64.1	63.1	112.8
5000.	55.3	57.8	65.3	64.8	61.3	61.3	62.8	59.8	60.8	64.3	65.8	65.3	65.3	61.8	59.3	58.8	51.8	51.8	56.3	108.8
6300.	61.8	63.3	65.8	64.3	68.3	64.8	55.8	64.3	61.8	61.8	69.3	65.8	62.3	65.8	63.3	56.3	43.8	47.8	49.3	110.6
8000.	62.5	65.0	65.0	64.0	70.0	65.0	63.5	66.5	61.0	65.5	71.5	69.5	66.0	68.0	63.5	60.5	51.5	54.0	54.0	112.4
10000.	60.3	60.8	61.3	64.8	69.8	60.8	65.3	65.8	60.8	68.3	70.3	64.3	68.3	67.3	61.3	63.3	56.7	57.7	57.7	112.3
CASPL	90.0	79.5	80.3	81.7	85.3	84.5	85.6	86.5	87.0	88.2	90.1	90.1	89.7	87.8	85.2	83.8	85.1	87.1	88.6	132.5
CEIA)	74.9	75.4	76.5	79.6	81.7	79.6	80.5	81.2	81.2	81.4	82.8	85.7	85.0	83.0	79.0	76.8	75.2	77.2	78.7	
PNL	88.8	90.0	90.6	93.1	95.6	93.3	94.6	94.8	94.5	97.3	100.1	98.8	98.5	96.6	92.6	91.3	88.5	92.0	94.5	
PNLT	88.8	91.1	90.6	93.1	95.6	93.3	94.6	94.8	94.5	97.3	100.1	98.8	98.5	96.6	92.6	91.3	88.5	92.0	94.5	
THE FOLLOWING TWO LINES ARE FOR A 200. FOOT SIDELINE RATHER THAN A CONSTANT 200. FOOT RADIUS																				
PNL		70.3	78.9	86.1	91.2	90.7	92.2	94.2	94.4	97.3	100.0	98.3	97.0	94.0	88.3	84.2	79.3	76.8		
PNLT		71.4	78.5	86.1	91.2	90.7	92.2	94.2	94.4	97.3	100.0	98.3	97.0	94.0	88.3	84.2	79.3	76.8		

N_L = 39% (of 33,850 rpm)
N_H = 59% (of 43,450 rpm)
N_{PT} = 12% (of 24,500 rpm)

TEST – DECEMBER 1973 MIC LOCATION – 200 FEET

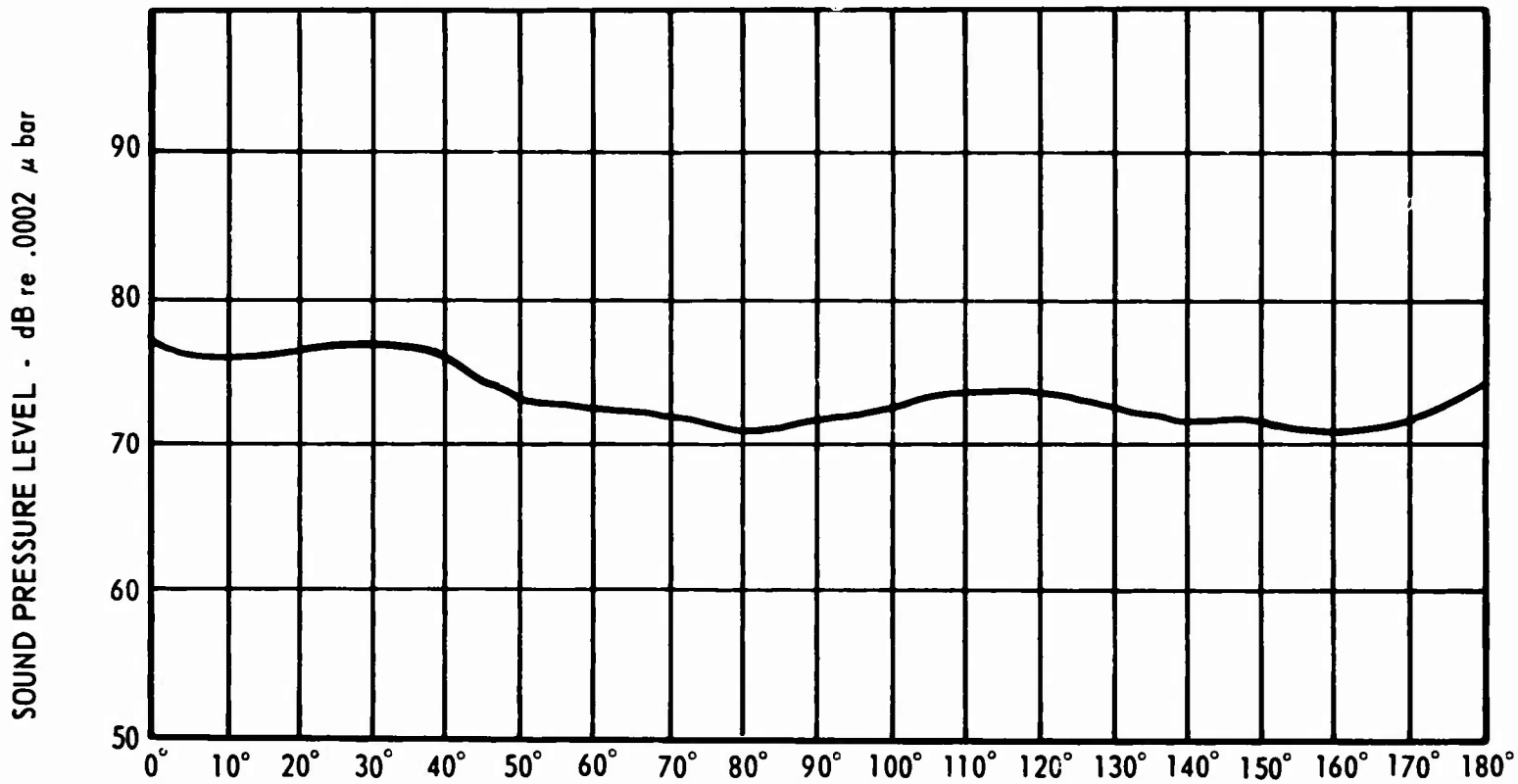

Figure 52. Overall Sound Pressure Levels at Idle.

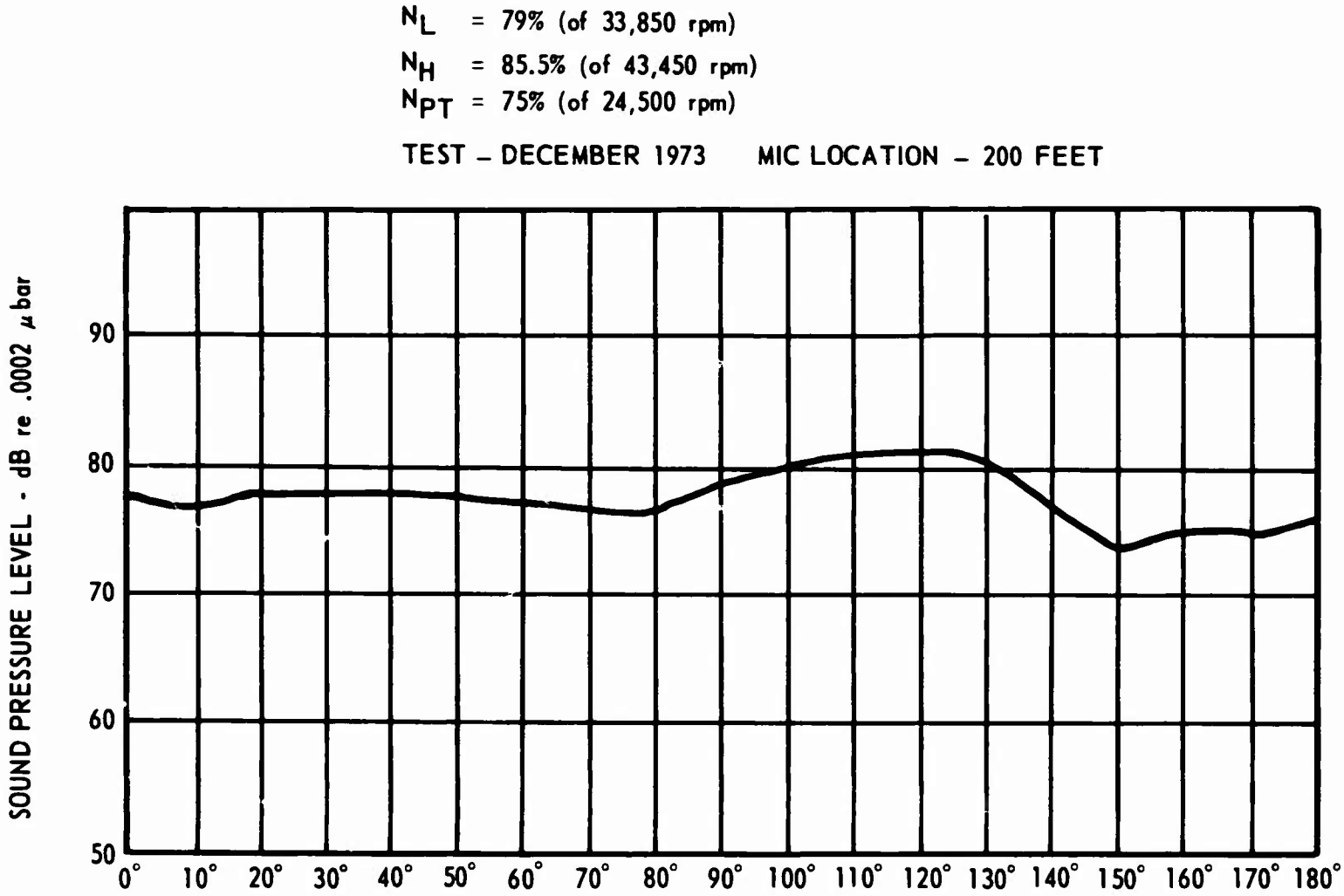

Figure 53. Overall Sound Pressure Levels at 600 SHP.

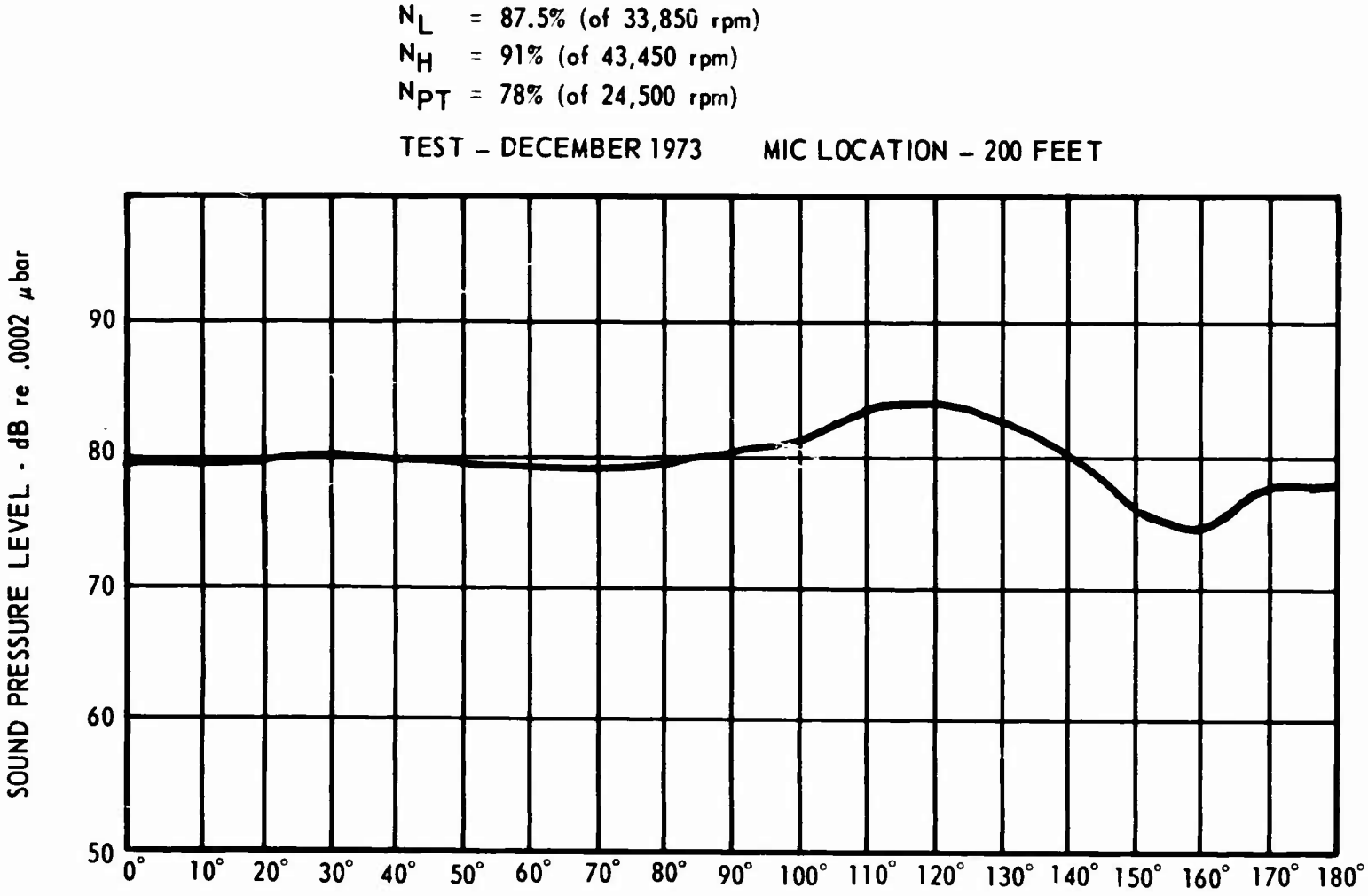

Figure 54. Overall Sound Pressure Levels at 1150 SHP.

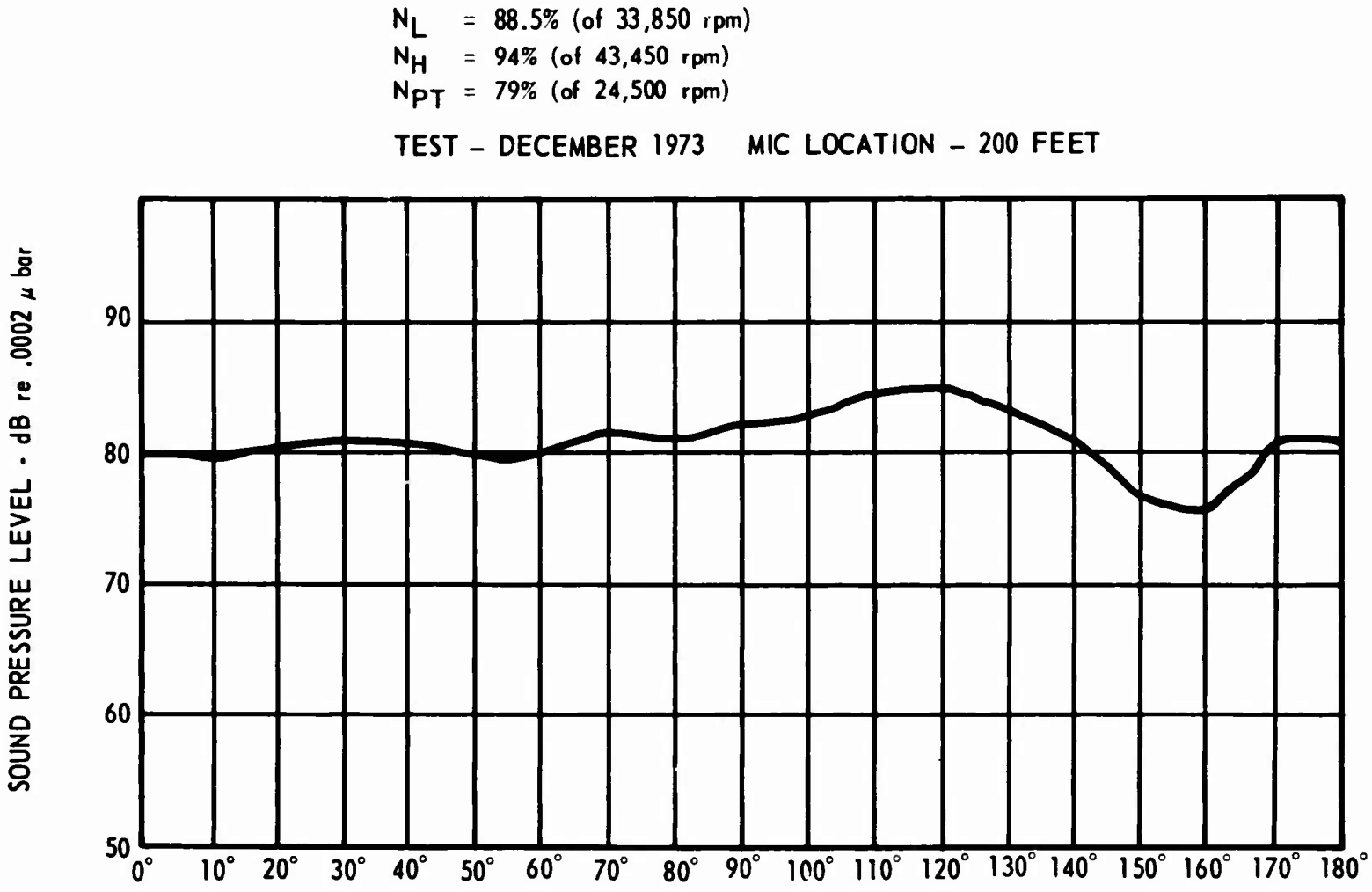

Figure 55. Overall Sound Pressure Levels at 1500 SHP.

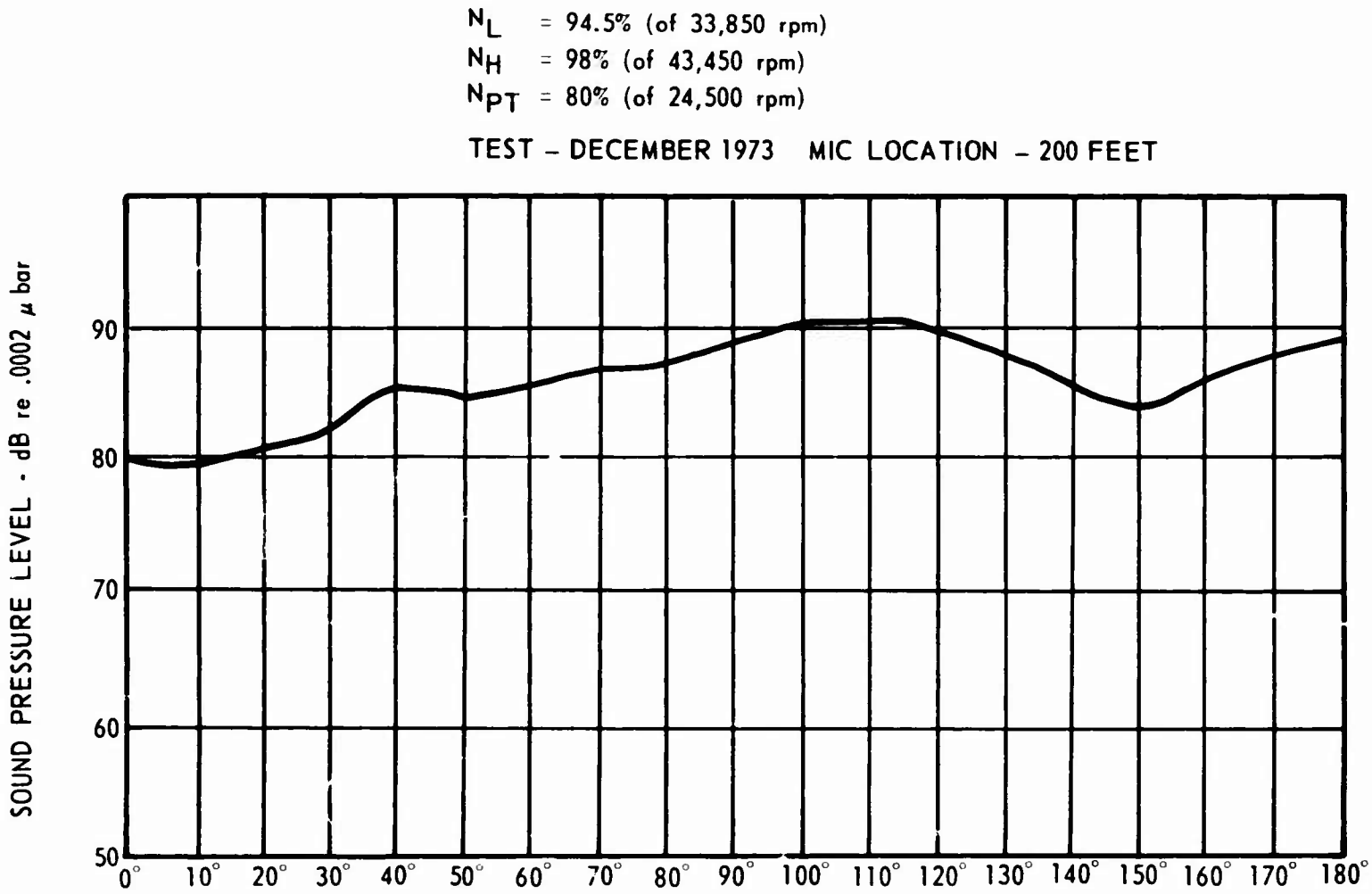

Figure 56. Overall Sound Pressure Levels at 2000 SHP.

The frequencies of the tones generated by the compressor and power turbine blade passage are above the range used for the calculation of PNL and "A" weighted noise levels for most of the operating range; i.e., they are above 11,200 Hz.

The dominant source of the PLT 27 engine is broad-band noise, which is comprised of the jet exhaust noise in the frequency range below 2000 Hz and the compressor noise in the range above 2000 Hz.

Multiple pure tones or combination tones are present at high engine power levels as a result of supersonic compressor rotor tip speeds but have little influence on overall sound levels because there is much less energy under the combination tone peaks relative to the energy contained in the broad band noise.

Far-field narrow-band plots of sound pressure level versus frequency for the power settings of 1500 shp and 2000 shp measured at a 100-foot radius are presented in Figures 57 and 58. The near-field (10-foot radius) narrow-band plot for 1500 shp is shown in Figure 59.

In order to evaluate the noise performance of the bare PLT 27 engine, its near-field and far-field sound pressure levels at maximum power in the 31.5 to 8000 Hz octave bands have been compared with the noise level criteria set forth for an advanced Army gas turbine engine in the medium power class. Following is a tabulation of this comparison.

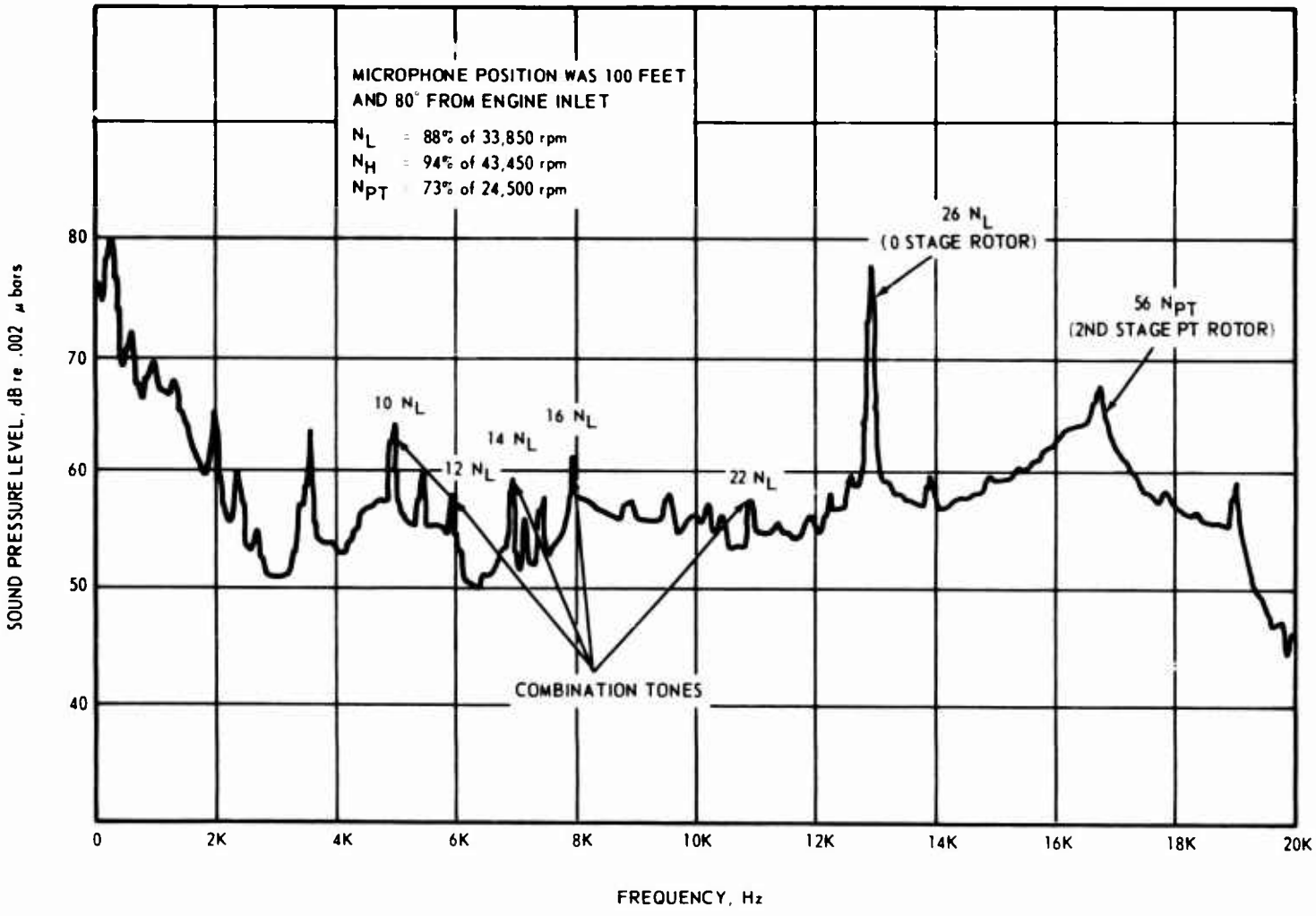

Figure 57. Far-Field (100-ft Radius) Narrow-Band Sound Pressure Levels at 1500 SHP.

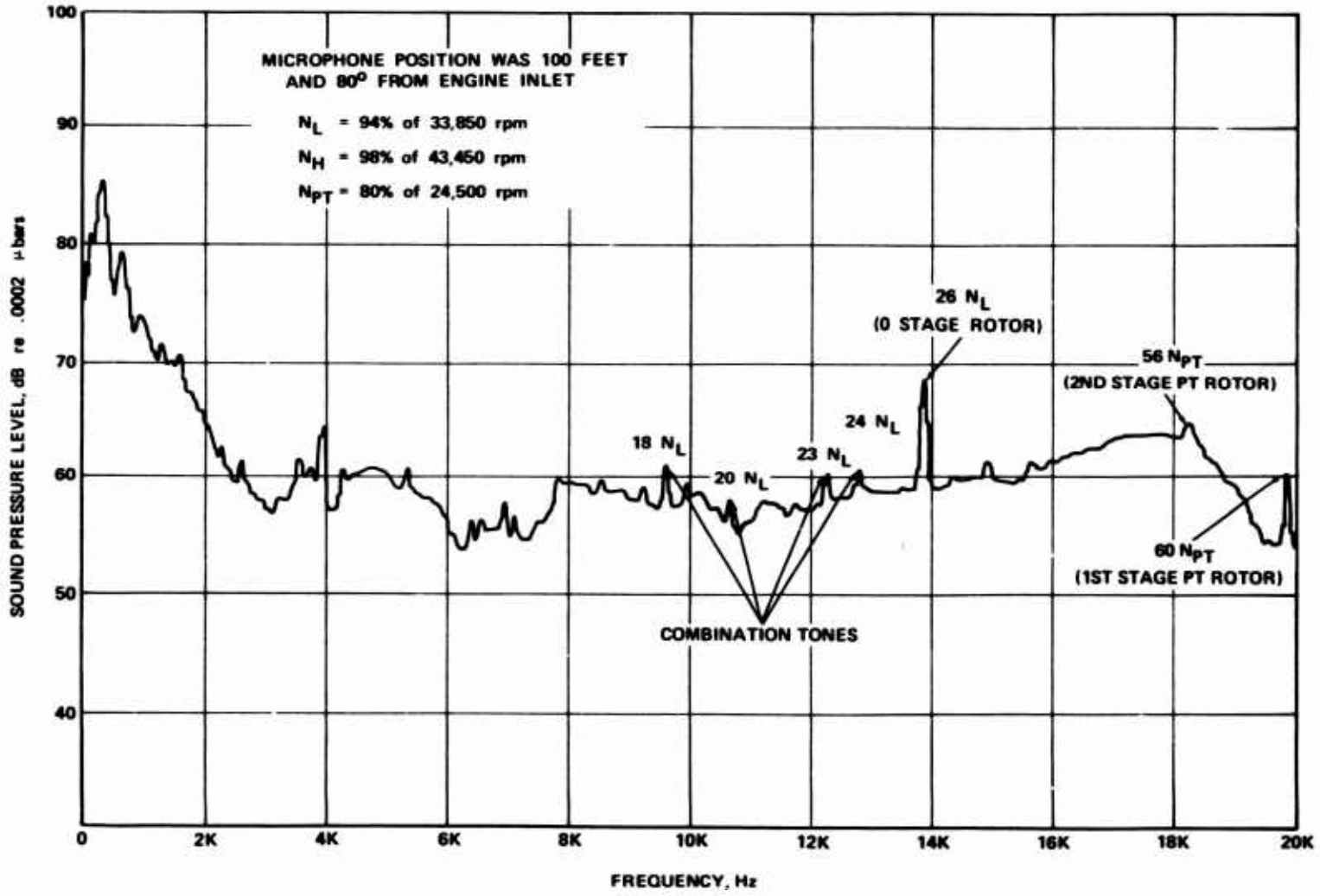

Figure 58. Far-Field (100-ft Radius) Narrow-Band Sound Pressure Levels at 2000 SHP.

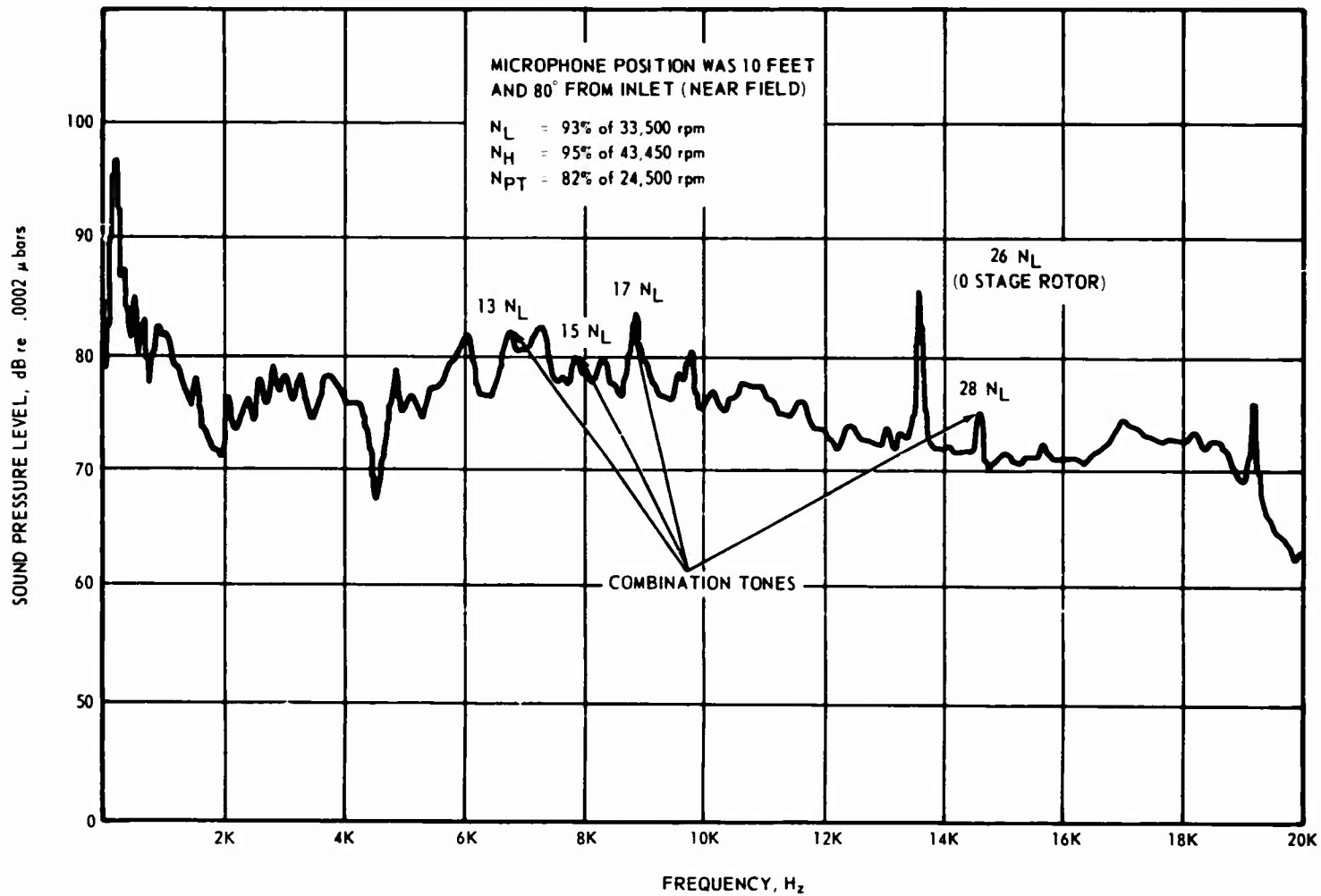

Figure 59. Near-Field (10-ft Radius) Narrow-Band Sound Pressure Levels at 1700 SHP.

Frequency (Hertz)		Maximum Sound Pressure Levels, dB referred to 0.0002 microbars			
		10-Foot Radius (Near-field)		200-Foot Radius (Far-field)	
Bandwidth	Center	Specified	PLT 27	Specified	PLT 27
22.4-45	31.5	102	87	76	76
45 -90	63	106	88	80	74
90 -180	125	108	92	82	81
180 -355	250	113	97.5	87	85
355 -710	500	110	92.5	84	78
710 -1400	1000	107	92.5	81	82
1400 -2800	2000	104	90.5	78	80
2800 -5600	4000	102	95	75	76
5600 -11200	8000	102	99	73	75
OVERALL (Linear)--		118	104.5	92	90

CONCLUSIONS

The bare PLT 27 meets the far-field (200-foot) noise level criteria set by the Army for advanced medium power class gas turbine engines in all octave bands except four. However, these four band levels at 200 feet are exceeded only by 1 or 2 dB. The overall PLT 27 sound pressure level is lower by 2 dB.

At near-field (10-foot radius), the engine is very quiet when compared with the Army specification. The PLT 27 octave-band sound pressure levels are lower than the near-field specification by 3 to 18 dB, and the overall level is lower by 13.5 dB.

The major noise sources of the PLT 27 at high powers in the 31.5 to 8000 Hz octave-band range are broad band in nature. They originate from the engine exhaust and the compressor blade broad-band noise. Multiple pure tones are present but contribute little energy to the broad-band noise. Compressor and power turbine blade passage tones are above 11,200 Hz, which is the upper limit of the 8000 Hz octave band.

CONCLUSIONS AND RECOMMENDATIONS

The results of the measurement and analysis of the exhaust gas and noise emissions show that the Lycoming PLT 27 gas turbine engine satisfies the present criteria or standards established for the exhaust gas and, with few exceptions, the noise emission characteristics of advanced gas turbine engines.

The engine demonstrated a high combustion efficiency throughout the operating range from idle to maximum-rated power. At idle, the combustion efficiency is 99.5 percent; above 10 percent maximum-rated power, combustion efficiency is approximately 99.9 percent. Consequently, the contents of unburned combustion products (hydrocarbons and carbon monoxide) in the exhaust gas proved to be low at all power levels. The amount of nitrogen oxides is in the upper part of the band obtained from the gas turbine engines reported by Lipfert. This condition is a result of the higher compressor pressure ratio produced in the PLT 27. Further development effort is indicated so that the contents of nitrogen oxides can be reduced in high-pressure-ratio gas turbines.

Overall, the PLT 27 turboshaft engine meets the EPA 1979 P2 exhaust gas emission standards for fixed-wing aircraft, turboprop engines.

The smoke levels produced by the PLT 27 are practically zero at all power levels.

The three types of fuel injector systems tested in the engine produced only minor differences in the emission characteristics. The Parker-Hannifin air-blast injector showed a slightly better overall performance than the dual-orifice and Delavan air-blast injectors.

With few exceptions the PLT 27 engine, as a bare engine without an inlet particle separator and specific acoustical treatment, operates quietly and meets emission criteria established by the Army for advanced turboshaft engines in the medium power class. These exceptions occur in the far-field range (200 feet) where the sound pressure levels in the high-frequency octave bands exceed the Army criteria slightly, i.e., by not more than 2 dB.

Operation of the engine is particularly quiet in the near-field range (10 feet) where its sound pressure levels are significantly below the Army criteria.

The overall far-field and near-field sound pressure levels are 2 dB and 13.5 dB, respectively, lower than the levels established by Army criteria.

REFERENCES

1. Stumke, F. B., Jr., ARMY MIPR AMRDL 71-6-T53-L-13A ENGINE; RESULTS OF EXHAUST EMISSIONS TESTS ON (Report), Naval Air Propulsion Test Center, AEFL:GS:er, 10340, Ser. 370, 19 July 1972.

2. Stumke, F. B., Jr., ARMY MIPR AMRDL 71-6-T55-L-11A ENGINE; RESULTS OF EXHAUST EMISSIONS TEST ON (Report), AEL1:GS:er, 10340, Ser. 322, Naval Air Propulsion Center, 22 March 1972.

3. Rubins, P. M., and Doyle, B. W., T53 and T55 GAS TURBINE COMBUSTOR AND ENGINE EXHAUST EMISSIONS MEASUREMENT, USAAMRDL Technical Report 73-47, U. S. Army Air Mobility Research and Development Laboratory, Ft. Eustis, Virginia, December 1973.

4. AIRCRAFT GAS TURBINE EXHAUST SMOKE MEASUREMENT, SAE Aerospace Recommended Practice, Report ARP 1179, 4 May 1970.

5. Rubins, P. M., GAS ANALYSIS EVALUATION OF GAS TURBINE ENGINES AND COMBUSTORS, Avco Lycoming Report 4235. 2. 18, May 1972.

6. Toone, B., and Arkless, R., THE APPLICATION OF GAS ANALYSIS TO COMBUSTION CHAMBER DEVELOPMENT, Seventh Symposium (International) on Combustion, Butterworths, London, 1959, pp. 929-937.

7. Perry, J. H., CHEMICAL ENGINEERS HANDBOOK, 4th Ed., McGraw-Hill, New York, 1969.

8. Doyle, B. W., GAS ANALYSIS DATA REDUCTIONS SYSTEM 370/155, Avco Lycoming Memo Program No. K-120, 27 July 1972.

9. Glenn, C., MEASUREMENT AND TEST EQUIPMENT CALIBRATION SYSTEMS, Avco Lycoming Memo IES-1, March 1972.

10. CALIBRATION SYSTEM REQUIREMENTS, Military Specification MIL-C-45662A, 9 February 1962.

11. Dick, R., and Hartmann, C. H., CRITICAL EVALUATION OF THE RESPONSE CHARACTERISTICS OF THE HYDROGEN FLAME DETECTOR, Varian Aerograph Tech. Bull. 133-67, 1966.

12. PROCEDURE FOR THE CONTINUOUS SAMPLING AND MEASUREMENT OF GASEOUS EMISSIONS FROM AIRCRAFT TURBINE ENGINES, SAE Aerospace Recommended Practice, ARP 1256, 1 October 1971.

13. Lipfert, F. W., CORRELATION OF GAS TURBINE EMISSIONS DATA, ASME Paper 72-GT-68, March 1972.

14. THE DESIGN AND PERFORMANCE ANALYSIS OF GAS TURBINE COMBUSTION CHAMBERS, VOLUME I, THEORY AND PRACTICE OF DESIGN, Northern Research and Engineering Corp., NREC Report No. 1082-1, 1964, P 124ff.

15. Watkins, S., PERFORMANCE OF PLT 27 MANIFOLDS USED IN EMISSIONS TESTING, Avco Lycoming Memo D12-b-012-74, 23 January 1974.

LIST OF SYMBOLS

A	area of combustion chamber cross section, $in.^2$
a	parameter in chemical reaction (Equation 2)
b	parameter in chemical reaction (Equation 3)
b	parameter used in θ combustor loading equation
F/A	fuel-air ratio (or W_f/W_a)
HC	abbreviated term for unburned hydrocarbon components mixture
m	hydrogen atoms in fuel molecule
n	carbon atoms in fuel molecule
P	combustion chamber pressure, psia
SHP	shaft horsepower
T	temperature, ^oR or ^oF
W	mass flow
ΔH	lower heating value of fuel, Btu per lb
η_b	combustion efficiency
ϕ	equivalence ratio = $(F/A)/(F/A)_{stoich.}$

Subscripts

a	air
f	fuel
p	primary zone
ref	reference
stoich.	stoichiometric
3	combustor inlet
7	power turbine inlet